A Feedback Controlled Gas Mixing System For the Ram Accelerator

by

Matthew Jardin

A thesis submitted in partial fulfillment of the
requirements for the degree of

Master of Science in Aeronautics and Astronautics

University of Washington

1992

Approved by_____
(Chairperson of Supervisory Committee)

Program Authorized
to Offer Degree_____

Date_____

In presenting this thesis in partial fulfillment of the requirements for a Master's degree at the University of Washington, I agree that the library shall make its copies freely available for inspection. I further agree that extensive copying of this thesis is allowable only for scholarly purposes, consistent with "fair use" as prescribed in the U.S. Copyright Law. Any other reproduction for any purposes or by any means shall not be allowed without my permission.

Signature _____

Date _____

University of Washington

Abstract

A Feedback Controlled Gas Mixing System for the Ram Accelerator

by Matthew R. Jardin

Chairperson of the Supervisory Committee: Professor Adam P. Bruckner
Department of Aeronautics
and Astronautics

The development of a feedback controlled gas mixing system is presented here along with the operation results for a prototype control system which has been developed for the Ram Accelerator facility at the University of Washington. The purpose of the control system is to fill high pressure chambers with as many component gases as are required (four for the Ram Accelerator) at a desired set of molar ratios. A further objective is to perform this task as quickly and efficiently as possible to serve as an example for the design of gas fill systems for future Ram Accelerators and other facilities which require precise gas ratios at high pressure.

A flow rate controller is designed to keep the flow rate of a primary gas constant while the secondary gas controllers make use of a control law which drives their molar ratio errors to zero, thereby ensuring that the final gas composition is correct. The sensing elements are resistive thermal detection (RTD) mass flowmeters, the control elements are nonlinear servo-actuated metering valves, and the control laws are implemented using a Macintosh IIci running Labview software from National Instruments. The flow rate controller makes use of a simple first order linear control law, but a more advanced second order control law in conjunction with a feedback path filter is required to obtain optimal time responses for setting molar ratios. Experimental results for the operation of the prototype system are reported.

TABLE OF CONTENTS

LIST OF FIGURES

LIST OF TABLES

LIST OF SYMBOLS

A = Area

CF = Conversion factor from Kg/sec to Standard Liters per Minute

C_p = Specific heat at constant pressure

C_v = Valve C_v factor, a measure of pressure loss

D = Diameter; Denominator polynomial of a transfer function

d_{min} = minimum fill line diameter

d_p = fill pipe diameter

ε = Pipe roughness coefficient (inches)

F_w = Shear force on a pipe wall

$G_{ol}(s)$ = Open loop transfer function

K_{cf} = Conversion constant in mass flow rate equation

K_{cl} = Control law gain

K_{cv} = Relational constant between orifice area and C_v factor

K_{eff} = Effective closed loop system gain

K_{fd} = Relational constant between C_v factor and molar flow rate

L = Length of fill pipe

M = Mach Number

MW = Molecular weight

$\dot{M}$ = True molar flow rate in SLM

$\dot{M}_{cl}$ = Voltage signal from control law in feedback loop

$\dot{M}_e$ = Error signal in feedback loop and input to control law

$\dot{M}_m$ = Molar flow rate reading from flow meter

$\dot{M}_{max}$ = Maximum molar flow rate

$\dot{M}_{ref}$ = Input reference molar flow rate

$\dot{M}_{SLM}$ = Molar flow rate in Standard Liters per Minute

$\dot{m}$ = Mass flow rate in Kg/sec

N = Numerator polynomial of a transfer function

P = Pressure; Pole of a transfer function

P_s = Standard pressure (1.01×10^5 MPa

P_t = Total pressure

R = Ideal gas constant for a given gas

$\Re$ = Molar ratio of two gases

R_u = Universal ideal gas constant

$\dot{R}_n$	= Angular speed of valve actuator motor shaft (revolutions/second)
rev	Number of revolutions of the valve actuator motor stem
s	Complex variable used in Laplace Transform analysis
SLM	Standard Liters per Minute (the number of Liters a given mass of gas would occupy if at standard temperature and pressure, T_s & P_s)
T	Temperature (absolute)
T_s	Standard temperature (273.15 K)
T_t	Total Temperature
u	Axial flow velocity
V_e	Error Voltage
Z	Zero of a transfer function
z	Axial displacement

Greek

γ	Ratio of specific heats
Φ	Friction coefficient
ρ	Density
τ	Shear stress

Operators

$d(\ )$	Derivative
$\Delta(\ )$	Finite Difference

Subscripts

1	Conditions upstream of the valve orifice
2	Conditions downstream of the valve orifice
f	Conditions in the fill tank
v	Conditions at the valve orifice

ACKNOWLEDGEMENTS

<u>A List of Key Players</u>

1. **Parents: Mr. Robert Jardin and Mrs. Anne Fox**

   My parents have been a source of encouragement and have made my educational pursuits possible.

2. **Professors Adam P. Bruckner and Abraham Hertzberg**

   Hired and supported me as a Research Assistant. Both professors have always managed to make time to answer any abstract question I have ever devised. They have both been very inspirational in my decision to seek a graduate degree and to complete this thesis.

3. **Fellow Research Assistants: Edward A. Burnham Jr., Gilbert Chew, Barbrina Dunmire and Jacqueline Auzias de Turenne, John Hinkey, Carl Knowlen.**

   Inspired my work by setting examples with their own dedication to their research projects. Allowed me to live after using a significant portion of equipment money for the hardware needed for this thesis.

4. **Gregg Murphy**

   An excellent friend who has always supported my work. He even selflessly aided in a trip I had to make to Las Vegas in order to secure more funding for my project. I wish him as much satisfaction with his newly initiated studies as I've had with mine.

5. **Alfa Zinkus and the staff at the Red Door Alehouse, 3401 Fremont Ave.**

   A significant amount of the work for this thesis has been accomplished while working at the Red Door, a truly inspirational pub.

6. **Professor Juris Vagners**

   Without the equipment and help made available by Professor Vagners, this thesis may have remained a paper study. I am truly grateful for his help along with the understanding of his research group in parting with some of their equipment as this thesis developed.

7. **The Office Staff at the Department of Aeronautics and Astronautics: Marlo Anderson, Diane Collum, and Jane Lybecker**

   Without their administrative help, many supporting tasks in my graduate work may have become overwhelming. They are fun to go out to lunch with too.

8. **Andrew J. Higgins**

   A swell *individual*, and a wonderful photographer though no one may ever know.

CHAPTER 1 INTRODUCTION

The Ram Accelerator has been an ongoing research project in hypervelocity launch methods at the University of Washington since 1986. As research is conducted, areas for hardware and operating procedure improvements are continually discovered. This thesis presents the design of a prototype system which may be used to simplify one aspect of the operating procedures of the Ram Accelerator. The background information regarding the Ram Accelerator and the motivation behind the work presented here will now be given.

1.1 The Ram Accelerator

The Ram Accelerator is a device used for accelerating objects to hypersonic velocities by use of a chemical propulsion cycle very similar to that of a conventional ramjet. In the Ram Accelerator, however, the projectile takes the shape of the centerbody of a ramjet and travels freely through a tube filled with a mixture of combustible gases. The shock structure developed by the projectile as it moves through the gases initiates combustion behind the projectile causing acceleration (Fig. 1).

One important area of research is to study the effects of mixture composition upon Ram Accelerator performance. Although no complete studies have yet been made, research to date suggests that even slight changes in gas composition can have significant effects upon Ram Accelerator performance so that obtaining accurate gas mixtures is very important. Additionally, the system used to fill the Ram tubes prior to a projectile launch must be quick and efficient to operate if the Ram Accelerator is to become a viable hypersonics testbed or orbital launch facility in the future.

1.2 Current Gas Mixing Systems

The current gas fill system at the University of Washington makes use of a set of choked orifices to achieve constant mass flow rates for any given upstream gas pressure (Fig. 2). The orifices are set with micrometering valves, and the mass flow rates are calibrated by setting the upstream pressures to known values and then recording dp/dt in a fill tank into which the gases flow. As long as the ratios of

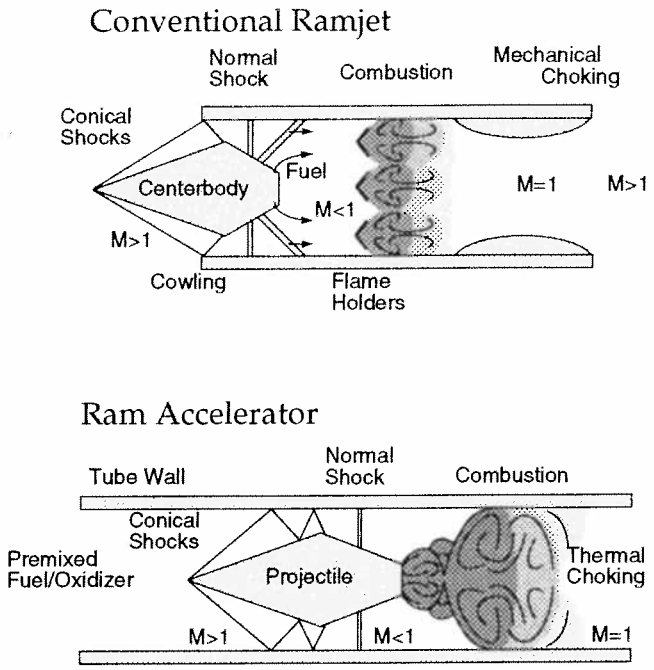

Figure 1. The Ram Accelerator

downstream to upstream pressures are held below the critical value, defined in Eq. 1, the flows through the orifices are choked, and the mass flow rates are dependent only upon the upstream pressure which can be set by system operators via Nitrogen gas dome regulators. Once the orifices are calibrated at a given setting, a wide range of mass flow rates, and therefore ratios, can be obtained by varying the upstream pressures.

$$\left[\frac{P_2}{P_1}\right]_{critical} = \left(\frac{\gamma+1}{2}\right)^{\gamma/(\gamma-1)} \qquad \text{(Eq. 1)}$$

In order to achieve proper molar ratios for a given shot configuration, the gases are set to their corresponding mass flow rates and are then flowed together through a high Length to Diameter ratio fill line into the Ram tube sections so that mixing of the gases occurs prior to insertion into the tubes. This method was originally chosen for its simplicity, but some inherent problems have necessitated the search for a better fill system. The main problem is that the orifice calibrations must be relied upon since no direct measurements of mass flow rate can be made during operation and this leaves open the possibility that plugging of an orifice,

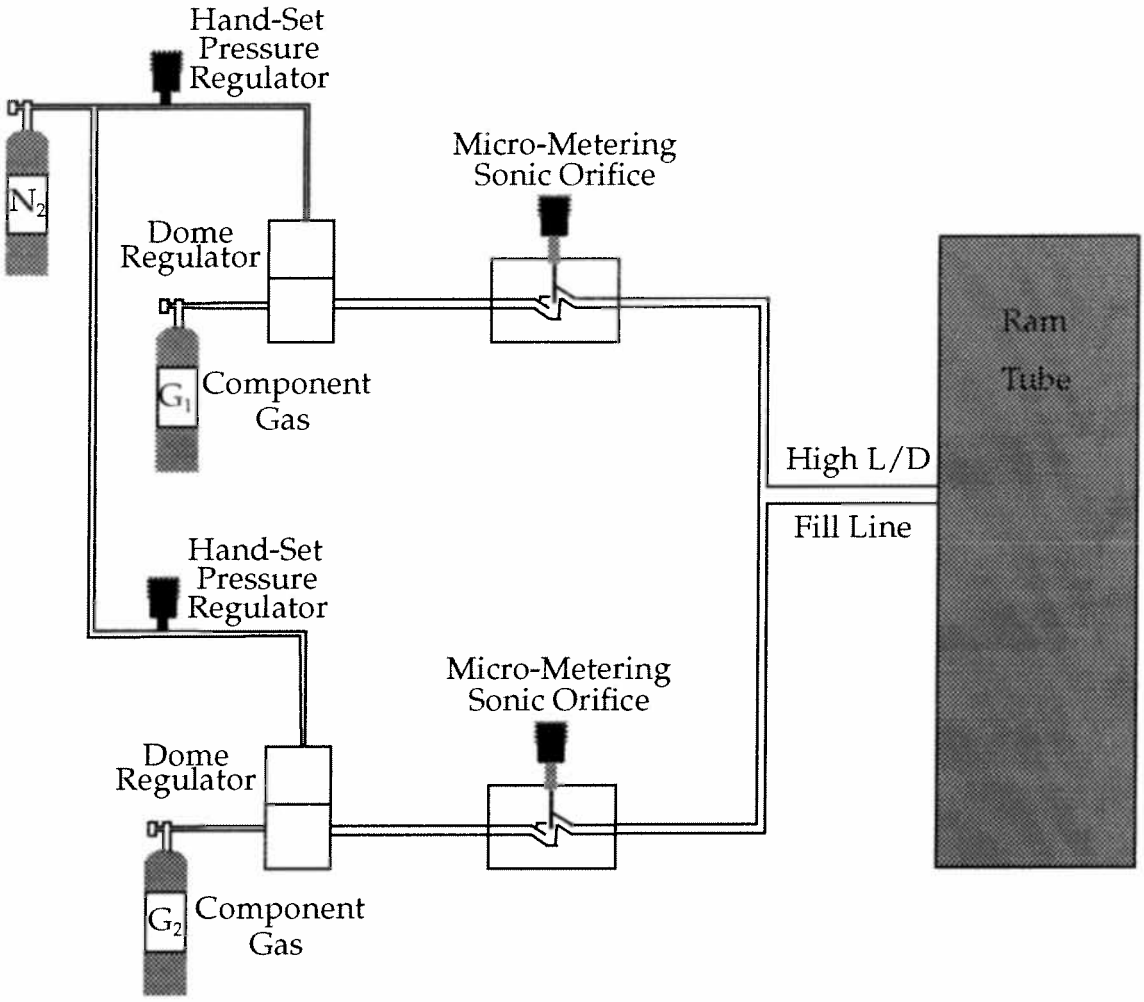

Figure 2. Current University of Washington Gas Fill System

inaccurate upstream pressure settings, or inadvertent displacement of the orifice can cause large errors in the final gas mixture which would not be known until after a sample of the gas mixture could be analyzed. A further problem is that maintaining choked flow conditions requires that the upstream pressure be roughly two times greater than the downstream pressure. Since fill pressures of about 600 psig are commonly used, this renders source gas bottles useless when source gas pressures approach 1200 psig. For some of the gas components, such as high purity Methane, this becomes a needless expense at $350 per gas bottle.

At the Army Ballistics Research Laboratory, the method of partial pressure filling has been attempted with some initial experimental success. As the name

suggests, each gas is introduced into the ram tube sequentially, and the mass is determined based upon the pressure rise in the ram tube. One reason partial pressure filling has not been attempted at the University of Washington facility and the reason that this method may prove to be undesirable in the future is that the question still remains of whether or not the gases become uniformly mixed before a firing is attempted. Studies need to be made to determine which fill system hardware configurations will consistently mix the gases to an adequate degree. A further problem with partial pressure filling is that individually flowing each gas into the tubes may require a significant amount of time. In the case of current research where four component gases are in use, fill times could be reduced by 75 percent over partial pressure filling by flowing all four gases simultaneously.

In an automated gas mixing system, three major requirements need to be met in order to improve upon current systems: 1) Direct measurement of mass flow rate, or of total mass must be made in real time, 2) All gas components should be allowed to flow simultaneously for more efficient operation, and 3) Mass flow *ratios* should be measured and should be able to be set to a specified high degree of accuracy.

A feedback control mechanism which makes use of true mass flow meters along with integrating capabilities can meet all of the requirements. By using computer control law implementation, some additional benefits can be realized by allowing routine aspects of Ram Accelerator operation to be programmed into a fully automated system.

1.3 The Control Concept

The idea for an automated gas mixing system is to employ feedback control in order to set the final mass ratios of gases which have been introduced into a high pressure chamber. The general concept is to set the flow rate of a primary gas component (this can be any one of the gases) by use of a mass flow *rate* controller, and then to run mass *ratio* controllers on the secondary gases using the flow rate of the primary gas as a reference input. Block diagrams for these feedback loops are given below in Fig. 3.

The components of the control system such as the control valves and flow meters must first be chosen before the control law design may begin. The sizing of

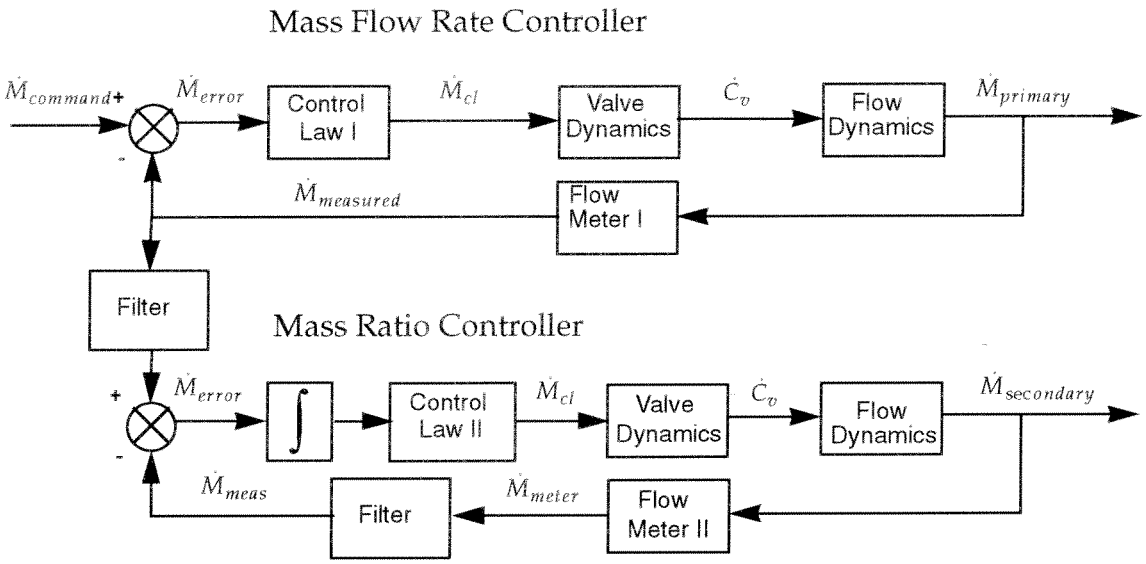

Figure 3. Block Diagrams of Basic Control Loops

valves and flow meters is a relatively open ended problem and requires a significant amount of work to properly accomplish. After the system hardware has been chosen, dynamic models are created either theoretically, or empirically if possible. The design of the control laws then consists of straightforward single input/single output linear system analysis with the aid of nonlinear computer simulations. The nonlinear simulations allow much more thorough control law adjustments to be made before the actual control hardware is operated. Finally, experimental results are obtained with the prototype system in order to verify the operation of the control systems.

CHAPTER 2 CONTROL COMPONENT SELECTION

As previously mentioned, a prototype gas controller has been designed, built, and tested for use with the Ram Accelerator at the University of Washington. In this chapter, the analysis used to determine the proper sizes for the controller components is detailed. When sizing the components, the important factors are the limitations imposed by the Ram Accelerator hardware and any new limitations imposed by the choice of controller components. In this sense, the design process is somewhat iterative since all of the hardware parameters are not known until component choices have been made, but the components cannot be chosen until the hardware parameters are known. For example, the type of flow meter which has been decided upon limits the operating pressure to 1000 psig which, along with other parameters, determines the size of valve which is used.

2.1 General Component Selection

The very first part of the component selection process is to decide what types of control and sensing elements to use for the controller. In making these decisions, at least some of the system limitations could be discovered before performing computations to determine the exact sizes the components should be.

2.1.1 Flow Meter Selection

Much research went into the different types and limitations of gas mass flow meters available. Only one type of commercially available mass flow meter has been found which meets the requirements mentioned in Chapter 1. This is the Resistive Thermal Detection (RTD) type of mass flow meter which is the only one that accurately measures the true mass flow rate (not volume flow rate) of gases without the need for extensive pressure or temperature corrections [1].

The RTD mass flow meter measures mass flow rates by transferring heat to a diverted stream of the flowing gas and measuring this heat transfer a little further downstream by the use of resistive thermal heating coils in a bridge circuit (Fig. 4). Since heat transfer to a flowing gas is primarily dependent upon mass transport, the mass flow rate can be detected by this principle. The heat transfer is also

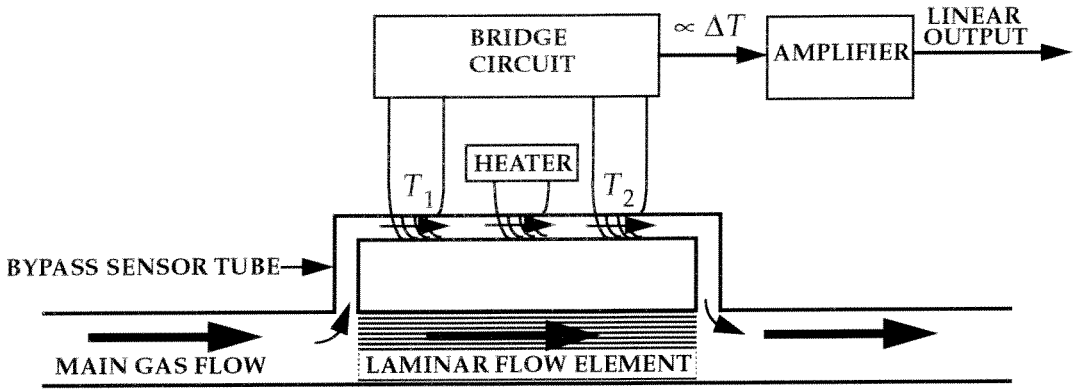

Figure 4. RTD Mass Flow Meter

dependent upon the specific heat, c_p, of the flowing gas, and since c_p is a weak function of temperature, a very small correction factor is needed for variations in gas temperature (± 0.2% of full scale flow per °C between 0-50 °C)

The measurement stream is diverted into a high L/D ratio tube by the use of a laminar pressure reducing flow element in the main flow stream. When the flow through both streams remains laminar, the pressure drops through each stream are nearly linear, and this causes the ratio of diverted gas flow to main gas flow to remain constant over a specified operating range of the flow meter. This allows the heat transfer measurements to be made on a very small portion of the gas flow which greatly increases accuracy. The amount of diverted flow is a very small percent of the total, and this requires only very slight drops of gas total pressure when the gas passes through the mass flow meter.

Of course, some fluctuations in RTD response to mass flow rate exist which are dependent upon the type of gas being flowed. Most obviously, the change in specific heat for different gases is large so that a meter which has its electrical output calibrated for gas '1' will give readings that are a factor of c_{p_2}/c_{p_1} off if the mass flow rate of gas '2' is measured with the same meter. Other second order effects such as differences in gas viscosity can alter the reading of the flow meters slightly, so the accuracy of the meters is guaranteed by the manufacturers to be fairly high (± 1% of full scale flow) by running calibrations of the electrical output for each specific gas. These calibrations may also be performed by the user of the flow meter if some other mass flow rate proving method is available. This allows

one RTD meter to be used to measure the flow rate of many different gases with just a simple function applied to the electrical output of the flow meter.

The transient response time of RTD mass flow meters to unit step changes in flow rate is on the order of 10 seconds. This limits the use of RTD flow meters to control systems in which the measurement of rapid flow rate changes is not necessary. For the Ram Accelerator, these response times will not cause problems since fill operation times on the order of a few minutes are acceptable. One other limitation is that the operating pressure rating for these meters is generally limited to 500 psig, and is often lower. Only a handful of manufacturers offer special pressure rating tests to ensure safety up to at least 1500 psig, but the highest calibrations are still only performed up to 500 psig. Therefore, the mass flow meter must somehow be calibrated before mixture ratio accuracy can be guaranteed.

2.1.2 Valve Selection

Many different metering valves are commercially available with a large variety of characteristics and ratings so that the choice of valve type or manufacturer can not be safely made before more detailed analysis is performed. However, from the data books for the metering valves currently in use with the Ram Accelerator, and for similar metering valves, no further limitations are placed upon the flow system such as pressure ratings or maximum flow ratings.

2.1.3 Valve Actuator Selection

Again, many different actuation types are readily available, so no exact specifications can be determined for the valve actuators. The important parameters for the actuator are torque rating and motor speed which would determine the speed with which flow rates could be set. The actuation in concert with the valve should have a bandwidth somewhat similar, or perhaps slightly faster than that of the flow meter. If the frequency of operation becomes too fast, the controller will have a very difficult time maintaining stability.

In the search for actuator manufacturers, one company has been found which offers a complete system of servo valve actuation fit to a customer specified valve, and powered by a custom made printed circuit board. This system offers flexibility since many of the actuator parameters can be adjusted via the circuit board. An

additional benefit of this system is inherent in the method of powering the actuator motor. A control circuit on the circuit board measures the input signal and, in the manner of a switch, either sends positive or negative V_{max}, the maximum operating voltage, to the actuator depending upon whether the input signal is positive or negative. A small dead zone exists between ± 0.02 volts so that the valve will remain at rest once setpoint has been reached. In this way, the actuator always responds at the maximum rate so that the control system can react as quickly as physically possible. This type of response is nonlinear as will be discussed in further detail later in the chapter regarding controller design, and can cause some stability problems, but with the proper control law, these problems can be overcome.

2.1.4 Computer Control Implementation Hardware and Software

The choice of computer is fairly simple since a Macintosh IIci has been made readily available along with National Instruments Labview version 2 software. Labview 2 is graphical interfacing software which is useful for both data acquisition and data conditioning tasks such as implementing control laws. A National Instruments NB-MIO-16L multifunction analog/digital and timing board is also available for use in connecting electronic hardware to the computer and a special termination board, the National Instruments SC-2070, has been purchased for its thermocouple cold-junction compensation capabilities.

2.1.5 Other Hardware

The control system also requires the use of two pressure probes and two thermocouples in order to monitor the source gas pressure and temperature, and the pressure and temperature of the gas that has accumulated in the Ram Tubes. The necessary equipment has been obtained from Omega Engineering Inc., and consists of one each of a PX603-1KG5V 1000 psig pressure transducer and a PX603-3KG5V 3000 psig pressure transducer, and two JTIN-18E-12 J-type thermocouple probes.

2.2 Flow Meter Sizing

The flow meter must be chosen such that the measurement range covers as

much of the mass flow rate range as possible while maintaining high accuracy. The range of flow rates for which the meters must operate can be determined by placing limits upon the time that the fill system should take to fill the Ram Accelerator with a mixture of gases. While shorter fill times are better, sufficient time must be allowed for the controller transients to damp out so that the final mixture ratios will be as accurate as possible. For the prototype system, conservative estimates of the transients can be made so that the full operation of the controller can be easily tested.

The data books for a variety of RTD flow meters report response times on the order of 10-15 seconds. Presumably a valve/actuator combination can be found which sets flow rates much quicker than the response time of the meter so that the flow meter is the limiting element of the control system. While the controller will allow the flow rates to be set as quickly as the valve can set them, the meters will not be able to completely verify the settings for at least 10-15 seconds so that having the entire fill process be shorter than this may risk overall accuracy. For this reason, the flow meter response times are used as a guideline for how quickly the filling of the Ram Accelerator should take place. After the prototype has been built and tested, the effectiveness of the controller in setting flow rates quickly, even with the significant lag in the flow meters, may allow faster systems to be employed in the future.

2.2.1 Ram Accelerator Fill Process

The Ram Accelerator at the University of Washington is comprised of eight tube sections, each of which are 2 meters long. These tubes may be sectioned into any possible shot configuration by placing mylar diaphragms in between the tubes in order to separate the stages. The U.W. facility has been operated both as one large single stage Ram Accelerator, and in multistage configuration with the smallest stages being made of only one tube section. The volumes for which the fill system must operate are therefore bounded by the volume of one tube, and the volume of the entire Ram Accelerator operated as one stage. In Table 1 appears a listing of the internal dimensions of a single Ram Accelerator tube as well as those for the entire Ram Accelerator.

The mixture ratios of gases varies with each use of the Ram Accelerator, but several common mixtures are given below (Table 2) which are used to determine

Table 1: Ram Accelerator Tube Internal Dimensions

# Of Sections	Diameter (mm)	Length(m)	Volume (L)
1	38.1	2	2.28
8	38.1	16	18.24

Table 2: Common Ram Accelerator Gas Mixtures

Mixture #	Molar Ratios
1	$2O_2 + 5.8N_2 + 2.75CH_4$
2	$2O_2 + 3.9N_2 + 4.5CH_4$
3	$2O_2 + 12He + 3CH_4$
4	$2O_2 + 20H_2 + 3.2CH_4$

the necessary flow rates for each of the component gases.

Following the discussion earlier in this chapter, the fill times should be at least 10-15 seconds long for the prototype gas mixing system so that the controller operation may be verified by the RTD mass flow meters. For a safety margin, some extra time will be allowed so that fill times of no less than 30 seconds will initially be attempted. As previously mentioned, the fill times for a single Ram tube will be the shortest, so the mass flow rates necessary for a single tube fill of 30 seconds will determine the range that the mass volumeters should be able to measure.

Adhering to the molar ratios given in Table 2, a table of fill times has been compiled with all of the flow rates scaled such that 30 seconds are required to achieve a fill pressure of 400 psig. The molar flow rates are determined by first computing the necessary flow rate of Oxygen using

$$\dot{M}_{O_2} = \frac{P_f V_f}{P_s}\left(\frac{1}{2}min\right)\left[1 + \left(\frac{\dot{M}_{N_2}}{\dot{M}_{O_2}}\right) + \left(\frac{\dot{M}_{CH_4}}{\dot{M}_{O_2}}\right)\right]^{-1} \qquad \text{(Eq. 2)}$$

and then multiplying the desired molar ratios of the other gases by the computed flow rate of Oxygen. The same procedure can be used for any of the gas mixtures.

Table 3: Molar Flow Rates for a 400 psig Fill in 30 seconds

Mixture #	Molar Flow Rates (SLM)	V_{fill} (L)
1	$24.4O_2 + 70.7N_2 + 33.5CH_4$	2.28
2	$24.7O_2 + 48.24N_2 + 55.6CH_4$	2.28
3	$15O_2 + 90.8He + 22.7CH_4$	2.28
4	$10.2O_2 + 102H_2 + 16.3CH_4$	2.28
1	$195O_2 + 566N_2 + 268CH_4$	18.24
2	$198O_2 + 386N_2 + 445CH_4$	18.24
3	$121O_2 + 726He + 182CH_4$	18.24
4	$81.7O_2 + 817H_2 + 131CH_4$	18.24

Table 3 gives the ranges of flow rates that the flow meters for each of these gases must be able to measure for fill times to be kept at 30 seconds. Since the accuracy of an RTD flow meter is usually given as a percent of maximum rated flow, slightly longer fill times can be accepted for the full Ram Accelerator fills in order to narrow the required ranges of the flow meters so that greater accuracy can be achieved for the smaller volume fills. Additionally, the large volume fills are not as common.

The prototype controller is being built for Nitrogen gas so the flow meter needs to be chosen for the Nitrogen flow range. If the flow rate of Nitrogen is limited from the maximum in the table of 566 SLM to 200 SLM and the other gases are scaled accordingly, the full Ram Accelerator fill will still only take about 1.5 minutes while the smaller fills can still take place within the 30 second limit.

When cost, performance, and delivery time are considered along with the flow range specifications, the model HFM-201 mass flow meter by the Teledyne-Hastings Raydist corporation has been chosen as the sensor for the prototype system. The specifications for this meter appear at the end of this chapter along with the specifications for the other controller components.

2.3 Control Valve and Actuator Sizing

When taking all of the flow hardware into consideration, estimating the correct size for the control valve consists of calculating flow losses due to friction in the gas delivery lines as well as discovering limitations upon other independent system variables such as the upstream fill pressure. The flow rate for the prototype has already been limited to 200 SLM by the choice of flow meter, so this narrows the search for the valve somewhat.

2.3.1 Hardware Limitations

From section 2.1.1, the flow system pressure has been limited by the flow meter to 1500 psig. The maximum fill pressure required by the Ram Accelerator is only about 750 psig, so that upstream flow system pressures of 1500 psig are unnecessary. Operating the control system well below the proof pressure of the flow meter is prudent, and a quick approximate calculation assuming one dimensional incompressible flow [Note: More detailed calculations of mass flow rates are given later] shows that with an upstream pressure of 1000 psig, the mass flow rates of the system are more than adequate. By keeping the pressure at or below 1000 psig, the expense of the control valves is kept lower as well since the high pressure options required by some manufacturers are then not necessary. This pressure also poses no problems for the high pressure steel tubing used to transport the gases from their source tanks into the Ram tubes.

2.3.2 Valve Sizing Calculations

The end result of these calculations is to obtain a numerical algorithm which gives the valve C_v factor (described in the nomenclature list in section 2.3.2) as a function of the measurable and independent parameters in the fill system, namely molar flow rate ($\dot{M}$), Upstream total pressure (P_{t_1}), Ram Tube fill pressure (P_f), and all of the physical hardware parameters such as tube diameter and the friction coefficient of the tube walls. One dimensional compressible fluid dynamics with friction accounted for will be used to form the necessary relations among the appropriate variables. Steady and uniform flow is also assumed in these calculations. Refer to Fig. 5 when necessary.

The first expression to obtain is one for the molar (and therefore mass) flow rate

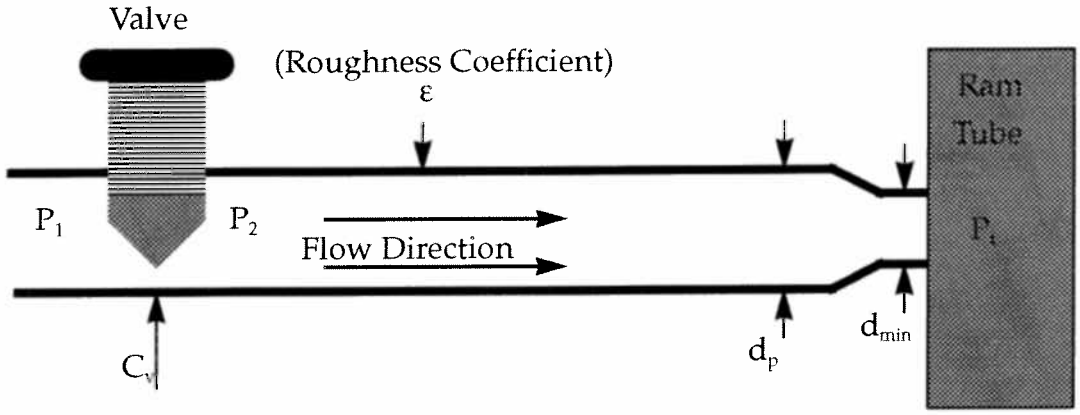

Figure 5. Model of Gas Fill System for Use in Sizing Calculations

of a gas through an orifice with a pressure differential across the orifice. Beginning with the continuity equation written at station *1* and station *2*, the expression for the mass flow rate is

$$\dot{m} = \rho_1 A_1 u_1 = \rho_2 A_2 u_2 = \rho_v A_v u_v \qquad \text{(Eq. 3)}$$

Then, for an ideal gas,

$$P = \rho RT \qquad \text{(Eq. 4)}$$

Using the ideal gas assumption here makes the resulting equations easier to manipulate and demonstrates the calculation process, but if conditions need to be computed for a non-ideal gas such as CH_4 or CO_2, Eq. 4 need only be replaced by an equation of state which adequately models non-ideal effects. Furthermore, these calculations are only required to give the approximate valve sizes which should be used for the flow control system, and will therefore be applicable to most gases as long as the departure from the ideal gas model does not become too large.

Now we add the adiabatic energy equation which implicitly assumes a perfect gas as well since c_p has been assumed constant,

$$c_p T_1 + \frac{u_1^2}{2} = c_p T_v + \frac{u_v^2}{2} \qquad \text{(Eq. 5)}$$

Solving Eq. 5 for u_v and making use of Eq. 3, we arrive at

$$\dot{m} = \frac{A_v P_1}{RT_1}\left[2C_p(T_1 - T_v) + u_1^2\right]^{1/2} \qquad \text{(Eq. 6)}$$

Now, if station *1* has a large enough area, the flow through this station can be kept slow, and therefore, u_1 can be neglected in the above expression. Then, applying the ideal gas relation (Eq. 4) to both station *1* and the valve station, we get

$$T_1 - T_v = \frac{1}{\rho R}(P_1 - P_v) \qquad \text{(Eq. 7)}$$

Additionally, noting that $c_p = \frac{\gamma R}{(\gamma - 1)}$, and manipulating slightly, Eq. 6 becomes

$$\dot{m} = A_v\left(\frac{2\gamma}{(\gamma-1)RT_1}\right)^{1/2} P_1\left[\left(\frac{P_v}{P_1}\right)^{2/\gamma} - \left(\frac{P_v}{P_1}\right)^{(\gamma+1)/\gamma}\right]^{1/2} \qquad \text{(Eq. 8)}$$

Remember that some simplifying assumptions have been made. The restrictions will now be removed by replacing the A_v term with an empirically determined function of the area which computes an effective area for a valve orifice that takes pressure losses into account. This removes the incompressible and frictionless assumptions. Since the ambient temperature will be very near to that of the flowing gases, the adiabatic assumption can remain and will be reasonably accurate.

The empirically determined function is called the C_v factor and is dependent upon the type and size of valve being used. Theoretical approximations can be made for the C_v factor, but for accurate results, this function should be measured directly with the actual valve to be used. The units for the C_v factor are gallons per minute of water which would flow through the valve in question with a pressure drop of 1 psi across the valve. Modifying the A_v term in Equation 10 then yields

$$\dot{m} = A_v(C_v)\left(\frac{2\gamma}{(\gamma-1)RT_1}\right)^{1/2} P_1\left[\left(\frac{P_v}{P_1}\right)^{2/\gamma} - \left(\frac{P_v}{P_1}\right)^{(\gamma+1)/\gamma}\right] \qquad \text{(Eq. 9)}$$

which shows A_v as a function of the C_v factor.

In order to have a realistic approximation to the C_v factor, the values given in data sheets for similar micro metering valves to those that have been used in the sonic orifice gas fill system can be used. The C_v factor is actually a nonlinear function of the area, but for the range of values of interest here, a linear approximation can be used which forces the line to pass through the origin of the C_v vs. A_v curve. Then, the $A_v(C_v)$ function becomes, simply, the C_v factor multiplied by a constant which will be called K_{cv}.

A conversion factor can now be added to this equation to obtain an expression for the molar flow rate in units of SLM as explained in the nomenclature. If SI units are used for all variables in Eq. 9, the mass flow rate is in units of Kg/sec. With this in mind, the conversion to SLM is given by

$$CF = \frac{RT_s}{P_s} \bullet \left(1000 \frac{L}{m^3}\right) \bullet \left(60 \frac{\text{sec}}{min}\right) \qquad \text{(Eq. 10)}$$

Replacing R with $R_u/(MW)$ and substituting SI values for T_s and P_s, and combining this conversion factor with the γ term in Eq. 9, a conversion constant can be derived as

$$K_{cf} = 1315.74 \sqrt{\frac{\gamma}{(MW)\ (\gamma - 1)}} \left(\frac{Liters}{Newton \cdot minute}\right) \qquad \text{(Eq. 11)}$$

Substituting this into Eq. 9 and solving for the C_v factor yields

$$C_v = \dot{M}_{SLM} \left\{ K_{cf} \cdot K_{cv} \cdot P_1 \left[\left(\frac{P_v}{P_1}\right)^{2/\gamma} - \left(\frac{P_v}{P_1}\right)^{(\gamma+1)/\gamma} \right]^{1/2} \right\}^{-1} \qquad \text{(Eq. 12)}$$

This expression is almost enough for us to compute approximate C_v factors so we may choose a proper valve for the control system, however, Eq. 12 is not yet set up so that desirable independent parameters may be input into the equation. The independent system parameters are the molar flow rate, the upstream pressure, and the Ram tube pressure. With the frictional and compressible effects of the valve neatly tucked into the C_v factor, the static pressure at the valve orifice can be obtained in terms of P_2. A similar relationship can be used to then obtain P_2 in terms of the Ram tube pressure which would empirically model the frictional

losses in the fill tube, but no accurate approximations to this empirical relationship exist for the particular fill tube configuration at the Ram Accelerator. This makes calculations quite difficult because now a theoretical friction approximation must be done. The result of the calculations will give us P_2 as a function of the known independent parameters.

For this analysis of pressure loss for a gas flowing through a tube, the derivation follows that in reference [2], but some alterations have been made which tailor the analysis to this particular problem. The assumptions made for this derivation are that a perfect gas is flowing through a constant area duct in which compressible and frictional effects are significant. Two-dimensional flow effects are not being considered.

We now write out the basic one dimensional flow equations, beginning with the First Law of Thermodynamics:

$$C_p dT + d\left(\frac{V^2}{2}\right) = 0 \qquad \text{(Eq. 13)}$$

Next, the continuity equation is written after taking the logarithmic differential as

$$\frac{d\rho}{\rho} + \frac{dV}{V} = 0 \qquad \text{(Eq. 14)}$$

Now the linear momentum equation can be written including a term for the force due to the shear stress on the tube walls as

$$-AdP + dR = (\rho VA)\,dV \qquad \text{(Eq. 15)}$$

By referring to , the tube wall friction force term can be written as

$$dR = -(\pi DL)\,\tau_w dz \qquad \text{(Eq. 16)}$$

where (πDL) is the perimeter of the duct cross section, τ_w is the wall shear stress, and dz is an infinitesimal axial displacement. Referring to Fig. 6 below, we can write Newton's Law as

$$\Sigma F = \Delta P\left(\frac{\pi D^2}{4}\right) = \tau_w (\pi DL) \qquad \text{(Eq. 17)}$$

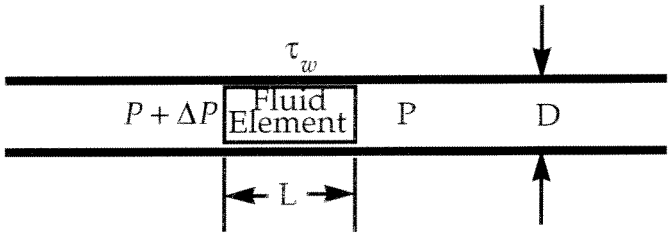

Figure 6. Force Diagram for an Element of Fill Tube

Multiplying Eq. 17 by ρ/ρ, Newton's Law can be written as

$$\Sigma F = \rho \left(\frac{\Delta P}{\rho}\right) \left(\frac{\pi D^2}{4}\right) = \tau_w (\pi D L) \qquad \text{(Eq. 18)}$$

The term $\Delta P/\rho$ represents the head loss of the fluid element and can be written as a function of the following variables,

$$\frac{\Delta P}{\rho} = \Phi \frac{L}{D} \frac{V^2}{2} \qquad \text{(Eq. 19)}$$

where Φ is a friction coefficient that is a function of the Reynolds Number that has been determined empirically [2] to be

$$\Phi = \frac{0.25}{\left[\log\left(\frac{\varepsilon}{3.7 \cdot D}\right) + \left(\frac{5.74}{(Re)^{0.9}}\right)\right]^2} \qquad \text{(Eq. 20)}$$

This equation is valid for $5\times10^3 \le Re \le 1\times10^8$ and $1\times10^{-6} \le (\varepsilon/D) \le 1\times10^{-2}$. Additionally, ε and D must be in the same units, typically inches. That these limits are adhered to by the Ram Accelerator hardware can be verified later after the flow calculations show what values of ε and Reynolds number are involved. By combining Eq. 18 and Eq. 19, we now have an equation for the shear stress in terms of the friction coefficient which is

$$\tau_w = \left(\frac{\Phi}{4}\right) \left(\frac{\rho V^2}{2}\right) \qquad \text{(Eq. 21)}$$

and when this is substituted inEq. 15, the result is

$$-dP = \frac{\Phi}{D}\left(\frac{\rho V^2}{2}\right)dz + \rho V dV \qquad \text{(Eq. 22)}$$

One further equation, the equation of state written in logarithmic differential form is required before we can compile these equations into one useful expression,

$$\frac{dP}{P} = \frac{d\rho}{\rho} + \frac{dT}{T} \qquad \text{(Eq. 23)}$$

The combination of Eqs. 13, 14, 22, and 23 along with the definition of the Mach Number ($M = V/(\gamma RT)$), the following equation is arrived at

$$\frac{dM^2}{M^4}\left[\frac{1-M^2}{1+(\gamma-1)(M^2/2)}\right] = \frac{\Phi\gamma}{D}dz \qquad \text{(Eq. 24)}$$

The remainder of this derivation will now stray from that in reference [2] somewhat. With the help of formulas 37 & 40 on pages 240 & 241of reference [3], and assuming the friction coefficient roughly constant over the length of the tube (which is not a bad assumption since the Reynolds Number is mostly a function of mass flow rate which is constant along the tube), the integration of Eq. 24 can be fairly easily carried out to give

$$\left(\frac{1}{M_2} - \frac{1}{M_f}\right) + \left(\frac{\gamma+1}{2}\right)\left[ln\left(\frac{M_2^2(2+(\gamma-1)M_f^2)}{M_f^2(2+(\gamma-1)M_2^2)}\right)\right] = \frac{\Phi\gamma}{D}L \qquad \text{(Eq. 25)}$$

where M_2 is the Mach Number at station 2, and M_f is the Mach Number at the entrance to the Ram tube just prior to the fitting into the tube. An expression for this Mach Number in terms of the independent parameters is easily found in the following way: First, begin with the Mach Number definition,

$$M_f^2 = \frac{u_f^2}{\gamma RT_f} \qquad \text{(Eq. 26)}$$

Now, writing the velocity in terms of the molar flow rate by use of the

continuity equation and the ideal gas equation, we have

$$u_f^2 = \left[\frac{\dot{M}_{SLM} P_s}{P_f A_f (6\times10^4)} \right]^2 \qquad \text{(Eq. 27)}$$

where SI units must be used and $\dot{M}_{SLM}$ is, of course, in Standard Liters per Minute.

Compiling the two equations above, the expression for M_f becomes

$$M_f^2 = \left[\frac{\dot{M}_{SLM} P_s}{P_f A_f (6\times10^4)} \right]^2 \frac{MW}{\gamma T_f R_u} \qquad \text{(Eq. 28)}$$

And, since Eqs. 25 and 28 can be used to solve for M_2, an expression can now be developed which gives us the static pressure at station 2, and finally the pressure at the valve orifice in terms of the independent parameters.

Isentropic relations along with the continuity equation, the definition of the Mach number, and the ideal equation of state can be combined to give

$$P_2 = \frac{\dot{m}}{A_2 M_2} \left(\frac{R \cdot T_{t_2}}{\gamma \{1 + [(\gamma-1)/2] M_2^2\}} \right)^{1/2} \qquad \text{(Eq. 29)}$$

At the exit plane of the valve orifice, subsonic flow is assumed so that the static pressure within the orifice can be assumed equal to the static pressure at the downstream station. Eq. 29 may then be written as

$$P_v = \frac{\dot{m}}{A_2 M_2} \left(\frac{R \cdot T_{t_2}}{\gamma \{1 + [(\gamma-1)/2] M_2^2\}} \right)^{1/2} \qquad \text{(Eq. 30)}$$

The final work which needs to be done before the preceding equations can be used to determine the required C_v factors is to empirically determine values for the roughness coefficient, ε, the Ram tube fitting internal diameter, d_{min}, and the constant relating the valve area and the C_v factor. This will be accomplished in the next section.

2.3.3 Empirical Determination of Parameters ε, d_{min}, and K_{cv}

The friction parameter, ε, and the fitting internal diameter, d_{min} can be determined by running a few experiments and using the previously developed mathematical flow model to adjust these two values until the model agreed closely with experiment.

First, two different cases have been run using the actual Ram Accelerator gas fill system hardware with the metering valve removed so that the system could be modelled as shown in Fig. 7. Then, The pressures P_1 and P_f were set such that

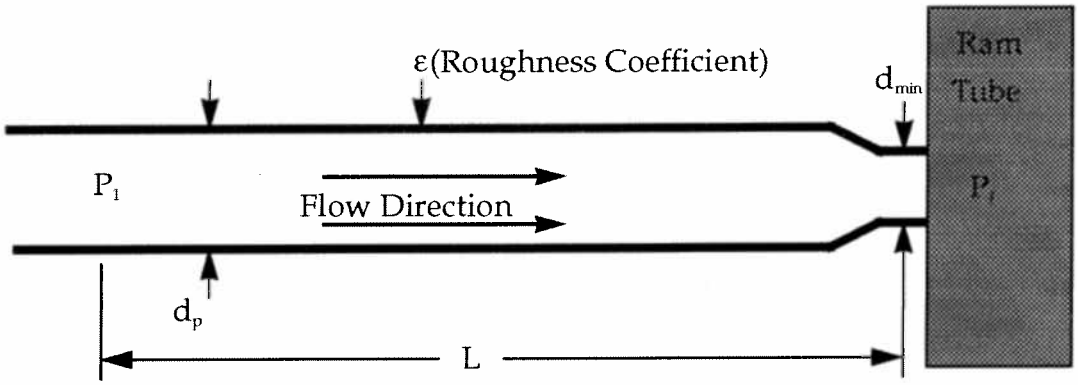

Figure 7. Configuration for Experiment to Determine E & d_{min}

choking would occur at the fitting into the Ram tube. Gas was then flowed through the system into the Ram tube for a known amount of time after which the final Ram tube pressure was measured. From this data, the mass flow rate could easily be determined.

For the theoretical model, Eq. 25 was used with M_f set to unity since the flow would be choked at the minimum orifice point, and M_2 was solved for. M_2 could then be used to compute a theoretical mass flow rate for this system which could be compared to the experimentally obtained values. In the theoretical model, ε and d_{min} were varied until theory and experiment agreed for two different experimental cases.

The computations for this procedure were written into a computer program using Matlab software from Mathworks [4], and the resulting program, *mdot.m* appears in appendix A along with corresponding subprograms *mach1.m* and *mach2.m*.

The program *mdot.m* contains the data taken for two different cases and allows the user to iteratively enter values for ε and d_{min} until the theoretical and experimental mass flow rates agree to the user's satisfaction. Appearing in Table 4 are the results of the calculations performed with *mdot.m*.

Table 4: Results of E and d_{min} Calculations

Gas	L(m)	P_1 (Pa)	$\dot{m}_{meas}$ (Kg/sec)	$\dot{m}_{theory}$ (Kg/sec)	ε (in)	d_{min} (m)
N_2	18	6.97×10^6	.0158	.0157	.00125	.00143
N_2	10	6.97×10^6	.0169	.0167	.00125	.00143

A valve data book with information regarding five different valves from two manufacturers has been used to obtain typical values for K_{cv}. The information given was maximum C_v factor and effective orifice diameter at maximum C_v factor so this could be used to obtain the constant K_{cv}. The necessary information is given below (Table 5). From the table, K_{cv} can be seen to have a range of

Table 5: Valve Data

Manufacturer	Series	Orifice Diameter (mm)	C_v	$K_{cv}\frac{m^2}{C_v}$
Nupro	"S"	0.79	0.004	12.25×10^{-5}
Nupro	"M"	1.40	0.03	5.13×10^{-5}
Nupro	"L"	3.18	0.15	5.29×10^{-5}
Whitey	SS-22RS4	0.51	0.007	2.91×10^{-5}
Whitey	SS-31RS4	1.59	0.04	4.9×10^{-5}

$2.91\times10^{-5} \le K_{cv} \le 12.25\times10^{-5}$ which causes significant differences in the C_v calculations. For this reason, The two limits for K_{cv} will be used for the

calculations in order to allow a more rational judgement to be made about which valve to order for the prototype system. Other considerations will also affect the decision and will be discussed later.

2.3.4 Computer Algorithm for Calculation of C_v Factors

All of the preliminary work required to compute necessary C_v factors for the gas mixture control system has now been completed. Since the equations do not result in an analytical expression which may be solved for the C_v factors directly, a numerical scheme must be employed. The algorithm for the computations appears in this section, and the computer program called *maxvalve.m* appears in appendix A along with the subprograms *mach1mv.m* and *gas.m*. Six separate functions have been created which contain information about each of six different gases that the computations can be performed for, but only the function for Nitrogen, *N2.m*, appears in the appendix as an example.

- Have user choose desired Ram tube fill pressure, P_f, and desired molar flow rate, $\dot{M}_{SLM}$
- Input other system hardware parameters such as fill pipe diameter, fill pipe length, and the previously determined roughness coefficient.
- Use Eq. 11 to compute K_{cf}.
- Compute M_f using Eq. 28.
- Compute the Reynolds Number based upon the user's input choice of molar flow rate, type of gas, and fill pipe diameter.
- Compute the friction coefficient using Eq. 20.
- Make use of Eq. 25 to compute the Mach Number at station 2.
- Compute the static pressure at the valve orifice with Eq. 29.
- Obtain the C_v factor from Eq. 12 for a desired range of upstream pressures (not to exceed the critical pressure ratio).

This algorithm allows plots to be made of the C_v factor vs. the required upstream stagnation pressure. In this way, a C_v factor can be chosen which gives desirable system characteristics. For example, too small of a C_v factor would require upstream pressures far greater than the system hardware could withstand.

Too large of a C_v factor would lead to an unrealistic case where the source gas pressure was nearly equal to the Ram Tube pressure. The results of the computer manifestation of this algorithm will be presented in the next section.

2.3.5 Results of Valve Sizing Program Calculations

The program *maxvalve.m* has been run for Nitrogen gas so that the prototype valve could be designed. The input parameters are the following:

Table 6: *maxvalve.m* Input Parameters

Gas	$\dot{M}_{SLM}$	P_f (psig)	K_{cv}
Nitrogen	200	400	2.91×10^{-5} or 12.25×10^{-5}

The flow rate was determined by the choice of mass flow meter, and the Ram Tube fill pressure of 400 psig was chosen as a common lower limit so that the largest necessary C_v factor could be computed. The output of the program is a plot of C_v factor vs. required upstream stagnation pressure. These plots have been made for both $K_{cv} = 2.91\times10^{-5}$ and for $K_{cv} = 12.25\times10^{-5}$ and appear in Figures 8 and 9 .

The maximum C_v factor can be read from these plots at the point where the upstream stagnation pressure reaches an arbitrary lower limit. From Table 5, the various valve C_v factors can be checked against the plots, and this reveals that the Whitey SS-31RS4 with a C_v factor of 0.04 might be the best match since this would allow the upstream gas bottle pressures to be brought down as low as possible over the full range of K_{cv}. This might cause control problems if the valve needs to be operated at lower flow rate settings, however, so a check of the minimum required C_v factor needs to be made.

The minimum required C_v factor will occur when the upstream pressure is a maximum (1000 psig), the orifice is choked, and the required flow rate is a minimum. The minimum flow rate for Nitrogen can be read from Table 3 to be about 50 SLM. Using these input parameters, a table of minimum required C_v

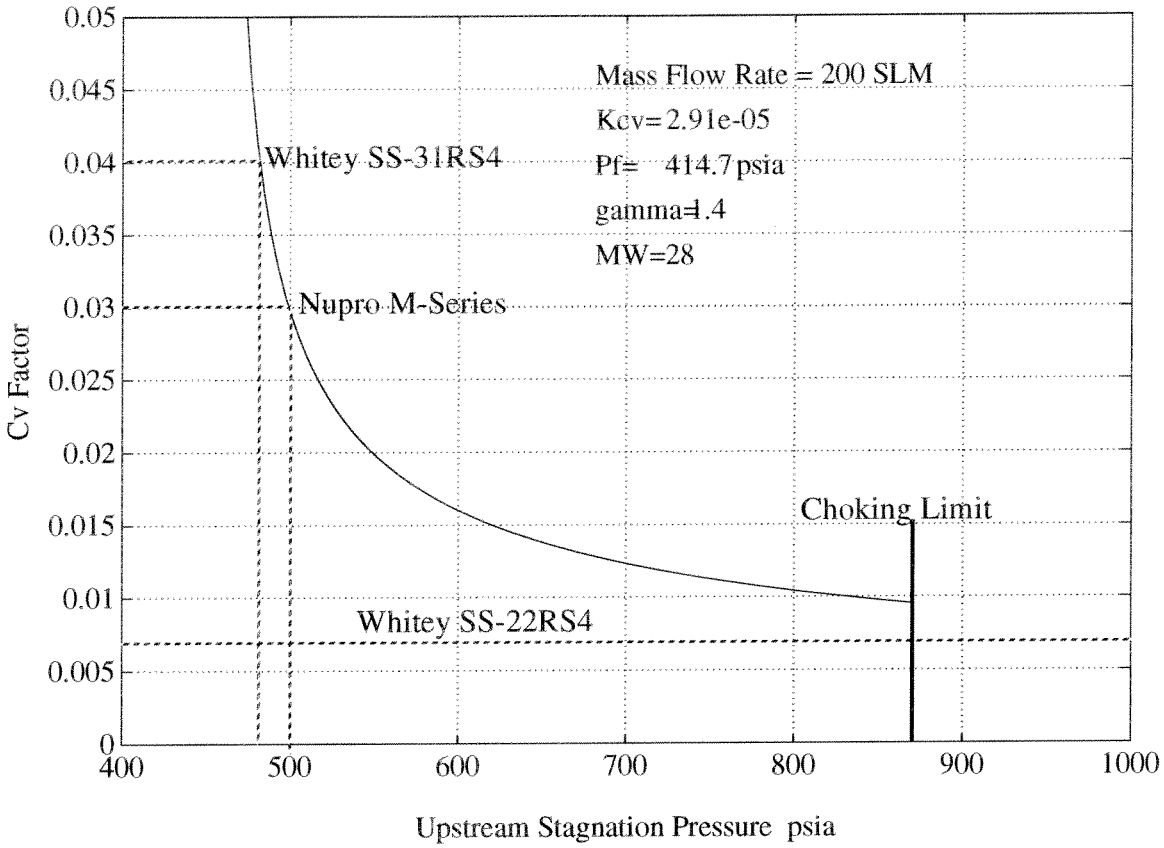

Figure 8. C_v Factor vs. Upstream Stagnation Pressure $K_{cv} = 2.91\times10^{-5}$

factors (Table 7) has been compiled with the use of Eq. 12:

Table 7: Minimum Required C_v Factors For Nitrogen

P_{t_1} psig	$\dot{M}_{SLM}$	K_{cv}	$\left(\frac{P_v}{P_{t_1}}\right)_{crit}$	$C_{v_{min}}$
1000	50	2.91×10^{-5}	0.528	.00205
1000	50	12.25×10^{-5}	0.528	.00049

The case used to determine the minimum C_v factor is actually the most

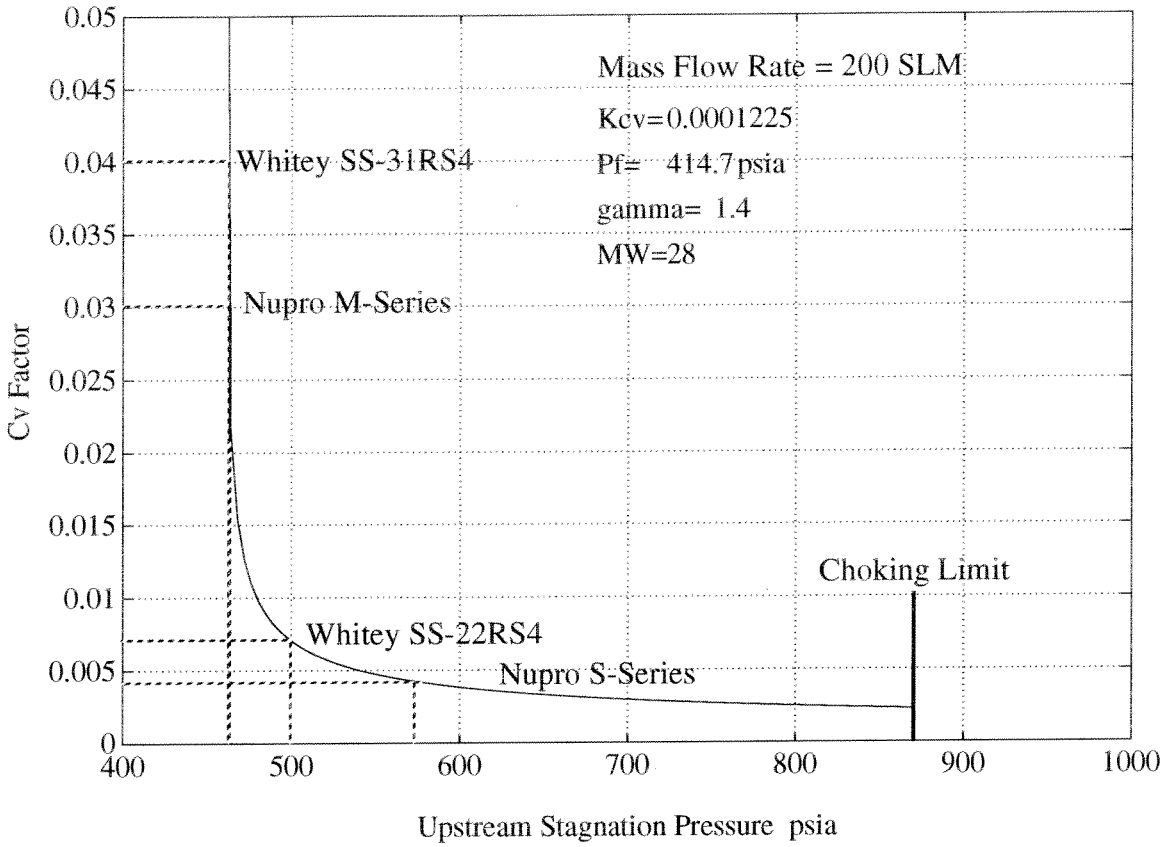

Figure 9. C_v Factor Vs. Upstream Stagnation Pressure $K_{cv} = 12.25\times10^{-5}$

common operating condition that the control system will operate under since single tube fills are normally encountered and since the source gas bottles will be at pressures above 1000 psig for most of their use. For this reason, accommodating the minimum C_v requirements takes precedence over fill speed. While the valve with a maximum C_v factor of 0.04 might still be useful in these lower C_v ranges, the data book shows that factors on the order of 10^{-3} and 10^{-4} are at the end of the useful flow range. Additionally, the C_v vs. valve stem turns curve becomes nonlinear in these lower regions. The Whitey SS-21RS4, however, only has a maximum C_v factor of 0.007 but can still operate in a nice linear region down at the lower values where controller operation will be more common. For this reason, the Whitey SS-21RS4 has been chosen as the valve for the control system.

Ironically, the same type of valve has been in use with the University of

Washington Ram Accelerator for a few years now in the sonic orifice gas mixing system. Now, however, the analysis has been performed to show why these particular valves work so well with this fill system.

In the future, two valves may be placed in parallel which would allow for both fine and coarse control of mass flow rates. This would be the ideal solution for fully operating control systems so that the controller could operate with fine accuracy across a much larger range of flow conditions. For the prototype, however, using the one valve will perfectly well demonstrate the necessary concepts.

2.4 Valve Actuator

Now that the valve size had been chosen, a corresponding actuator would need to be found that could operate at the proper speed. Too slow of a response would limit the performance of the control system, and to quick of a response could cause stability problems. The actuator should be compatible with the choice of valve, and should have desirable electrical characteristics so that no special extra equipment would be required.

While researching different valve actuator manufacturers, one was found which obtains the customer's choice of valve and fits an actuator to the valve, complete with a custom designed printed circuit board. The standard motor speed was determined to be slower than optimal but would work well enough for proving the prototype and could still be adjusted later after the prototype had been tested. An estimate of the rate of change of molar flow rate for the most common operating conditions that the controller would experience was made with some simple calculations and some parameter estimates obtained from valve and actuator data books.

As a first order estimate, Eq. 12 can be differentiated with respect to time while assuming everything constant except for C_v and $\dot{M}_{SLM}$ and rearranged to give:

$$\frac{d}{dt}(\dot{M}_{SLM}) = \frac{d}{dt}(C_v) \cdot K_{cf} K_{cv} P_1 \left[\left(\frac{P_v}{P_1} \right)^{2/\gamma} - \left(\frac{P_v}{P_1} \right)^{(\gamma+1)/\gamma} \right]^{1/2} \qquad \text{(Eq. 31)}$$

The rate of change of the C_v factor was estimated by obtaining the change of

C_v factor per revolution of the valve stem from the valve data book, and obtaining the revolutions per minute of the actuator motor from the actuator data book. These values were found to be:

$$\frac{\Delta C_v}{\Delta rev} \cong 8.75\times10^{-4}\frac{C_v}{rev} \qquad \text{(Eq. 32)}$$

and

$$\frac{\Delta rev}{\Delta time} = 8rpm = 0.133\frac{rev}{\text{sec}} \qquad \text{(Eq. 33)}$$

Using these relations, a plot was created which shows the rate of change of molar flow rate as a function of upstream pressure for a critical pressure ratio (choked flow) with Nitrogen gas. This plot is shown below in Fig. 10 .

The most common conditions will be with the upstream pressure equal to 1000 psig and the flow choked through the valve so that the rate of change of molar flow rate will typically be about 3 SLM/sec as seen in the plot. This is somewhat slow in that making large changes in molar flow rate will require fairly long times, but the control around a setpoint should be more accurate for the same reasons. For the prototype, this should cause no problems so that the extra expense of changing the standard actuator would not be necessary.

2.5 Summary of Control Components

2.5.1 Mass Flow Meter

•Type	Resistive Thermal Detection Mass Flow Meter
•Manufacturer	Teledyne-Hastings Raydist
•Model Number	HFM-201
•Gas Type	Nitrogen (N_2)
•Flow Range	0-200 SLM (P_s = 1 atm., T_s = 0°C)
•Special	1500 psig proof testing

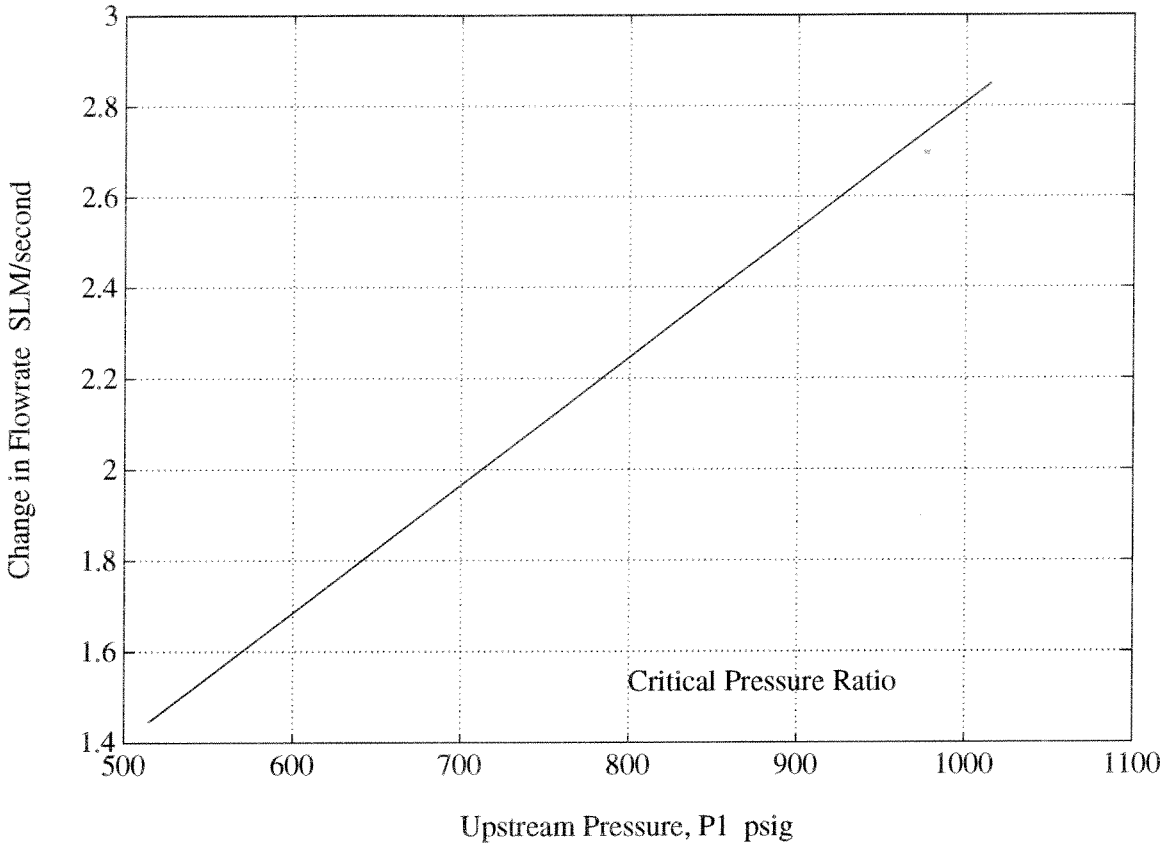

Figure 10. Rate of Change of Molar Flow Rate vs. Upstream Pressure

2.5.2 Control Valve

- Type — Micrometering Valve
- Manufacturer — Whitey
- Model Number — SS-21RS4
- C_v Factor — 0-0.007
- Orifice Size — 0.51 mm
- Pressure Rating — 3000 psig

2.5.3 Valve Actuator

- Type — Switched Servo-Motor With Driver Board

- Manufacturer ETI Systems Inc.
- Model Number Board: MC6501
- Voltage Input 0-5 Vdc
- Motor Speed 8 R.P.M.
- Motor Input Voltage 12 Volts maximum

2.5.4 Computer Hardware

- CPU Macintosh IIci
- A/D Board National Instruments NB-MIO-16
- Connector Board National Instruments SC-2070

2.5.5 Computer Software

- Type Labview 2
- Manufacturer National Instruments

CHAPTER 3 PROTOTYPE DYNAMIC MODELLING

Before the design of appropriate control laws could begin, the dynamic response characteristics of the control components needed to be determined. This was accomplished by a combination of theoretical and empirical approximations.

3.1 Description of Prototype Facility

A schematic of the prototype gas mixing system appears in Fig. 11 for reference

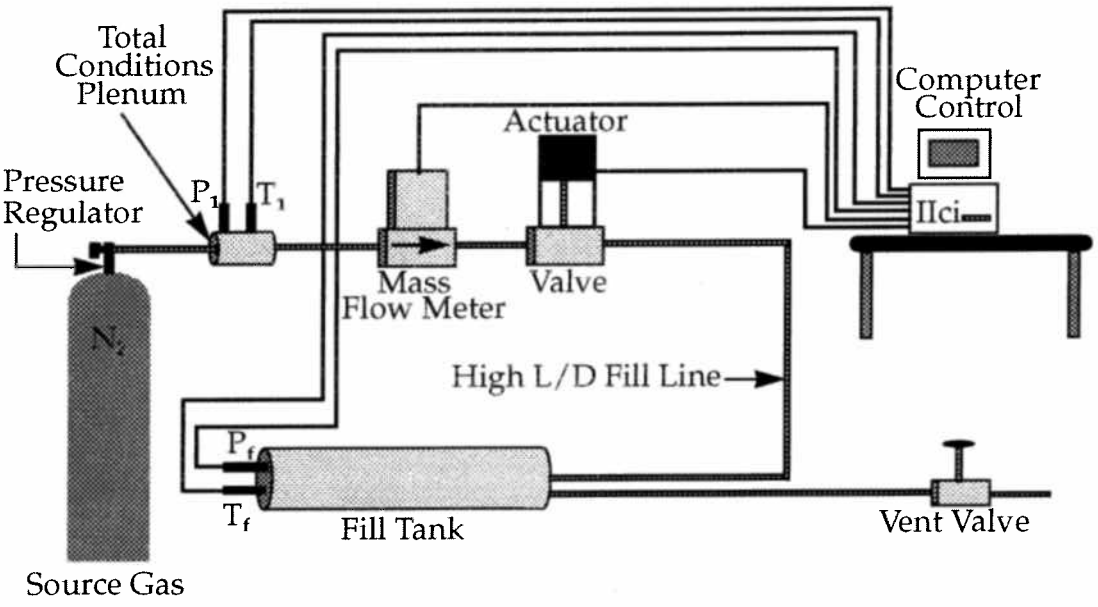

Figure 11. Prototype Control System Schematic

in the following description.

The prototype system has been created such that the flow conditions would closely approximate those of the actual Ram Accelerator fill system. In this way, problems with the controller due to fill system hardware could be discovered during the research phase. The source gas tank and the high pressure steel fill tubing are the same types which are currently used. The fill tank is an old section of a light gas gun driver and has a volume of 7 Liters which is almost exactly equal to 3 sections of Ram Tube. This size allows tests of actual Ram Accelerator conditions, and is large enough to give sufficient time when running other control

system experiments such as calibration of the flow meters.

The mass flow meter has been placed immediately upstream of the control valve. In this way, the meter and valve can be kept close together and compact and the turbulence added to the flow by the valve will not affect the meter. Additionally, having the meter upstream of the valve keeps the pressure of the gas flowing through the meter roughly constant which will increase the precision of the flow meter measurements.

The vent valve has been equipped with a back pressure regulator to ensure that the gas pressure exiting through the vent line cannot exceed the rated vent line pressure. By opening up the vent line during a flow process, the time for which gases can be flowed is greatly extended, indefinitely in the case of low flow rates.

In the laboratory, the valve and flow meter are encased within a steel 19" equipment rack which also houses the Macintosh CPU and has a front panel where all of the necessary electronic connections can be made. A really bad photograph of the entire flow system appears below in Fig. 12.

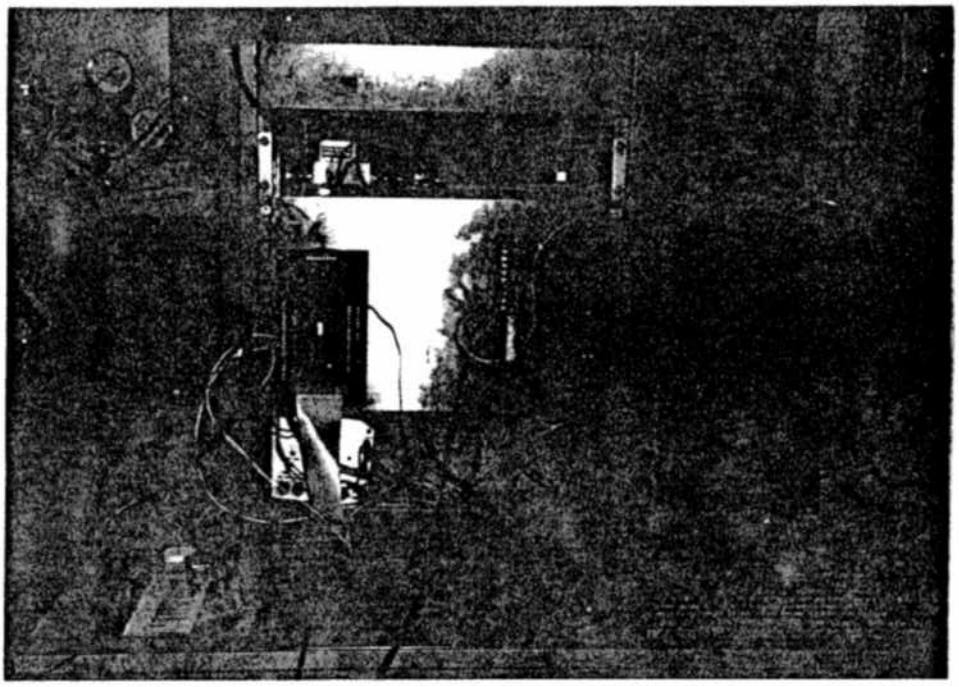

Figure 12. Photograph of Prototype Gas Mixing System

3.2 Modelling the Mass Flow Meter

3.2.1 Dynamic Response Measurements

The time response of the mass flow meter turned out to be very well behaved and could be modelled as a simple first order lag. This was accomplished by creating a either a step increase or a step decrease in the mass flow rate and then measuring the decay constant. By performing these measurements several times and for several different flow conditions, the resulting decay constants could be fit in a least squares sense to find the best fit to the data.

The step inputs in flow rate were achieved by temporarily replacing the actuated valve with a manual turn valve that could be very quickly opened by hand. The flow was either begun at some initial value when the valve would be quickly opened, or would be quickly closed. The resulting flow rates were then normalized to a standard value of unity so the results could be compared. A plot of the experimental data along with the least squares model curve are shown here in Fig. 13 . As shown on the plot, the transfer function for the flow meter has been determined to be

$$\frac{\dot{M}_m(s)}{\dot{M}(s)} = \frac{5.85\times10^{-3}}{(s+0.2339)}\frac{volts}{SLM} \qquad \text{(Eq. 34)}$$

with a conversion factor of $0.025\,(V/SLM)$ included since the output of the meter is in volts, and the mass flow rate is treated in SLM. The programs used to perform the least squares fitting are called metertf.m and foexpfit.m and they appear in Appendices A.8 and A.9 respectively. The data used for the computations then appear in Appendices A.10 to A.15.

3.2.2 Preliminary Calibrations

The flow meter was delivered with a calibration for 200 SLM of Nitrogen at 500 psig inlet pressure and a temperature of 295 K. Since the flow would be commonly run at 1000 psig, a preliminary calibration was performed to assure that the flow reading was accurate enough for a control law to be successfully developed. Once a working flow rate controller was developed, the controller itself could be used to calibrate the meter which will be demonstrated later in section.

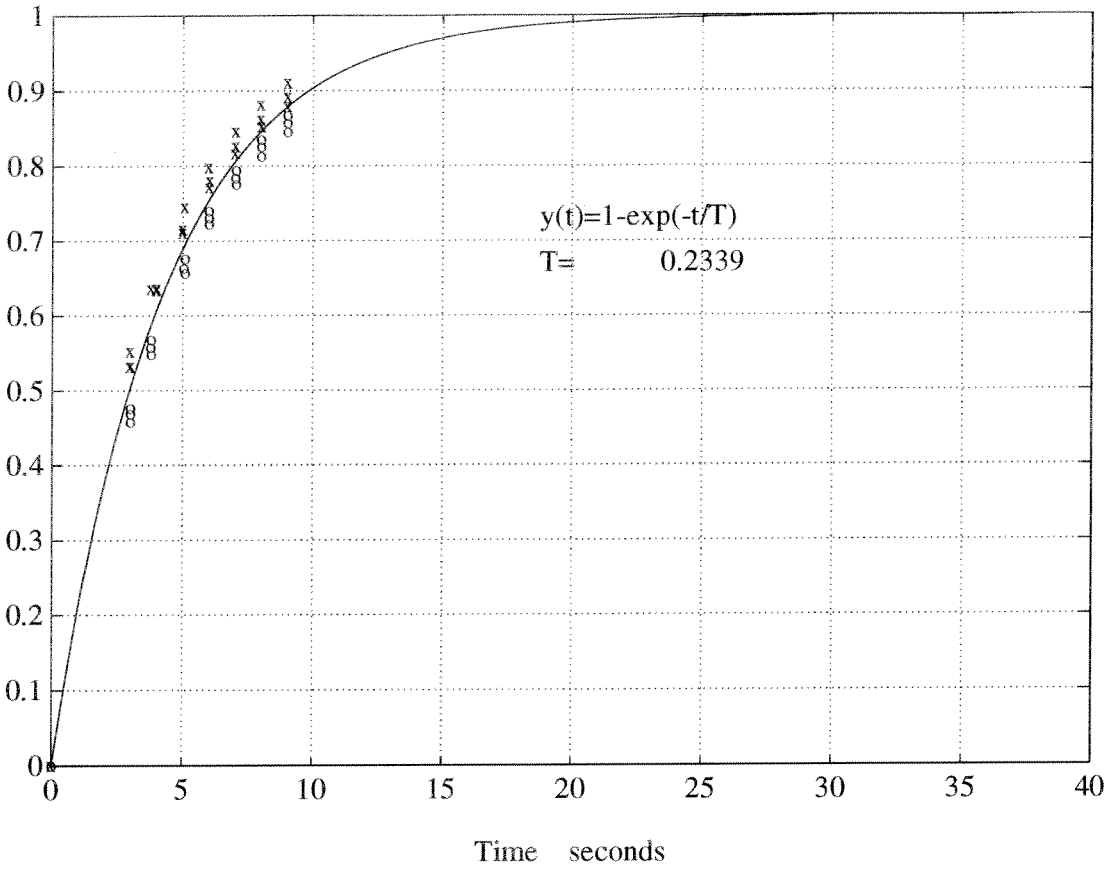

Figure 13. Empirical Determination of Mass Flow Meter Model

The preliminary calibration was performed by flowing the gas under choked conditions and comparing the flow meter reading to readings of dp/dt in the fill tank. The temperature was also monitored to make sure there was no significant change which would alter the flow rate readings. A program to perform the necessary functions was written into LabView and run for several different flow rates.

3.3 Control Valve and Actuator

The control valve was known to have a linear relationship between the C_v factor and the number of revolutions of the valve stem from the valve data book. Also, the motor speed of the actuator was expected to be a constant value, either

positive or negative depending upon the input to the motor. The mathematical model to be used for the valve would be the following:

$$\frac{dC_v}{dt} = \pm K_v \qquad \text{(Eq. 35)}$$

where the sign is dependent upon the sign of the input voltage to the actuator.

An equation can easily be written for K_v in terms of measurable quantities in the following way,

$$K_v = \dot{R}_n \frac{\Delta(C_v)}{\Delta(R_n)} \qquad \text{(Eq. 36)}$$

where R_n is the number of revolutions of the valve stem. These quantities will now be obtained.

The $\Delta(C_v)/\Delta(R_n)$ term can easily be obtained from the plot of C_v factor vs. number of valve stem revolutions which is reproduced here from the Whitey data book as Fig. 14. Now, if the number of revolutions of the valve stem per unit time can be measured, this can be combined with the data from Fig. 14 to give K_v as defined above in Eq. 36. An experiment was set up to obtain number of revolutions per unit time data which appears in the table below.. The value for K_v can now be obtained as:

$$K_v = (0.12608 \frac{rev}{\text{sec}}) \left(9.333 \times 10^{-4} \frac{C_v}{rev} \right) = 1.177 \times 10^{-4} \frac{C_v}{\text{sec}} \qquad \text{(Eq. 37)}$$

This completes the mathematical modelling of the valve and actuator. This model is nonlinear, however, due to the switching nature of the valve, so conversion to a transfer function will not be done until a linearization is made later in this chapter.

3.4 Flow Rate Dynamics

Measuring rapid fluctuations in mass flow rate is quite difficult, and was not possible with the equipment available. Theory is not of much help because determining unsteady flow characteristics in pipes is extremely difficult and is highly dependent upon system hardware configurations. The relationships for

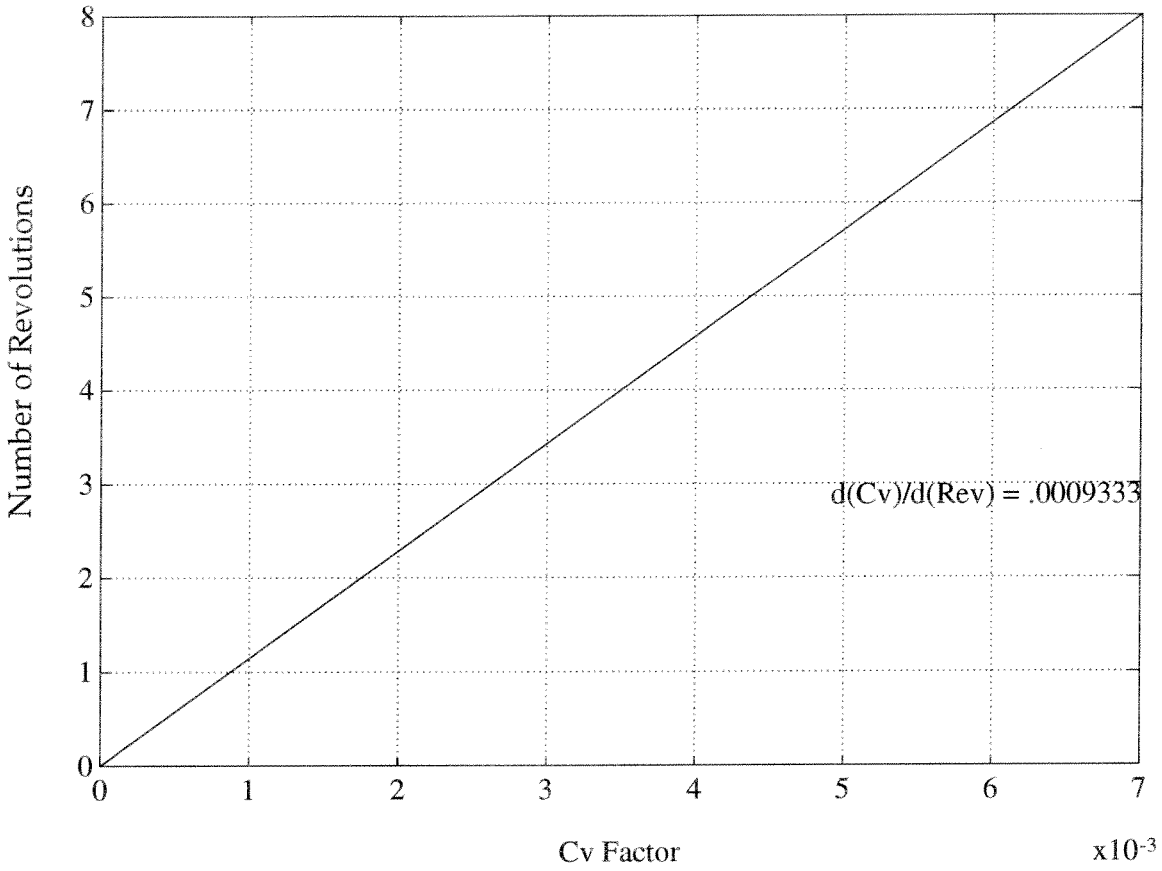

Figure 14. Cv Factor vs. Revolutions of Valve Stem for Whitey SS-21RS4

mass flow rate are generally nonlinear partial differential equations which are not compatible with linear control theory.

A qualitative look at the fluctuation of the mass flow rate with changes in the valve orifice opening showed that whatever higher order flow effects are happening are not measurable with the RTD mass flow meter so that quantitatively identifying these higher order effects would neither be possible, nor necessary for this control system. A theoretical justification can be made for neglecting the higher order flow dynamics by noting that if pressure related disturbances propagate through the system at the sound speed of the gas, which is roughly 350 m/s through most of the fill tube, then for a length of fill tube of 10 meters, the disturbances would propagate through the tube in about 0.03 seconds.

Modelling the flow rate dynamics can be done theoretically simply by

Table 8: Data For Speed of Revolution of the Control Valve

# of Revolutions	Seconds
1	7.97
1	7.96
2	15.63
2	15.8
3	23.72
3	23.80
4	31.83
4	31.54
5	40.07
6	47.87

rearranging Eq. 12 of section 2.3.2 to obtain:

$$\dot{M}_{SLM} = K_{cf} C_v K_{cv} P_1 \left[\left(\frac{P_v}{P_1} \right)^{2/\gamma} - \left(\frac{P_v}{P_1} \right)^{(\gamma+1)/\gamma} \right]^{1/2} \qquad \text{(Eq. 38)}$$

where K_{cf} was previously determined to be:

$$K_{cf} = 1315.74 \sqrt{\frac{\gamma}{MW\,(\gamma-1)}} \qquad \text{(Eq. 39)}$$

The value for K_{cv} was also estimated from the valve data books, but in order to tie Eq. 38 to reality, a new value can be empirically determined by opening the valve to a known value of C_v and setting known values of P_1 and P_v/P_1 and then measuring the mass flow rate.

The easiest experiment to perform is to set P_1 high enough that choking will occur so that P_v/P_1 will be the critical value, and then turning the valve stem through a known number of revolutions and using Fig. 14 to obtain the C_v factor. After flow transients have passed, the mass flow rate can be read from the mass flow meter. Eq. 38 can then be solved for K_{cv}. This was done at three different flow

rate settings and a least squares method was used to find the value of K_{cv} that best fit the data. A table of the results is presented here:

Table 9: Experimental Measurements of Molar Flow Rate

C_v	$\dot{M}_{volts}$	$\dot{M}_{SLM}$
9.33×10^{-4}	1.53	61.2
1.867×10^{-3}	2.815	112.6
2.8×10^{-3}	4.06	162.4

These measurements led to the following value for K_{cv}:

$$K_{cv} = 7.1475\times10^{-5} \qquad \text{(Eq. 40)}$$

Using the values determined here for the constants, Eq. 38 constitutes the mathematical model for the mass flow rate dynamics through the mixing system. This, too, is a nonlinear model since the pressure terms are generally functions of time. Turning this expression into a linear model so that control methods may be more easily applied will be done in the next section.

3.5 Linearization of Control System Models

Standard control theory is applicable only to linear mathematical models. Since most real systems are best modelled by nonlinear functions, assumptions must be made which linearize the equations in the most accurate way possible so that control laws may be designed.

The mass flow meter has already been modelled as a linear differential equation so that further linearization will not be necessary. At the end of this section in a summary of the linear control model for the gas mixing control system, the model for the flow meter will be repeated. In the next two sections, the linearization of the valve/actuator and the flow rate dynamics will be shown.

3.5.1 Valve/Actuator

As mentioned earlier, the switching action of the electronic conditioning board caused the valve/actuator model to be nonlinear. The actual model of the valve can be represented as shown in Fig. 15. What this means is that whether the input

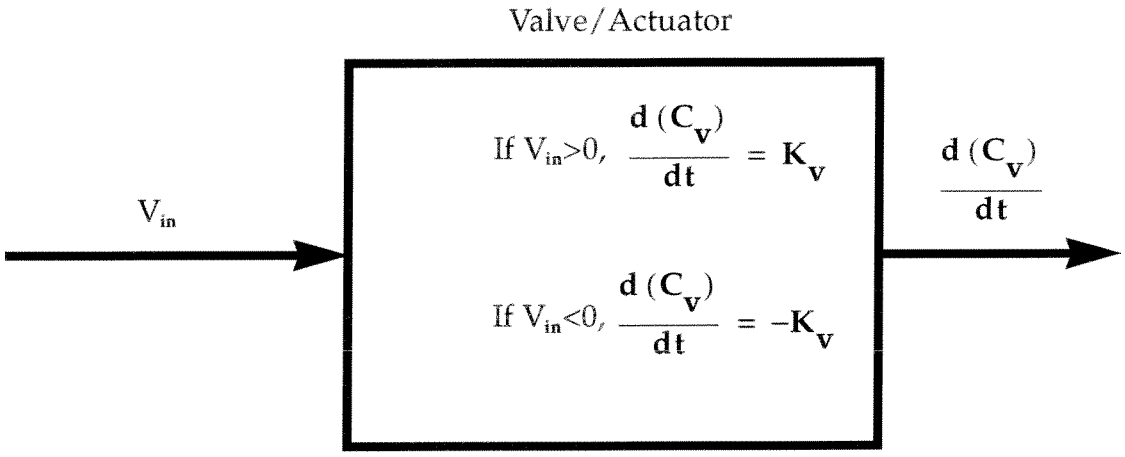

Figure 15. Valve & Actuator Model

voltage is 1 Volt, or 1000 Volts, the rate that the motor turns at is constant. If this behavior is modelled as a gain multiplied by the input voltage, then, in effect, this gain is a function of the input such that the output is kept constant.

When modelled as a gain, then, the gain value will have a range depending upon the maximum and minimum values of the input voltage. The range can be determined by applying the following equation to the minimum and maximum voltage values:

$$Gain = \left| \frac{K_v}{V_{in}} \right| \qquad \text{(Eq. 41)}$$

When the voltage to the valve actuator falls within the range of ±0.02 Volts, the actuator automatically shuts off so that steady state flow control may be maintained without constant small adjustments of the valve position. This sets the *minimum* voltage that will be sent to the actuator which therefore sets the *maximum* gain value for the valve actuator linear model. The minimum value will be different for the flow rate controller and the flow ratio controller. The input voltage to the valve/actuator will be the error voltage generated between the command

voltage input and the feedback signal from the flow meter. The commanded voltage will never be higher than 5 Volts since this corresponds to the maximum flow rate that the flow meter can safely measure, and the flow meter can never measure lower than 5 Volts. Therefore, the maximum input voltage to the actuator for the rate controller will be 5 Volts. The input voltage to the actuator in the flow ratio controller will be the integral of the error signal for the flow rate controller since in this case, the actual mass flow error is to be driven to zero. As a conservative worst case estimate, suppose that the valve somehow sticks shut for a few seconds after the controller has first been turned on so the reading of the secondary mass flow meter is 0 Volts, and that the primary gas with which the ratio is to be controlled has been flowing at the full 5 Volts. The integral error would then be 25 Volt-seconds. In such a case, an error would likely be reported to the operator and the system could be shut down until the problem could be resolved, but using this value as a worst case estimate allows us to have a minum gain value to use when designing the flow ratio controller. With the discussion in this paragraph, Eq. 41, and the value of K_v from Eq. 37, a table of gain ranges for the linearized valve/actuator dynamic model has been compiled below. The transfer

Table 10: Gain Range for the Valve/Actuator Linear Model

Controller Type	Maximum Gain	Minimum Gain
Mass Flow Rate	5.885×10^{-3}	2.354×10^{-5}
Mass Ratio	5.885×10^{-3}	4.708×10^{-6}

function is, therefore, just a simple gain which is bounded by the values found in Table 10.

3.5.2 Flow Dynamics

The nonlinearity in the flow dynamics arises from the fact that the pressures in the system do not generally remain constant. During most of the operation of the controllers, the pressures will be constant since the pressure ratio will usually be

below the critical value so that the orifice will be choked, and the upstream pressure will be kept constant by a regulator. In order for this control system to operate in an optimal manner for a wider range of flow conditions, however, the case where the orifice becomes unchoked must also be accounted for.

The variation in pressures only becomes a problem when the upstream pressure becomes nearly equal to the pressure in the tank being filled at which point the valve will have opened to its largest position. Since the upstream pressure will be regulated down to 1000 psig for most of the life of the source gas bottles and the required fill pressure for the Ram Accelerator will never be greater than 750 psig due to safety considerations, these conditions will not pose a problem. However, when the source gas bottle pressure falls below 1000 psig, checks must be made to ensure that the source gas pressure and the fill tube pressure will not become too nearly equal during the course of a fill. If so, the source gas bottle must be changed. The computations to determine whether or not a gas bottle must be changed may be easily performed on the control system computer as long as the pressure and temperature of both the source gas and the gas in the fill tanks are monitored in real time.

Since the rate of pressure variation will not be too large, the flow dynamics equation may be linearized in the same way as were the valve/actuator dynamics. The transfer function will become merely a gain, called K_{fd}, which can vary between a minimum and maximum limit.

The upper gain limit, easily determined by the use of Eq. 38, will occur when the valve is choked, the upstream pressure is at the maximum value of 1000 psig, and the flow rate is a maximum (200 SLM). The minimum gain is slightly more difficult to find, but can be computed with the help of the *maxvalve.m* (Appendix A.4) program that was used for sizing the control valve. By running the program for the case where P_f is a minimum, typically about 400 psig for the Ram Accelerator, and where the flow rate is a minimum, about 50 SLM for Nitrogen (see Table 3), the values of P_1 and P_v corresponding to the maximum C_v factor for the valve (0.007) are the conditions where the maximum gain will occur. The computations have been performed as described here and appear in Table 11. The gain limits in the table are only valid for Nitrogen since the computations are dependent upon γ and the molecular weight of the gas. The gain limits are also specific to this particular control system since the value for K_{cv} from Eq. 38 has

Table 11: Flow Dynamics Gain Limits for Nitrogen Gas

Limit	K_{cv}	K_{cf}	P_{t_1} MPa	P_vMPa	$\dot{M}_{SLM}$	K_{fd}
High	7.1475×10^{-5}	465.18	6.97	3.68	200	60×10^{3}
Low	7.1475×10^{-5}	465.18	3.92	3.88	50	7×10^{3}

been empirically determined (section 3.4) for this system.

3.5.3 Summary of Linearized Control Component Transfer Functions

The flow meter transfer function has been determined to be:

$$\frac{\dot{M}_m(s)}{\dot{M}(s)} = \frac{5.85\times10^{-3}}{(s+0.2339)}\frac{volts}{SLM} \qquad \text{(Eq. 42)}$$

The valve/actuator transfer function is given by:

$$\frac{C_v(s)}{V_e(s)} = \frac{K_v}{s} \qquad \text{(Eq. 43)}$$

with the ranges of K_v given in Table 10 for both the flow rate and the flow ratio controllers.

Finally, the flow dynamics transfer function has been determined to be:

$$\frac{\dot{M}(s)}{C_v(s)} = K_{fd} \qquad \text{(Eq. 44)}$$

where the term K_{fd} is defined by the limits given in Table 11.

CHAPTER 4 MASS FLOW RATE CONTROL LAW DESIGN

As mentioned in the introduction, the control method would be to set the flow rate of a primary gas constant by use of a flow rate controller, and then to use ratio controllers on the rest of the gases in order to keep the total mass flow ratios at the desired levels. This chapter details the development of the control law which is to keep the flow rate of the primary gas at a constant level.

The basic design method is to first develop linear control laws using well-known linear control system analysis. After some preliminary control law structures have been developed in this way, a nonlinear simulation may be employed which more accurately models the real system behavior so the controller designs may be validated before being implemented in the lab.

4.1 Linear System Analysis

The transfer functions for all of the hardware components have been determined in the previous chapter. These must now be compiled into a full system transfer function so that linear analysis may be applied. In Fig. 16 is a block

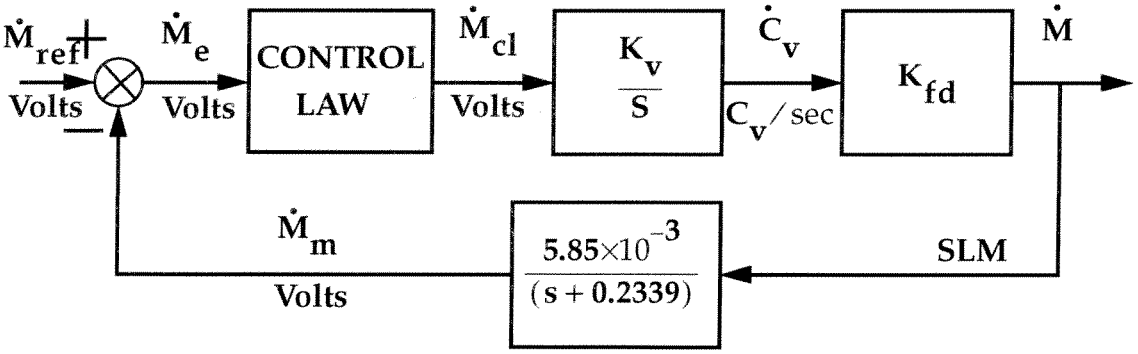

Figure 16. Block Diagram of Mass Flow Rate Control System

diagram of the linearized control model that has been used for control law design.

The first step in the design is to have a look at a root locus plot for the system with a simple constant gain control law to see what type of dynamic control might

be helpful. As developed in Chapter 3, the effective system gain will be within a range that depends upon the error term and the system pressures. By multiplying the appropriate K_v and K_{fd} values from Tables 10 and 11 together, the range of the effective system gain, K_{eff}, can easily be calculated (Table 12) .

Table 12: Effective Flow Rate Control System Gain

Limit	K_v	K_{fd}	K_{eff}
Maximum	5.885×10^{-3}	60×10^{3}	353.1
Minimum	2.354×10^{-5}	7×10^{3}	.165

Root locus is then to be performed for the following open loop system transfer function:

$$G_{ol}(s) = K_{eff} \cdot \frac{5.85\times10^{-3}}{s\,(s+0.2339)} \qquad \text{(Eq. 45)}$$

The root locus plot in Fig. 17 was formed using Eq. 45 and varying K_{eff} over the range specified in Table 12 and shows that a simple constant gain control law will provide stable control, but that the time response will be oscillatory due to the imaginary roots. Physically, what happens is that the actual mass flow rate will surpass the setpoint value before the flow meter reading catches up so that by the time the error signal has gone to zero, the flow rate is too high. This suggests that a control law with first order dynamics that could account for the delay in the flow meter reading might work well. This could be accomplished by mathematically cancelling the pole of the mass flow meter dynamics with a zero at the same location.

The transfer function model for a first order control law is given by:

$$\frac{\dot{M}_{cl}(S)}{\dot{M}_{e}(S)} = \frac{K_{cl}(S+Z)}{(S+P)} \qquad \text{(Eq. 46)}$$

The zero term will be used to mathematically cancel the relatively slow exponential decay term of the mass flow meter. The pole is then used to attenuate

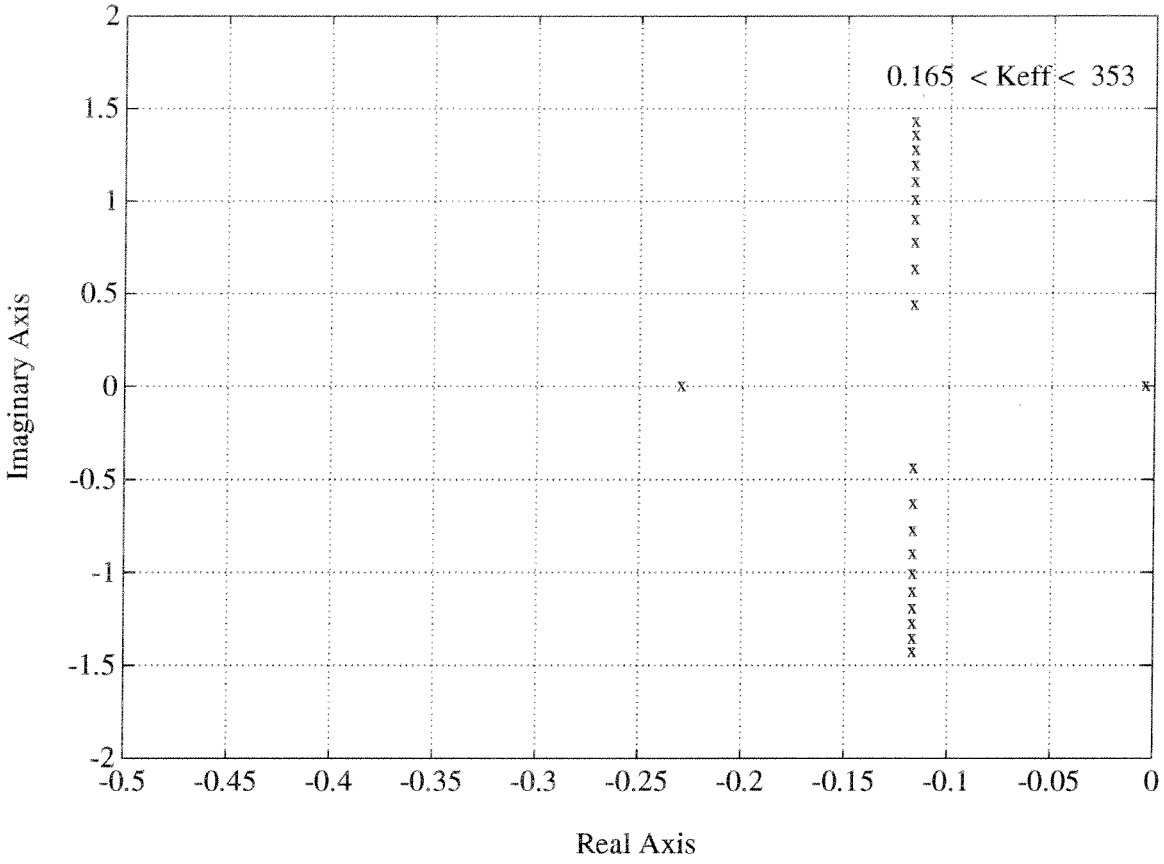

Figure 17. Root Locus -- Constant Gain Mass Flow Rate Controller

higher frequency system noise. The gain term, however, is not available as a design parameter in the usual way due to the switching action of the control valve. The dynamics of the control law and the input to the control law will determine the sign of the input to the valve actuator, and the gain will then only have a scaling effect. Since the actuator motor will then either open or close at the same rate regardless of the actual value of the input voltage, the control law gain will be hidden, and will have no real effect upon the system dynamics. The gain of the control law can, however, be used to adjust the accuracy limits of the control system as will now be discussed.

Since the valve actuator has a dead-zone between ±0.02 Volts, if the input to the actuator drops within this range, the control system will be in steady state. This should not happen until the flow has been set to within a desired percent of the

flow rate reference. An expression can be easily determined to compute the required control law gain to set the steady state percent error to a desired value.

An expression for the steady state error in terms of percent error is given by

$$\dot{M}_e = [\dot{M}_{ref} - \dot{M}_m] = \dot{M}_{ref}\left[1 - \frac{\dot{M}_m}{\dot{M}_{ref}}\right] \qquad \text{(Eq. 47)}$$

The term in brackets represents the percent error, E_p, between the measured mass flow rate and the reference command flow rate so we can write

$$\dot{M}_e = \dot{M}_{ref} E_p \qquad \text{(Eq. 48)}$$

The steady state gain is given by applying Eq. 46 when s goes to zero, and this leads to:

$$K_{ss} = \frac{K_{cl} Z}{P} \qquad \text{(Eq. 49)}$$

When the steady state gain is multiplied by the desired minimum steady state error term, the result should equal 0.02 Volts or greater so the valve actuator is still actively controlling the flow to this point. Multiplying Eqs. 48 and 49 and solving for K_{cl} gives

$$K_{cl} = \frac{(0.02)\, P}{Z \cdot \dot{M}_{ref}(E_p)} \qquad \text{(Eq. 50)}$$

This equation can be easily programmed on-line to allow the user of the controller to set the desired flow accuracy. At the same time, a check can be made to ensure that the voltage sent to the valve actuator driver board never exceeds ±5 Volts so the circuitry is not damaged. This will not affect the operation of the control system at all since the speed of the actuator motor is only dependent upon the sign of the input voltage, not the actual value.

Root locus plots may now be created for the following system model with the first order control law dynamics added:

$$G_{ol} = K_{eff} \cdot \frac{5.85\times10^{-3}\,(s+Z)}{s\,(s+0.2339)\,(s+P)} \qquad \text{(Eq. 51)}$$

Table 13 below will be helpful in determining which control parameters

Table 13: Root Locus Parameters -- First Order Flow Rate Controller

Figure #	Z	P
18	0.2339	1
19	0.2339	2.9
20	0.26	17.25
21	0.22	2.9

correspond to which root locus plot in the following discussion. Note that the gain term of the controller, K_{cl}, is not included here for the reasons mentioned earlier.

In the first plot (Fig. 18), the pole has been placed too close to the origin so that the pole from the origin comes out and pairs with the controller pole and causes imaginary roots to form at the higher gain values. Several quick iterations were performed to find the pole value at which imaginary roots were not formed for the entire gain range. This turned out to be at about $P = 2.9$ and the resulting root locus is shown in Fig. 19.

Since the model for the system can never be mathematically exact, the controller zero will never exactly cancel the pole of the flow meter. Root locus plots have been formed for the cases where the zero is at about ±10% of the expected flow meter pole value. At these points, iterations were performed to find the controller pole values for which imaginary roots never formed. The resulting values are given in Table 13 and the plots are shown in Figures 20 and 21. The values shown in these plots do not necessarily yield the best time responses, however. By moving the controller pole far enough away to keep the system from having oscillations, some response speed is sacrificed. This becomes more apparent in the nonlinear time simulation.

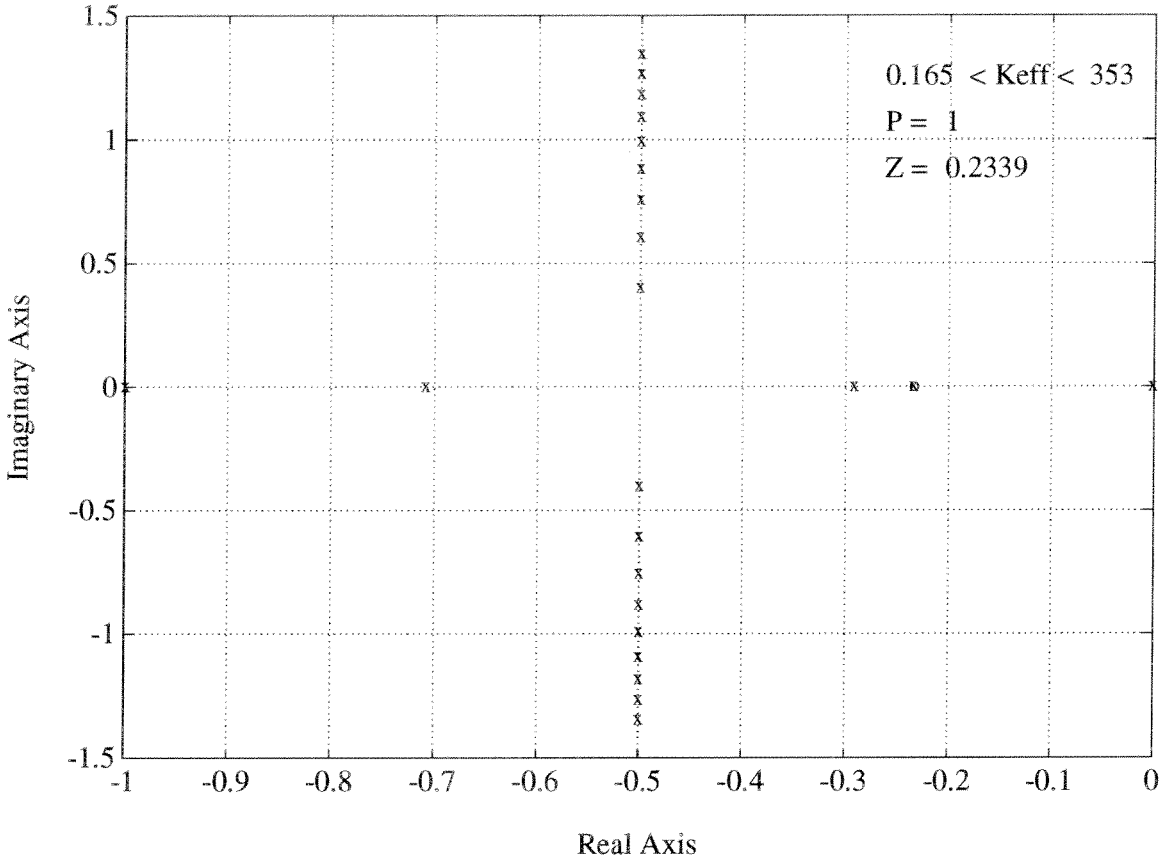

Figure 18. Root Locus -- First Order Mass Flow Rate Controller

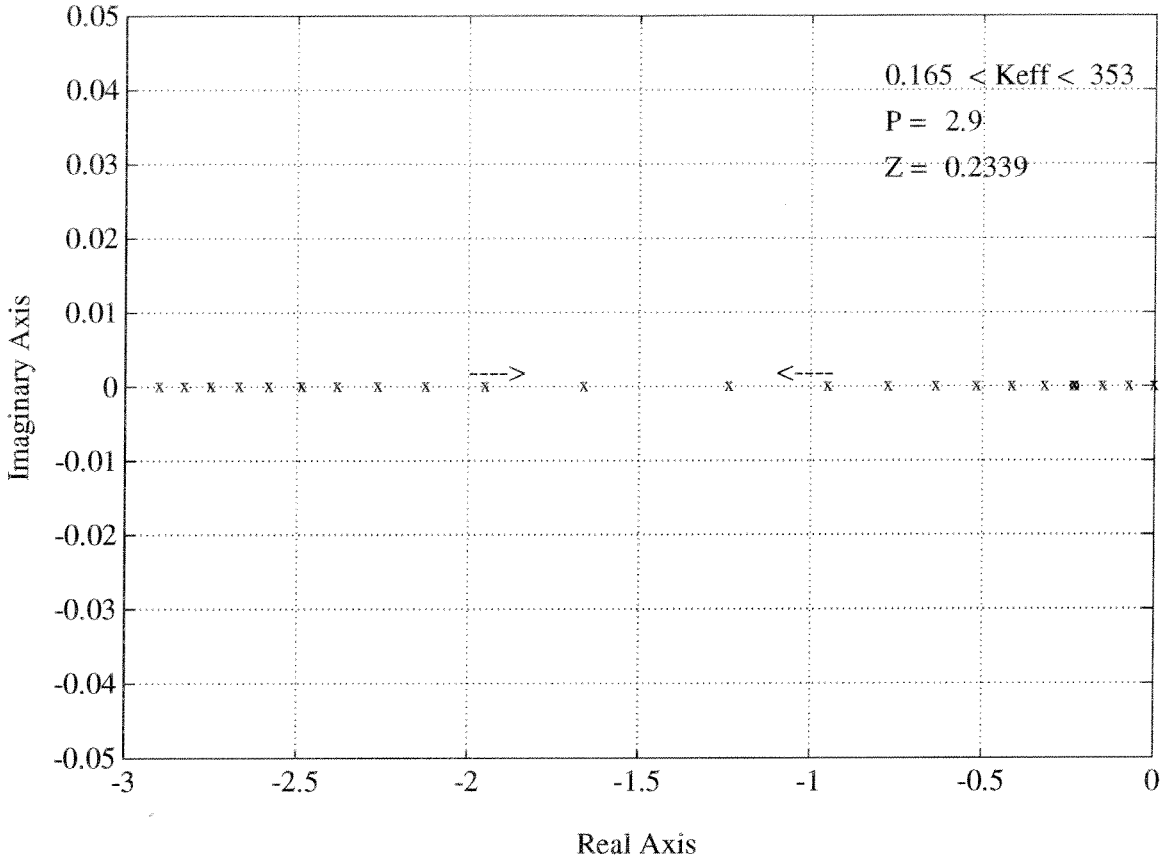

Figure 19. Root Locus -- First Order Mass Flow Rate Controller

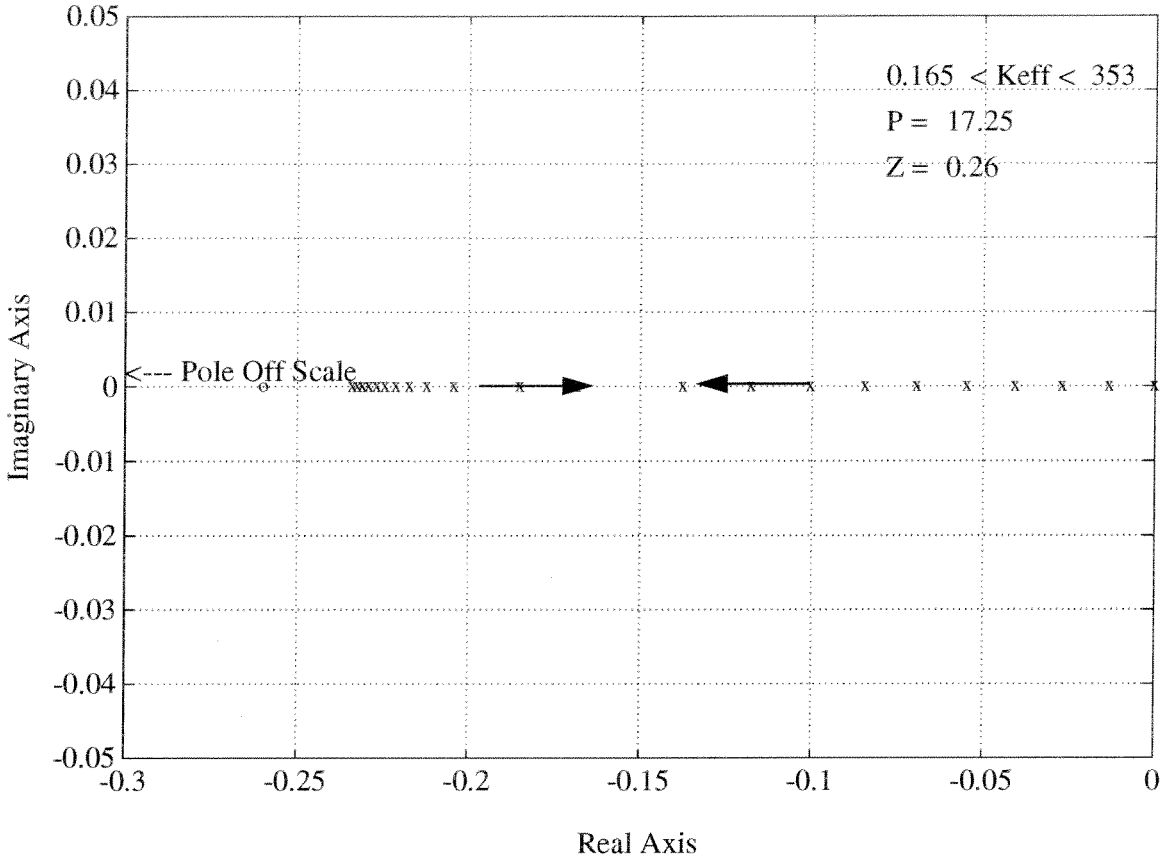

Figure 20. Root Locus -- First Order Mass Flow Rate Controller

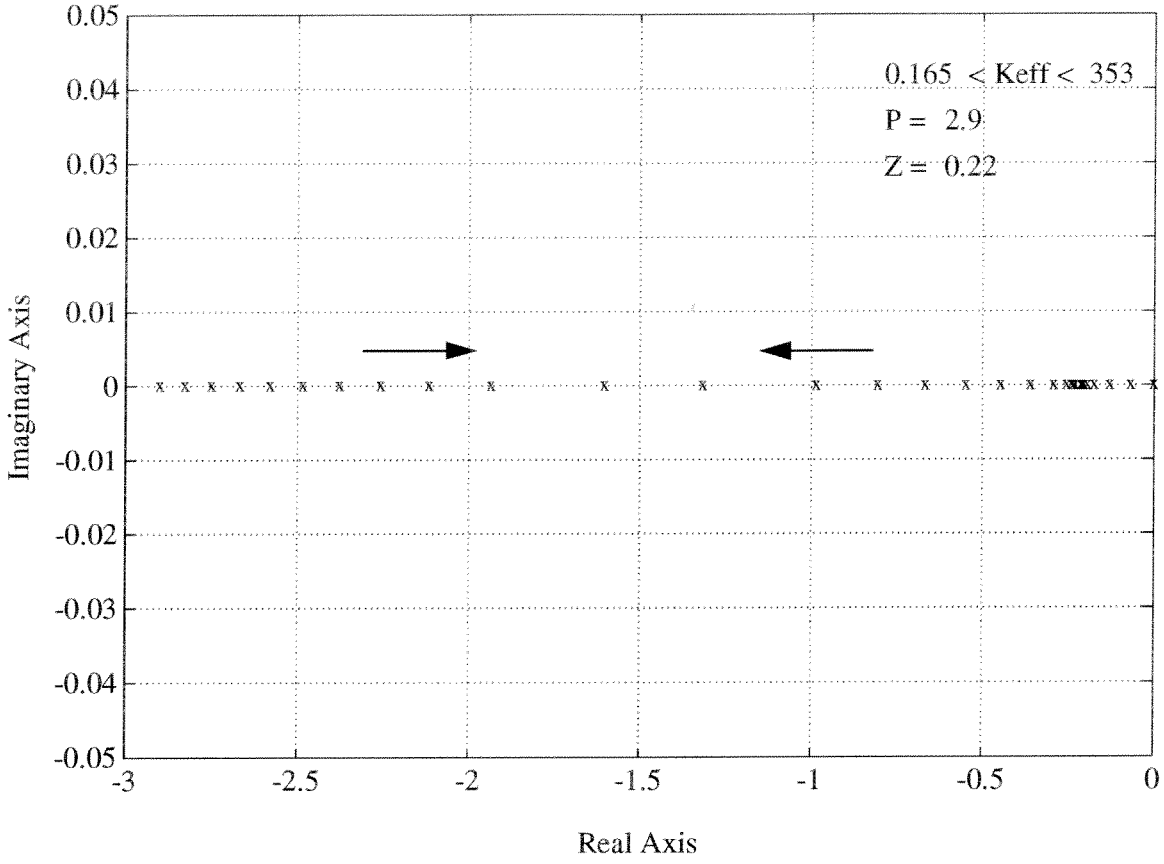

Figure 21. Root Locus -- First Order Mass Flow Rate Controller

4.2 Nonlinear Simulation of Mass Flow Rate Controller

The Simulab graphical programming interface from Mathworks provides a very convenient means of programming relatively complex nonlinear time simulations and is able to take full advantage of the convenient control system and output subroutines of Matlab, also from Mathworks. This was the software package used for the analysis in this section though many others may also have been used with similar results. With Simulab, familiar block diagrams may be drawn on the computer, compiled into the corresponding nonlinear time differential equations, and then solved by any of several numerical routines ranging from a simple Euler integration to a fifth order Runge-Kutta routine.

The Simulab graphical program and the corresponding Matlab code used to perform the calculations called *nlrateth.fig* and *nlrateth.m* are given in Appendices A.16 and A.17 respectively. This simulation takes into account the switching action of the valve as well as the voltage dead-zone for ±0.02 Volts. The gain term is also adjustable to allow the user to specify the desired steady state accuracy of the control system as specified in Eq. 50. The programming required to model the variable pressures in the flow system is fairly involved, and would cause the simulation to run quite slowly and is therefore not included in the simulation. The user is, however, able to specify the upstream pressure and the pressure ratio as constant values so that the control laws may be verified over the entire range of possible system gain values as given in Table 12. For the evaluation of the linear control laws from the previous section, the same step input of 2.5 Volts will be used which corresponds to a command of 100 SLM of Nitrogen. The simulation programs are currently set up for the simulation of flowing Nitrogen gas, but only minor changes are necessary to simulate the flow of a different gas.

For help in identifying the quantities used in the simulations that appear in the figures that follow, Table 14 has been compiled.

The first two simulations (Figures 22 and 23) show the response of the system to step input commands for both the maximum and minimum possible system gain configurations. The maximum gain occurs when the upstream pressure is at 1000 psig and the flow through the valve is choked, and the minimum gain occurs when the upstream pressure is at about 900 psig and the pressure ratio is 0.98. The conditions for the minimum gain were determined by running *maxvalve.m*

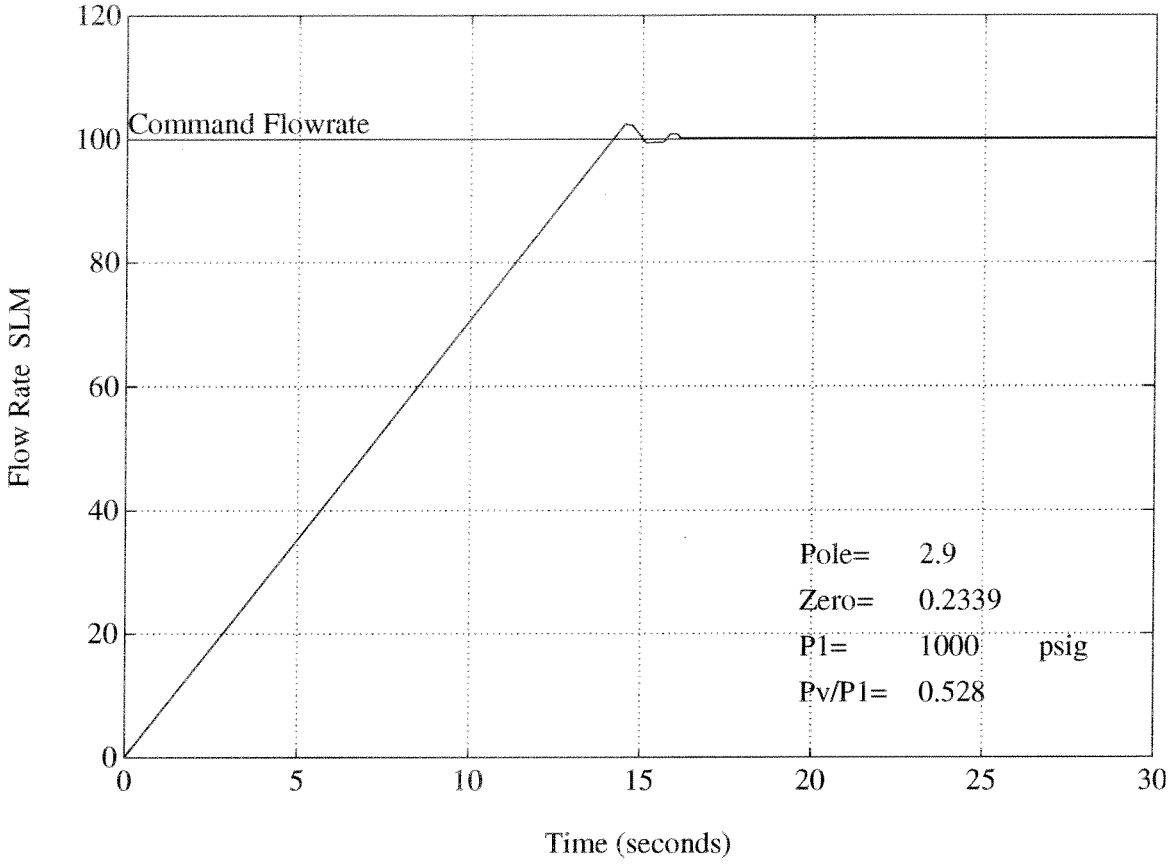

Figure 22. Nonlinear Simulation of Mass Flow Rate Controller at Maximum Gain

Table 14: Key to Nonlinear Simulation Figures

Figure #	Z	P	P_1 psig
22	0.2339	2.9	1000
23	0.2339	2.9	900
24	0.2339	10	1000
25	0.26	10	1000

(Appendix A.4) for the case where the Ram tube fill pressure is 400 psig and finding the corresponding upstream pressure which gives the prescribed flow rate

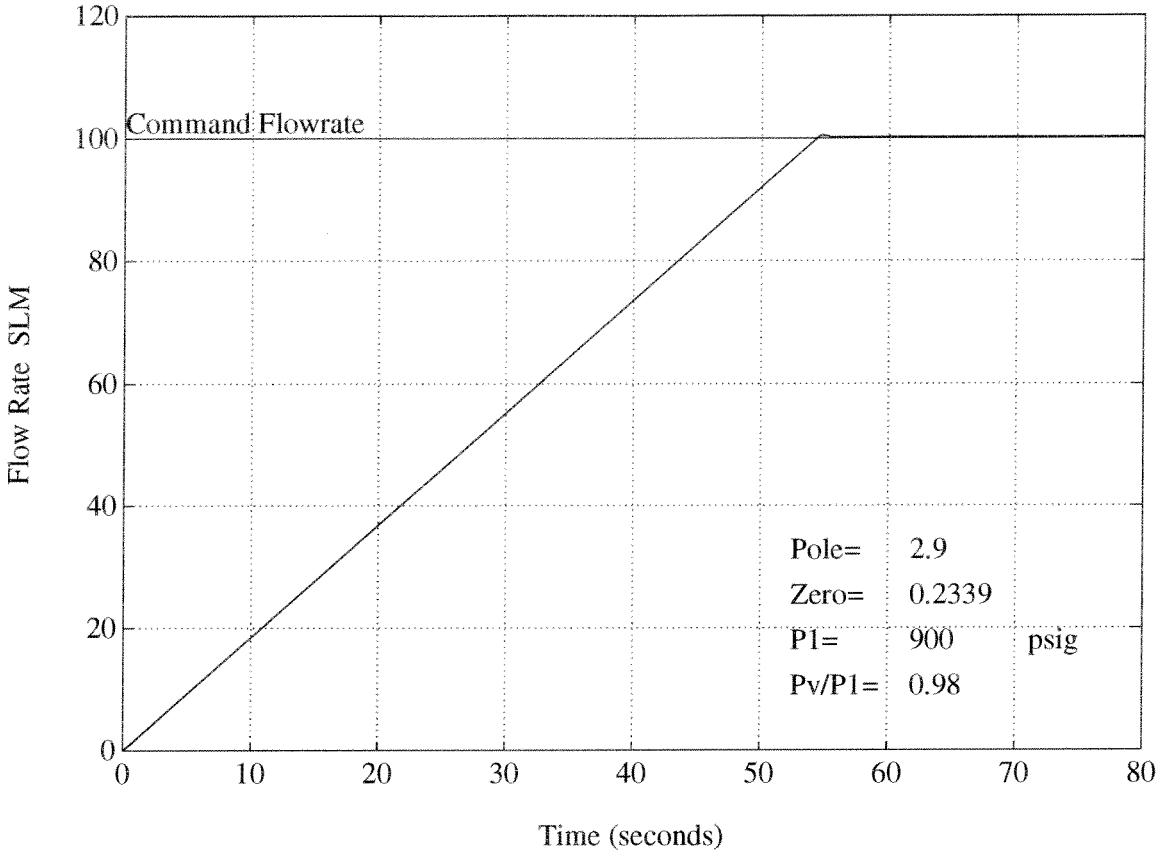

Figure 23. Nonlinear Simulation of Mass Flow Rate Controller at Minimum Gain

of 100 SLM at the maximum C_v factor of 0.007. These are the limiting conditions for which the prototype system can achieve a mass flow rate of 100 SLM. Notice that the time required for the flow rate to reach 100 SLM is much longer in the minimum gain case as would be expected. Also notice the slight overshoot in the maximum gain case. The corresponding root locus plot (Fig. 19) shows that the linear system should not have any overshoot, so the overshoot must be a result of the system's nonlinearities. The nonlinear simulation is also set up to make plots of the C_v factor of the valve vs. time which allowed a check to see that the C_v factor did not exceed 0.007.

A few iterations were attempted to try and limit or remove altogether the overshoot at the maximum gain level. For on-design conditions when the flow meter pole was exactly cancelled, by moving the pole further out along the

negative real axis, the overshoot could be eliminated. Since noise elimination might become an issue in the implementation of the controller by moving the pole too far along the real axis, a search was made to find the minimum pole value which would still keep the overshoot to about one percent of the setpoint mass flow rate. For a pole value at P = 10, the simulation (Fig. 24) shows that the

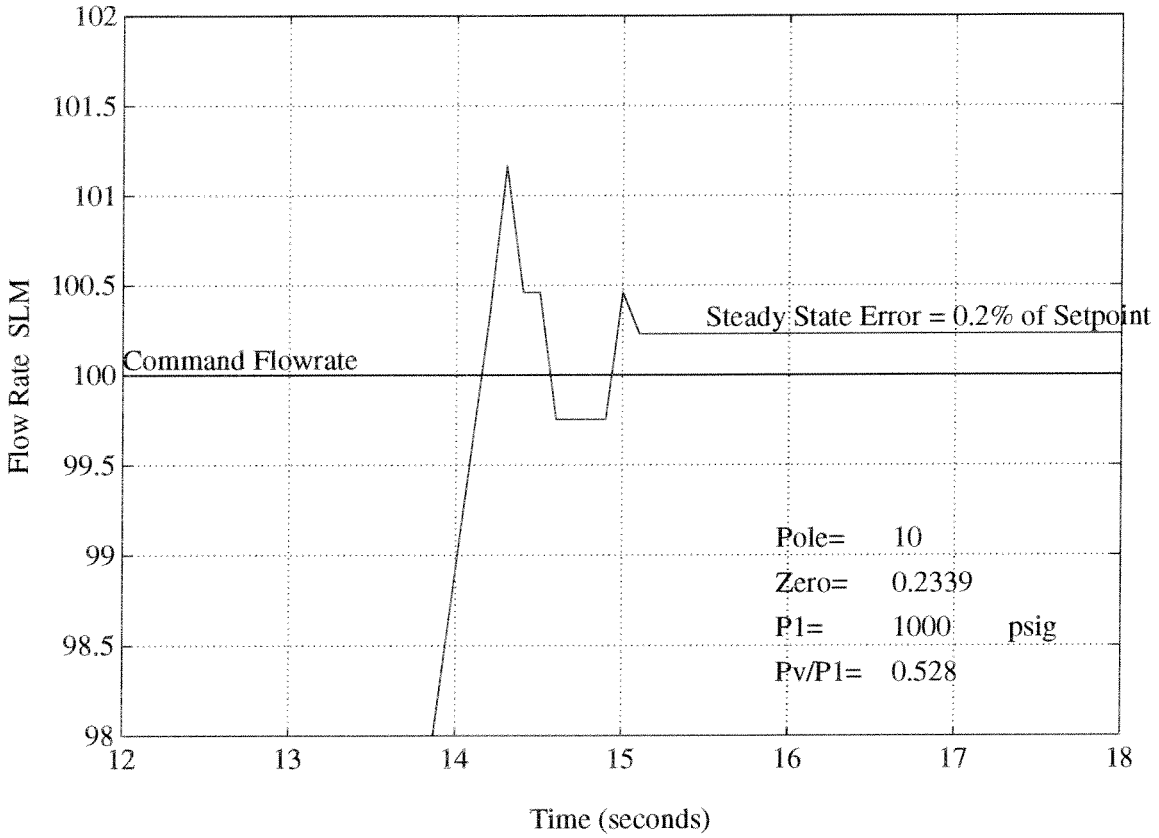

Figure 24. Mass Flow Rate Controller Simulation -- Detail of Overshoot

overshoot is kept within 1.1% of the setpoint flow rate of 100 SLM. On this plot, the steady state error can also be clearly seen which is caused by the dead operating zone of the valve actuator electronics. Remember that in these simulations, the controller gain has been set to give a steady state error of less than 0.5 percent.

The next simulations show how the controller will perform if the flow meter pole is not exactly cancelled as will likely be the case upon initial implementation

of the controller. As the root locus plots showed, underestimating the value of the controller zero by 10% caused no real overshoot problems and allowed a pole placement at P = 2.9 while overestimating the zero by 10% required the pole to be out at P = 17.25 before the imaginary roots were suppressed. Several iterations of the nonlinear simulation for the case of overestimating the zero showed that moving the pole further out along the negative real axis would limit the overshoot, but that complete elimination would not be practical. Furthermore, a point of diminishing returns was reached where reducing the magnitude of the overshoot began to increase the amount of time required for the flow rate to fall within 1% of the setpoint value. This point was reached at a pole placement of about P = 10. The following two simulation runs (Figures 25 and 26) show clearly that the slight

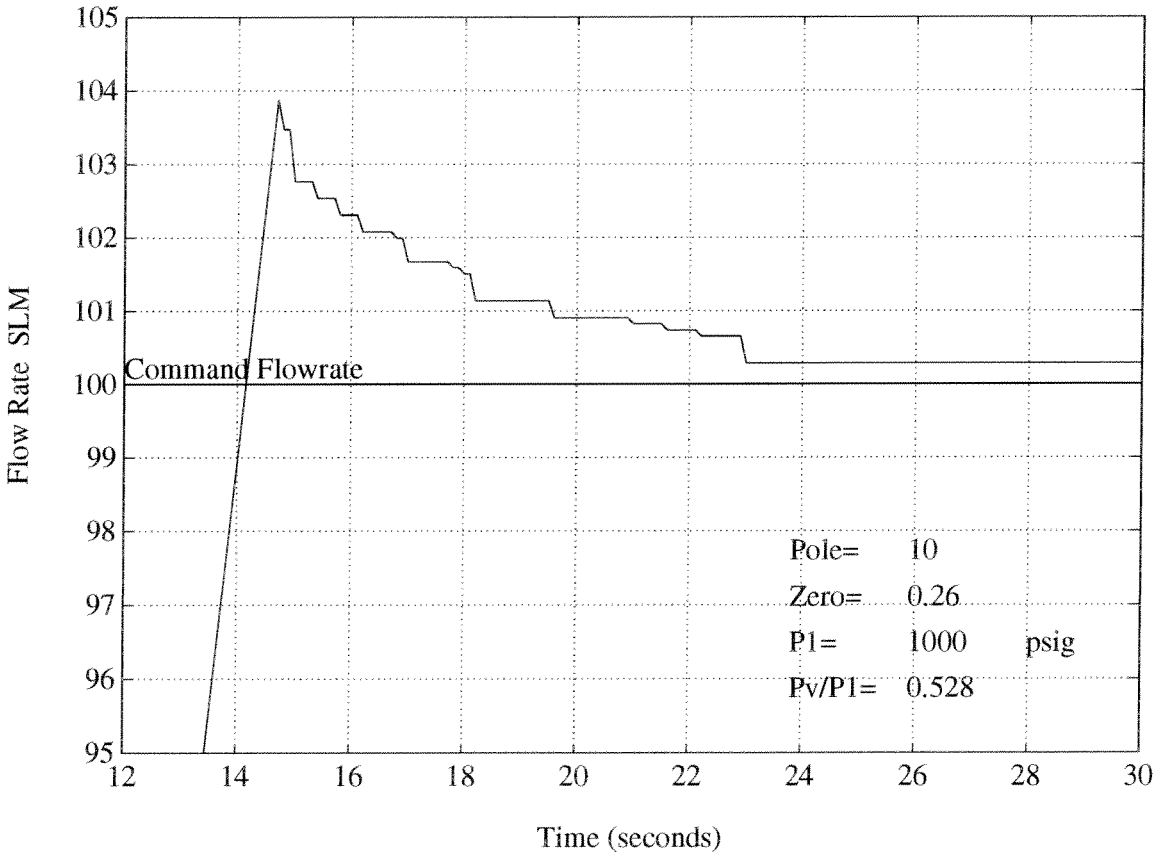

Figure 25. Mass Flow Rate Controller Simulation -- Off Design Operation I

reduction in overshoot from moving the pole from P = 10 to P = 50 results in a slight

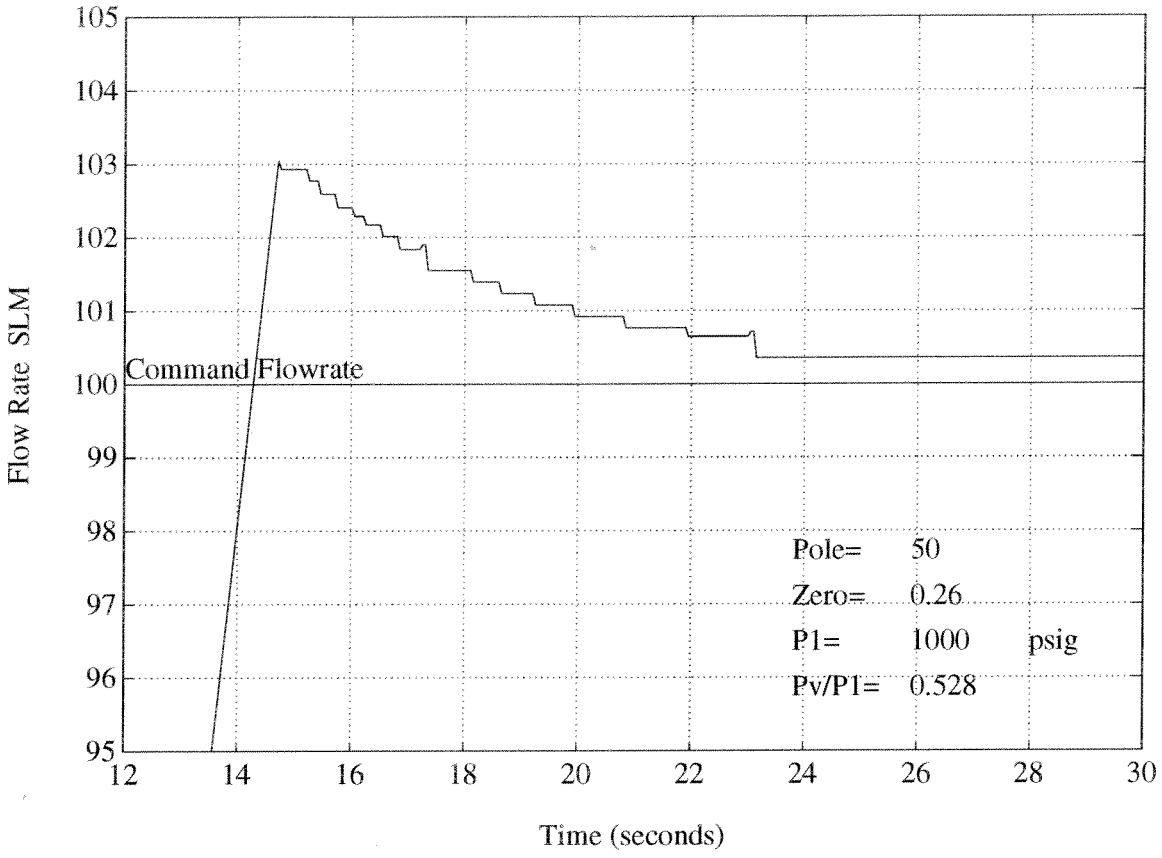

Figure 26. Mass Flow Rate Controller Simulation -- Off Design Operation II

increase in decay time. Since nothing is really gained by moving the pole out further than P = 10, the initial design to attempt for the prototype has been chosen as:

$$\frac{\dot{M}_{cl}(s)}{\dot{M}_e} = \frac{K_{cl}(s+0.2339)}{(s+10)} \qquad \text{(Eq. 52)}$$

CHAPTER 5 MASS RATIO CONTROL LAW DESIGN

For mass ratio control, as seen in the block diagram (Fig. 27), an integrator must be added to the control law in order to drive the mass ratio error (not just the ratio of mass flow rates!) to zero, and this places a second pole at the origin bringing the system transfer function to third order. An additional concern is present here that is not a factor in mass flow rate control which comes from the fact that mass measurements are not made directly but are obtained indirectly by integrating the signal from the mass flow meter. This makes the process of creating the proper error signal slightly more difficult than in the mass flow rate controller.

The basic design procedure here is the same as in the previous chapter but with the addition of the design of the filter in the feedback path which serves to condition the readings from the mass flow meter before the error signal is formed. In order to save time with the iterations involved with root locus design, a method of direct pole placement optimization has been employed as is discussed in section 5.1.

5.1 Linear System Analysis

The block diagram for the flow ratio controller (Fig. 27) is very similar to that

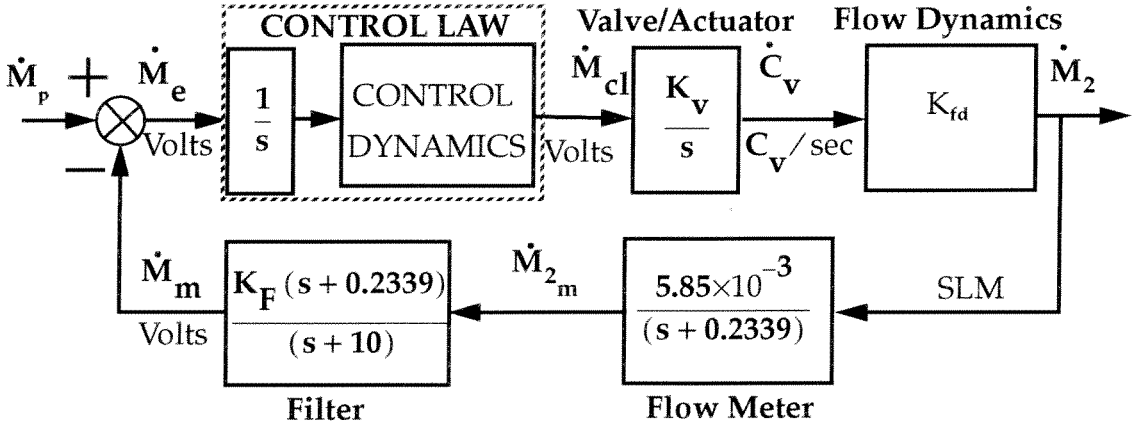

Figure 27. Block Diagram of Mass Ratio Control System

of the flow rate controller but with two notable exceptions. First of all, the control law must contain the integrator in order to force the ratio of flowed masses to zero

rather than merely forcing the rate of mass flow to zero. Secondly, the filter is necessary in the feedback path to condition the flow meter reading so that the proper error term can be formed.

Since the input value is the flow rate of the primary gas, the feedback value which is subtracted from the command value to form the error term must be made to represent what the mass flow rate of the primary gas should be in order that the integral of the error term represents the ratio of the mass of the secondary gas to that of the primary gas is the desired value. Defining the desired mass ratio in the following way

$$\Re_2 = \left[\frac{\dot{M}_2}{\dot{M}}\right]_{desired} \qquad \text{(Eq. 53)}$$

the feedback term we are looking for becomes, simply,

$$\dot{M}_m = \frac{\dot{M}_2}{\Re_2} \qquad \text{(Eq. 54)}$$

The desired mass ratio is known, but $\dot{M}_2$ is not directly available in this system. The only measure of the mass flow rate comes from the mass flow meter which equals the true mass flow rate only under steady conditions. The flow meter measurement of the mass flow rate may be used in Eq. 54 as an approximation, but since the dynamics of the flow meter are relatively stable and well known, a filter may be used which effectively shortens the delay in the reading of the mass flow meter. This minimizes the integral error so that the mass ratios may be much more accurately set. Without the filter, an overshoot of a few percent with a very long decay time constant must be tolerated as will be shown in the nonlinear simulations section.

The system transfer function with the flow meter pole cancelled is given by

$$\frac{\dot{M}_2}{\dot{M}_p} = \frac{K_{fd}K_vN_{cl}(s+10)}{\left[s^2(s+10)D_{cl} + K_{fd}K_vN_{cl}K_F(5.85\times10^{-3})\dfrac{(s+0.2339)}{(s+0.2339)}\right]} \qquad \text{(Eq. 55)}$$

where N_{cl} and D_{cl} are the numerator and denominator dynamic terms of the control law, and K_F is defined such that the steady state gain of the filter is equal

to $1/\Re_2$. The definition is, simply,

$$K_F = \frac{10}{(0.2339)\,\Re_2} \qquad \text{(Eq. 56)}$$

A plot of the root loci (Fig. 28) for a constant gain control law shows that some

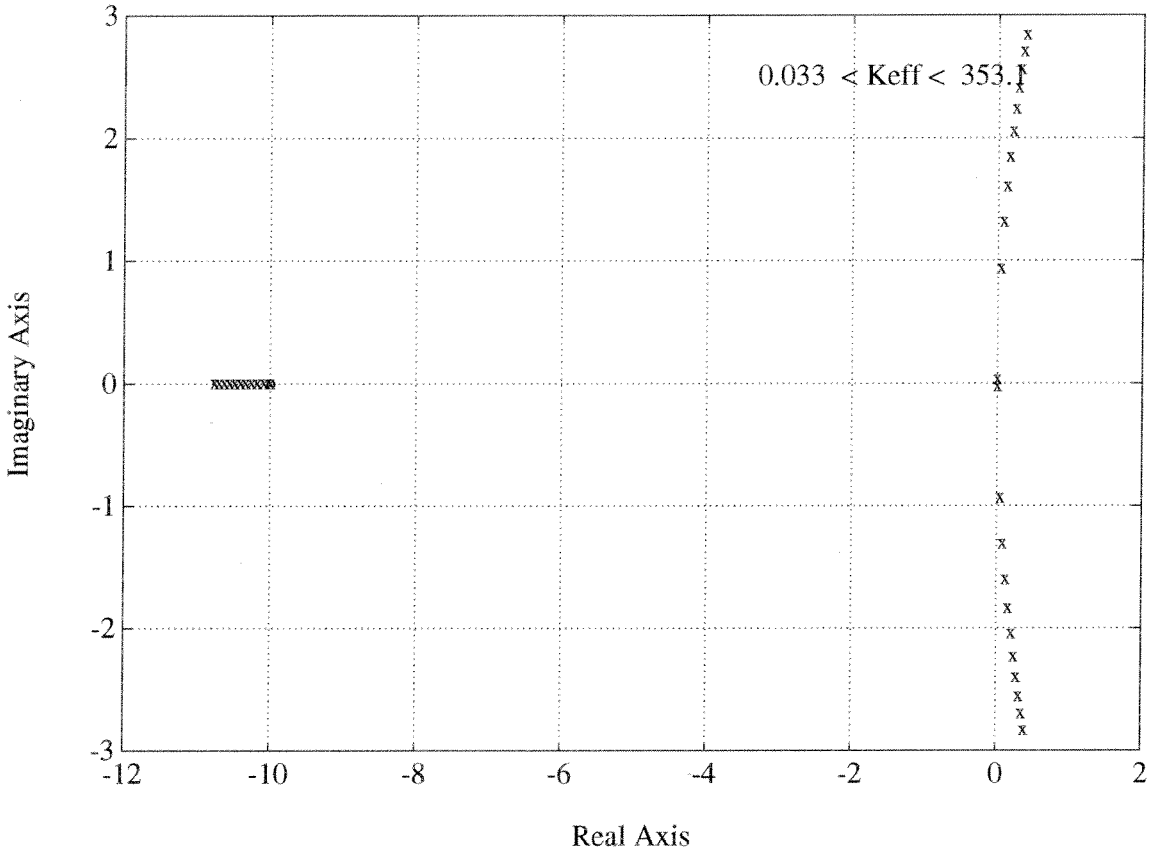

Figure 28. Mass Ratio Controller Root Locus -- Uncompensated

additional dynamics are necessary for system stability. As in the mass flow rate control system, the range of effective system gains is computed from the values in Tables 10 and 11 and is shown here in Table 15.

The design process proceeded similarly here to that of the mass flow rate controller, but promising results are not so easily found. A first order control law can stabilize the system, but to obtain a quality time response, a higher order

Table 15: Range of Effective System Gains for Mass Ratio Control System

Limit	K_v	K_{fd}	K_{eff}
Maximum	5.885×10^{-3}	60×10^{3}	353.1
Minimum	4.708×10^{-6}	7×10^{3}	.033

controller is necessary. Trial and error iterations, even when somewhat guided, are a very time consuming process by which to design a control law. This is especially true when the controller order is greater than one as is the case now. For this reason, a simple optimization routine for single input/single output systems has been developed here for use in speeding up the process of finding an adequate control law.

The use of a third order controller (in addition to the integrator) makes the characteristic equation of the closed loop transfer function sixth order. The third order controller has six parameters (three poles and three zeros) which may be adjusted by the designer to set the poles of the system transfer function as desired. One must only be careful to adhere to any physical limits imposed by the system hardware.

The simple equations for this process are developed by writing the general equation for the denominator of the system transfer function and setting this to zero. This is done six times, once for each system pole location which is substituted in for 's' in the equation and the result is a set of six linear equations which can be solved for functions of the poles and zeros of the controller. These functions can then be solved for the controller poles and zeros which will set the roots of the denominator as specified.

The denominator of the system transfer function is written as:

$$D_W(s) = D_G(s) \cdot D_H(s) \cdot [\,(s+P_1)\,(s+P_2)\,(s+P_3)\,] + N_G(s) \cdot N_H(s) \cdot [\,(s+Z_1)\,(s+Z_2)\,(s+Z_3)\,] = 0 \qquad \text{(Eq. 57)}$$

When the pole and zero terms are expanded, and the constant terms are placed on the right side, Eq. 57 can be written in the following summation form which is

easily implemented in a computer program:

$$\sum_{j=1}^{3}\left[\left(D_G(s_n)\cdot D_H(s_n)\cdot s_n^{(3-j)}\right)\cdot a_{(j-1)}+\left(N_G(s_n)\cdot N_H(s_n)\cdot s_n^{(3-j)}\right)\cdot a_{(j+2)}\right]$$

$$= -s_n^3\left(D_G(s_n)\cdot D_H(s_n)+N_G(s_n)\cdot N_H(s_n)\right) \qquad \text{(Eq. 58)}$$

where

$$a_0 = P_1 + P_2 + P_3 \qquad \text{(Eq. 59)}$$

$$a_1 = P_1\cdot P_2 + P_1\cdot P_3 + P_2\cdot P_3 \qquad \text{(Eq. 60)}$$

$$a_2 = P_1\cdot P_2\cdot P_3 \qquad \text{(Eq. 61)}$$

$$a_3 = Z_1 + Z_2 + Z_3 \qquad \text{(Eq. 62)}$$

$$a_4 = Z_1\cdot Z_2 + Z_1\cdot Z_3 + Z_2\cdot Z_3 \qquad \text{(Eq. 63)}$$

and

$$a_5 = Z_1\cdot Z_2\cdot Z_3 \qquad \text{(Eq. 64)}$$

Eq. 58 must then be written n times, once for each value of s_n that coincides with a desired pole location of the system transfer function. The resulting values for a_n must be used in conjunction with Eqs. 59 through 64 to solve for the pole and zero values.

The analytical solution of Eqs. 59 through 64 is somewhat involved and leads to an iterative process to find the poles and the zeros. Numerically, however, these Eqs. produce answers quickly when reasonable values are requested for the system poles. The program to form and solve Eqs. 58 through 64 is called *thor.m* and appears in Appendix A.18.

Using *thor.m*, an acceptable control law has been found fairly quickly. Starting values for the controller poles and zeros which stabilize the system are first found by educated trial and error. Then, the optimization program can be used to quickly show how to move the system transfer function poles in any desired direction

within one or two attempts. This is a far more satisfying design procedure than pure trial and error methods.

The third order transfer functions found for this system generally have a pole and a zero at nearly equal values which can be cancelled to reduce the control law to second order. This simplifies the implementation of the control system and doesn't alter the nature of the system response significantly.

One final consideration is necessary before the presentation of the chosen control law design. The effective system gain is still time varying, and the system poles can only be placed only for one gain value. The conditions for which the control system will be operating most often will be the maximum gain conditions. This is because the regulated source gas bottles will be at a constant 1000 psig for about 90% of their life-spans, and because the effective gain of the control valve actuator is a maximum when the system reaches steady state which will be most of the time. This suggests that the control law should be designed for operation at the maximum gain position. This is also a conservative design choice since the root locus plots show that the only time stability problems may occur is when the gain becomes higher than the value for which the controller is designed.

One more variable is significant in the mass ratio controller that does not appear in the flow rate controller analysis, and this is the choice of mass ratio for which the gas is to be controlled. This will be different for each type of gas, and will vary depending upon the chosen gas mixture. Usually, however, the variations in mass ratios for any one component of the gas mixtures are within ten to twenty percent of the median values which does not change the system dynamics significantly. For each type of gas, a slightly different control law will need to be developed if the control system is to operate under optimum conditions. If the variations in requested mass ratios cause significant degradation in the control system response, the control laws may be developed using the optimization program developed here as functions of the commanded mass ratios and varied on-line in the computer implementation system. For the demonstration of the mass ratio controller with the prototype system, a command mass ratio of unity will be used. The design process for any other command mass ratio is identical and leads to similar results.

The root locus plot (Fig. 29) for the control law developed with the *thor.m* program shows the variation in system poles across the range of possible system

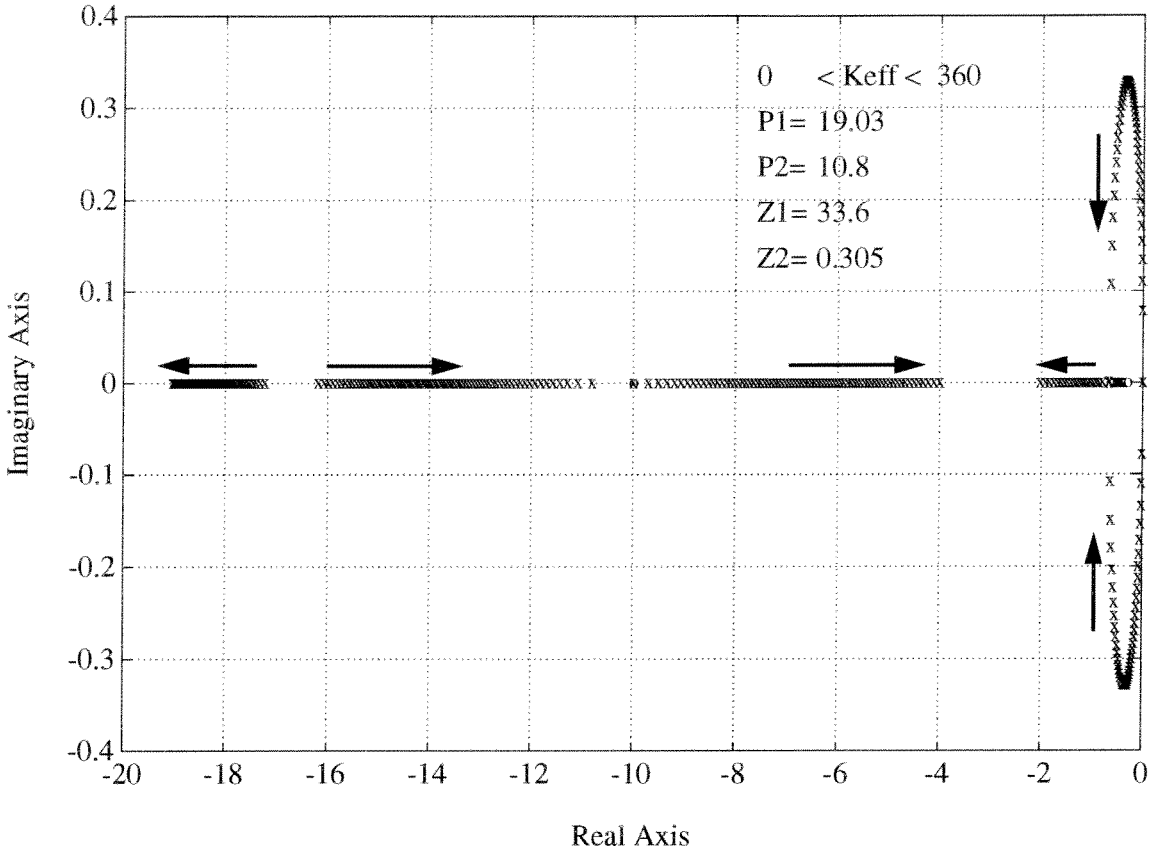

Figure 29. Mass Ratio Controller Root Locus

gains as given in Table 15. The optimization routine has been used to bring the integrator poles out from the origin and back down to the real axis for as large of a gain range as possible including the maximum gain value. If the gain is increased further, some of the roots will again pair and move off of the real axis, and will eventually travel into the right half plane. By removing the imaginary roots of the characteristic equation for a large gain range, oscillations in the system can be avoided. In Fig. 29, the gain at which the imaginary roots finally reach the real axis is about $K_{eff} = 260$. This effectively covers most of the operation range of the controller. Operation outside of this range occurs only when the controller is first switched on and the error term is relatively large. As discussed in Chapter 3, this makes the effective gain of the control valve actuator appear to be relatively low. As the error term is reduced, the effective gain comes back into a range where the

oscillatory system roots have disappeared. The nonlinear simulations for this control law design which appear in the next section show that the time response is more than adequate for mass ratio control.

5.2 Nonlinear Simulation of the Mass Ratio Controller

A program similar to that used for the mass flow rate controller has been written to simulate the time response of the flow ratio controller, and is called *nlratioth.m* (Appendices A.19 & A.20). The only changes from the mass flow rate simulator are the addition of the filter and the integrator, and the changing of the control law. Output connections have also been made to show the difference between the mass ratio formed with the direct mass flow meter reading and the filtered mass flow meter reading. This demonstrates why the filter is so necessary for mass ratio control. The simulations in this chapter show the operation of the mass ratio control system as changes are made in the effective system gain and in the command inputs. Additionally, a few simulations have been performed to demonstrate the operation of the controller if the filter does not exactly cancel the dynamics of the mass flow meter as will likely be the case. A compiled list of the figures that appear in this section along with the corresponding information about each simulation is given in Table 16. In the following series of simulation figures,

Table 16: Nonlinear Mass Ratio Controller Simulation Data

Figure #	Command Mass Ratio	$\dot{M}_{primary}$(SLM)	Filter Zero	Upstream Pressure
30	1	50	0.2339	1000 psig
31	1	50	0.2339	600 psig
32	1	100	0.2339	1000 psig
33	1	50	0.2105	1000 psig
34	1	50	0.2573	1000 psig

the solid lines represent the actual mass ratio, the dashed lines represent the mass ratio that the controller is measuring through the filter, and the dotted line represents the mass ratio formed with the integral of the unfiltered mass flow meter reading.

The first simulation (Fig. 30) demonstrates the operation of the controller during the most common operating conditions of 1000 psig upstream pressure. The actual mass ratio and the filtered mass ratio are seen to be nearly identical to

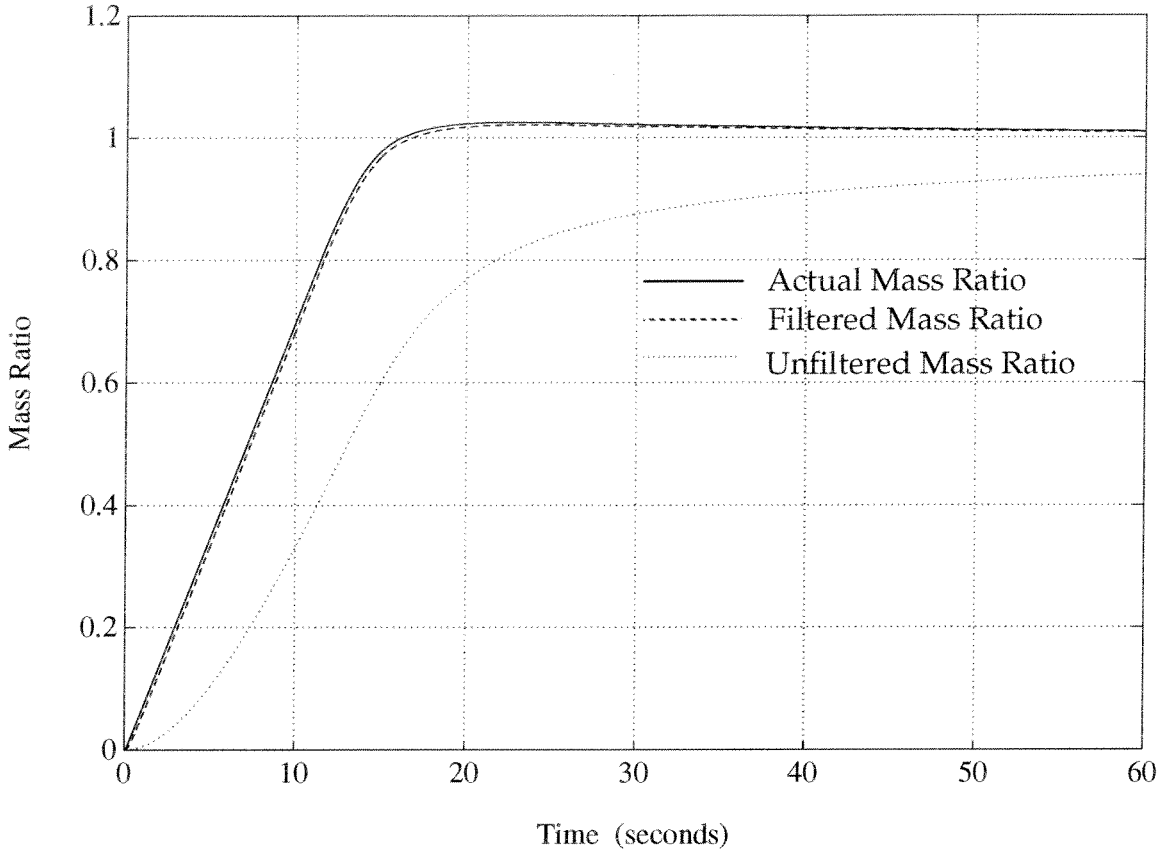

Figure 30. Nonlinear Simulation of the Mass Ratio Controller

one another. The slight discrepancy between the two readings comes from the fact that the filter does not entirely remove the delay but instead moves the delay time constant from near 4.3 seconds down to 0.1 seconds. The mass ratio formed from the unfiltered mass flow meter reading is quite a different value than the true mass ratio. The error in this reading will eventually go to zero, but this could take many minutes to occur. The actual mass ratio response does show some slight overshoot (about 2%), and this is likely due to the variable system gain as mentioned in the previous section, but this response is a large improvement over that of the unfiltered system.

As expected from the root locus analysis, when the controller is operating at lower gain levels due to a decrease in the upstream valve pressure from 1000 to 600 psig, the oscillations in the time response become more prominent (Fig. 31). The

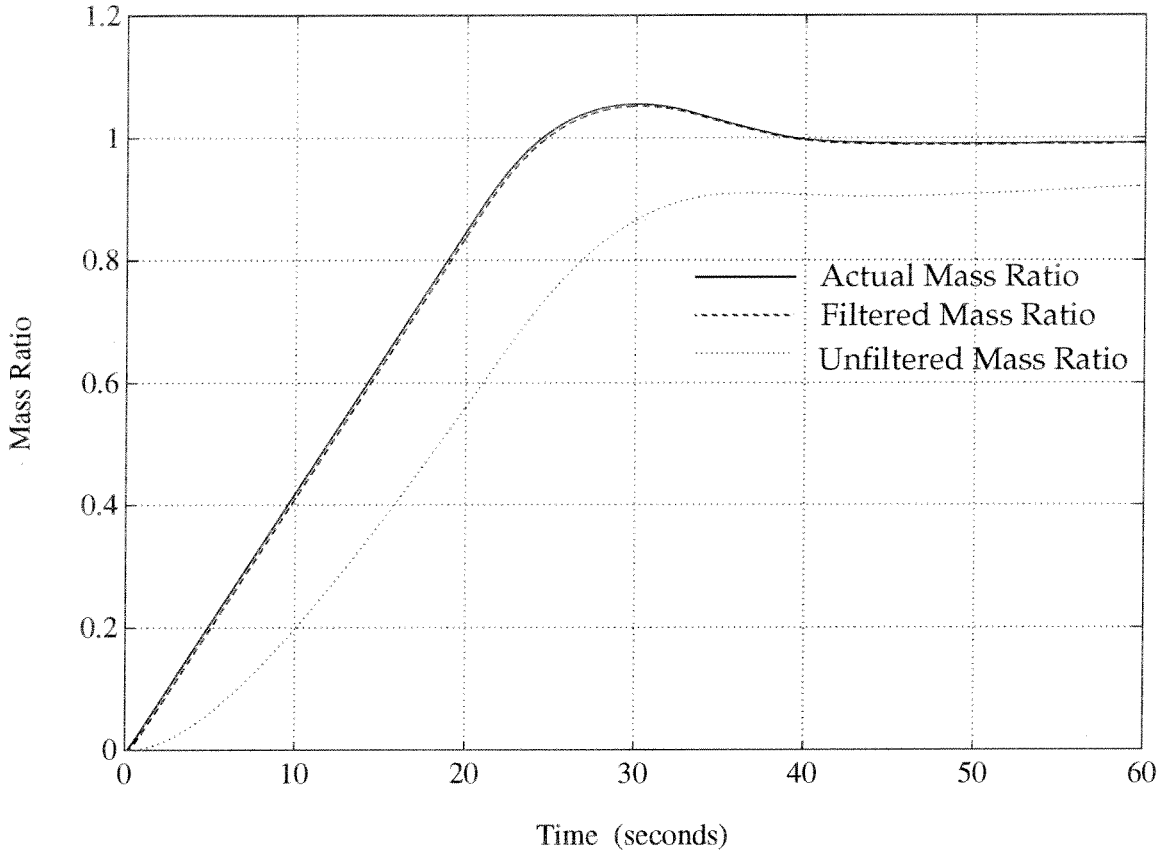

Figure 31. Nonlinear Simulation of the Mass Ratio Controller Operating at Reduced Upstream Pressure (600 psig)

maximum overshoot is now roughly 5% of the setpoint value but decays rapidly to within about 0.5%. Again, the filtered response follows the actual response very closely while the unfiltered response shows an extended lag time.

When the input mass flow rate is raised to 100 SLM from 50 SLM, the time to reach the set-point mass ratio doubles as is expected (Fig. 32). The maximum overshoot has increased somewhat over the corresponding plot for an input of 50 SLM (Fig. 22) and this probably occurs since the controller is now operating under the low effective gain conditions for a longer period of time while the valve is opening up and trying to reduce the feedback error.

The final two plots in this section (Figs. 33 & 34) demonstrate the operation of the mass ratio control system when the filter is set at off-design values of ±10%. These plots show that filter does not have to precisely cancel the pole of the mass

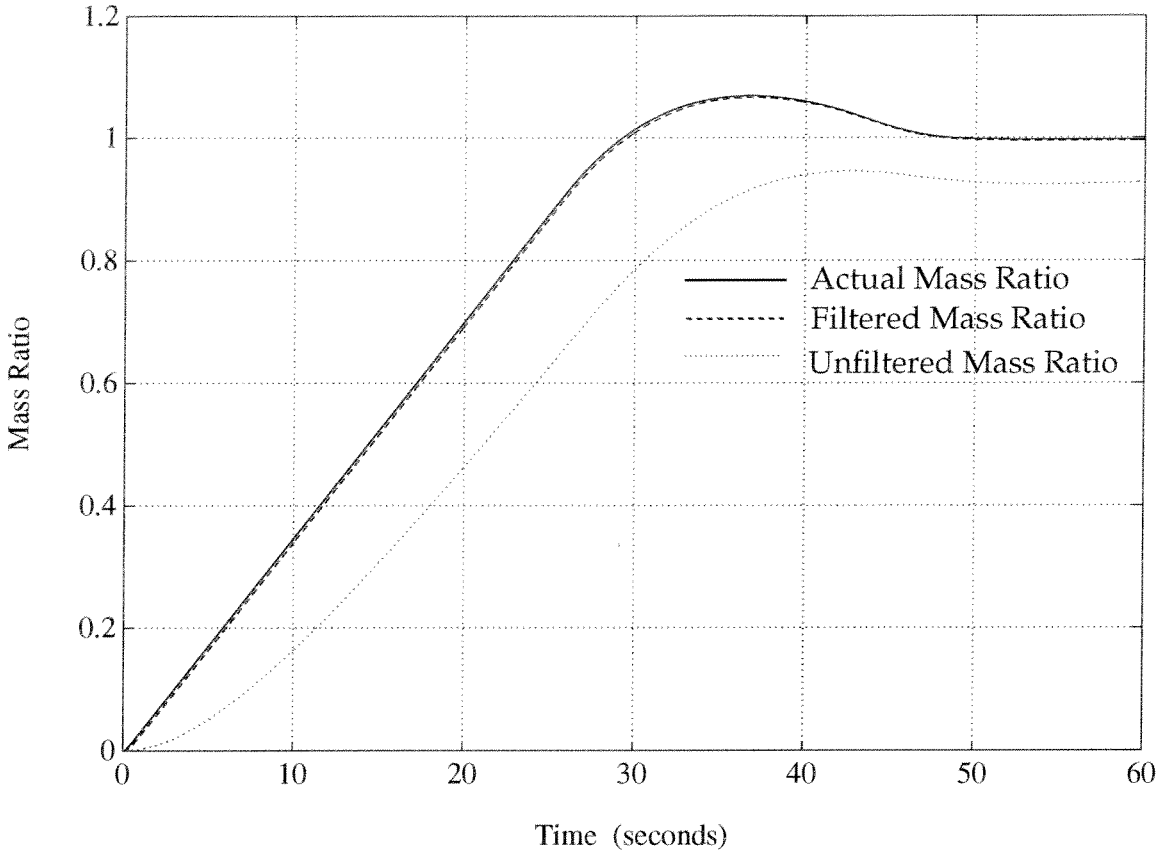

Figure 32. Nonlinear Simulation of the Mass Ratio Controller Operating at with a Command Input of 100 SLM

flow meter in order for the control system to work reasonably well. Oddly enough, the time response for the case where the zero is 10% lower than the design value appears to be better than for the on-design case. The overshoot of the actual mass ratio has nearly disappeared. This does not, however, mean that purposefully setting the filter zero slightly lower than the design value is a good idea. The best repair for the overshoot in the control system is to further adjust the control law in the forward loop. In this way, the control system will work better in all conditions.

5.3 Summary of Mass Ratio Control Law Design

The control law to be used for maintaining the mass ratio for two flowing gases consists of a second order linear transfer function with an integrator in the forward loop path and a first order linear filter in the feedback path. The mathematical

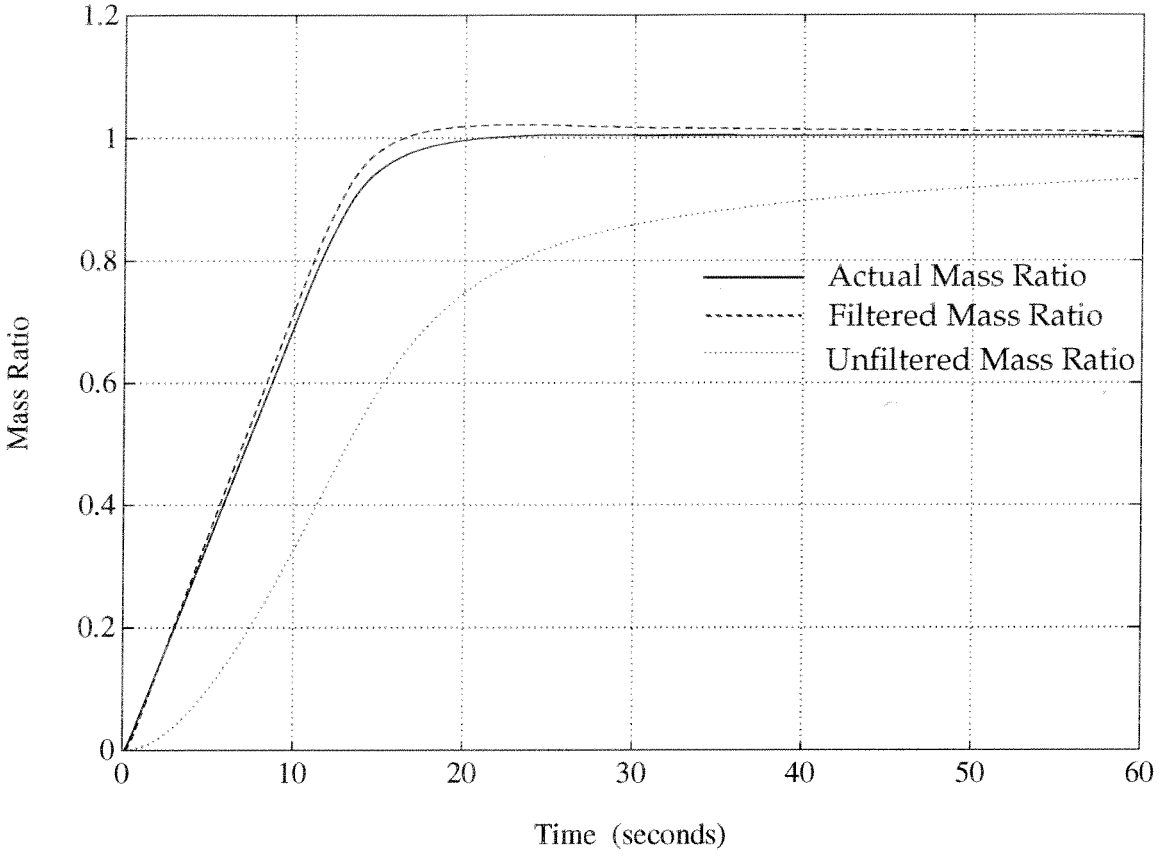

Figure 33. Nonlinear Simulation of the Mass Ratio Controller Operating with the Filter Zero at an Off-Design Value (Z_F = 0.2105)

description of the forward loop controller is given by:

$$\frac{\dot{M}_{cl}(s)}{\dot{M}_e(s)} = \frac{(s+33.6)\ (s+0.305)}{s\ (s+19.03)\ (s+10.8)} \qquad \text{(Eq. 65)}$$

and the filter transfer function is

$$\frac{\dot{M}_m}{\dot{M}_{2_m}} = \frac{(42.7533)\ (s+0.2339)}{\Re \cdot\ (s+10)} \qquad \text{(Eq. 66)}$$

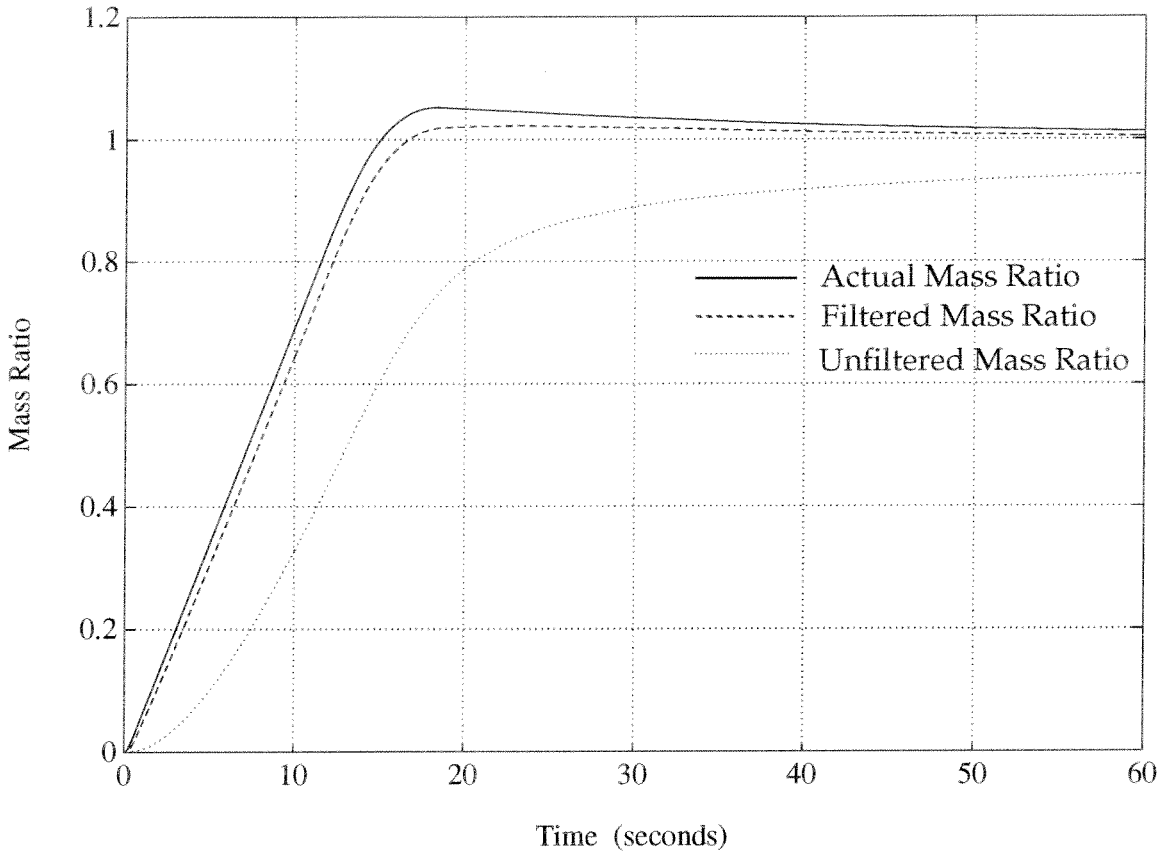

Figure 34. Nonlinear Simulation of the Mass Ratio Controller Operating with the Filter Zero at an Off-Design Value (Z_F = 0.2573)

CHAPTER 6 CONTROL LAW IMPLEMENTATION

The control laws developed in the previous two chapters are to be implemented on a digital computer so that additional automation may be more easily added to the gas mixing system. The procedure is simply to discretize the transfer function of the control law and to program this into the computer hardware and software of choice.

6.1 Computer Equipment

In section 2.1.4, the choice of computer hardware was revealed to be the Macintosh IIci with a National Instruments NB-MIO-16L multifunction analog/ digital and timing board along with a National Instruments SC-2070 termination breadboard for use in the connection of thermocouples. Also from National Instruments is the software package, Labview 2, that is used for programming all of the data acquisition, computation, control law application and output of results functions of the automated gas mixing system.

Labview 2 consists of a library of functions which greatly simplify data acquisition, analysis, and display of output programming. Further simplification of the programming procedures is made by the use of the high level graphical programming package that is a part of Labview. Programming in this language is accomplished by drawing block diagrams where each block performs some type of function upon the input. User defined blocks may also be created by writing a program first with the basic system building blocks and then compiling this into a single block with user defined inputs and outputs.

The screen graphics library incorporated into Labview is very sophisticated and allows the programmer to very easily program graphical interfaces for the operation of programs written in Labview. In this way, "Virtual Instruments" such as a gas mixing system can be quickly created.

The data I/O functions make the programming of laboratory measurements and voltage outputs very straightforward. All of the analog to digital and digital to analog functions could be easily manipulated by changing a few simple parameters within the built-in function blocks.

6.2 The Prototype Control System

The prototype control system (refer to Fig. 11, chapter 3) is capable of evaluating the performance of either the mass flow rate controller or the mass ratio controller separately, but not at the same time since only one each of the flow meter and control valve are currently available. The prototype system may also be used for running calibrations on the mass flow meters and valves which will need to be obtained in order to build the full four-gas mixing system. Pressure transducers and thermocouple probes are set up to measure the gas conditions in the source gas bottles and in the fill tank so that these conditions may be conveniently monitored and used in on-line computations. This allows some convenient features to be programmed into the gas mixing system which will allow the filling of the Ram Accelerator with a specified gas mixture to be performed fully automatically. For example, since the pressures and temperatures of the source gases are monitored, the masses are known, and the computations to determine whether or not enough gas is available for a prescribed gas mixture at a prescribed pressure will be possible. Additionally, since the fill tank temperature and pressure is monitored, the filling of the tank may be automatically terminated when the commanded conditions have been reached.

6.3 Programming the Control Laws

The concept behind the programming of the control laws is quite simple. The analog data from the mass flow meter must be read into the computer, the control law needs to be evaluated at that instant in time and multiplied by the flow meter reading, and the resulting voltage must be output to the valve. The difficult part of the process is not the application of the control law itself, but is the programming all of the necessary data acquisition and timing tasks.

The control laws, in order to be applied within the computer, must first be discretized. In this case since speed of operation was not considered to be very important due to the relatively slow bandwidth of the system dynamics, a simple zeroth order hold discretization was used. With this method, the solution to a first order linear differential equation may be written as a difference equation in the following way.

The transfer function of a generic first order control law where the gain has

been assumed to be equal to one will be written out and transformed into a time differential equation so that the pole and zero notation of the previous chapters may be preserved. The transfer function is given by

$$\frac{y(s)}{u(s)} = \frac{(s+Z)}{(s+P)} \qquad \text{(Eq. 67)}$$

which, when inverse transformed becomes

$$\dot{y}(t) + Py(t) = \dot{u}(t) + Zu(t) \qquad \text{(Eq. 68)}$$

The well known solution to this equation for the case when the input, u(t), can be assumed constant over the time interval, dt, is given as

$$y(t+dt) = \frac{(Z-P)}{P} u(t)\,(1-e^{-(P\cdot dt)}) + e^{-(P\cdot dt)}\,(y(t)-u(t)) + u(t+dt) \qquad \text{(Eq. 69)}$$

The solution to any higher order system of linear differential equations of any order may be obtained by connecting several first order systems in series. This is done by noticing that the output of the first system becomes the input to the second system, and so on. This is exactly how the third order control law equation was applied.

The only somewhat difficult parts of this are to accurately determine the time step, dt, and in the case of the variable pole/zero control law, to evaluate the appropriate functions in order to determine the values for the poles and zeros. This requires the knowledge of the effective system gain which isn't exactly straightforward.

For the mass ratio controller, the effective system gain is a function of the mass ratio error, the pressure upstream of the valve, the pressure at the valve orifice, and a few fixed system hardware parameters such as valve actuator speed. Everything to compute the effective system gain in real time is available directly except for the pressure at the valve orifice. Only the upstream pressure and the pressure in the fill tank are monitored, and measuring the pressure inside the micrometering valve directly will never really be an option. For this reason, the pressure at the valve orifice must be approximated so that the variable pole and zero values may be

computed.

Remember that the functions used to compute the valve pressure back in the chapter on valve sizing were somewhat involved and the solutions to which were iterative in nature. Solving these approximation equations at every measurement step would greatly increase the computational time for applying the control law, and this increase might actually be enough to cause some problems. However, since the valve in use is so small, the flow will often be choked passing through the valve. This conveniently provides us with the pressure ratio (the critical value) to use in computing the effective system gain. Furthermore, the effective gain term is a somewhat weak function of the pressure ratio so that even in the cases where the flow unchokes, using the critical pressure ratio still gives a good estimate of the pressure at the valve orifice. For example, the term in the equation to compute the effective gain that depends upon the pressure ratio is

$$P_{term} = \left[\left(\frac{P_v}{P_1} \right)^{2/\gamma} - \left(\frac{P_v}{P_1} \right)^{(\gamma+1)/1} \right] \qquad \text{(Eq. 70)}$$

Below in Table 17 , this term has been computed for a few values of the pressure

Table 17: Computed Pressure Term and % Difference From Critical Estimate

P_v/P_1	P_{term}	% Difference
0.528 (critical)	0.2588	0
0.6	0.2558	1.2
0.7	0.2413	7

ratio that might be encountered along with the percent difference between the critical value estimate and the actual value. This clearly shows that the critical pressure ratio estimate will provide reasonable results throughout most of the operating range of the mixing system.

With these ideas in mind, the programs to implement the control laws were developed. Most of the details of the program are very specific to the software that was used and will therefore not be covered here.

CHAPTER 7 EXPERIMENTAL RESULTS

The prototype system has been programmed with the control laws and implementation methods developed in Chapters 4, 5 and 6, and several data runs have been made in order to verify that the control laws work as expected. In the case of the mass flow rate controller, the following data set was taken directly: Control Law Output to Valve, Error Signal (difference between measured mass flow rate and commanded mass flow rate), Measured Mass Flow Rate, Fill Tank Pressure, and Fill Tank Temperature. Labview was used to program the experimental runs such that the data was directly stored in the desired units in a format that could easily be imported into Matlab where all of the theoretical results reside. This made the comparison between theory and experiment straightforward. Once the controller had been shown to function properly in a qualitative sense, data runs have been made to demonstrate the calibration procedures for the mass flow meters. The principle is to set the mass flow rate constant with the controller and then to measure the mass flow rate independently with readings of pressure and temperature in the fill tank.

One important thing to note here is that the measurements of the mass flow rate are available only through the delayed output response of the mass flow meter. This is the main reason that a feedback control law without dynamics would not work very well. Unless the system has reached steady state where the mass flow rate has been constant for at least ten seconds or so, the mass flow meters will be giving a reading that is delayed according to the exponential function determined back in Chapter 3 (Eq. 34). The object of designing the control laws, however, was to cause the true mass flow rate (or mass ratio) to go to the setpoint value as quickly as possible. This means that the actual mass flow rate should reach steady state before the readings from the mass flow meter. The only *direct* experimental verification of this fact comes from the measurements of the control voltages sent to the control valve actuator, and from the pressure time history in the fill tank. The important thing to watch for is that the control voltage goes to zero before the mass flow meter indicates that this is the case.

7.1 Mass Flow Rate Controller

Several experiments were recorded in order to show the performance of the

control system in both on and off design conditions. During the discussion of the results, refer to Table 18 for quantitative details of the conditions during the experiments shown in the figures such as the type of control law in use, the upstream gas pressure, and the setpoint mass flow rate.

Table 18: List of Verification Experiments for the Mass Flow Rate Controller

Figs.	Pole	Zero	$\dot{M}_{com}$	P_{t_1}	K_{cl}	Description
35	N/A	N/A	50	1000	1	No Control Law
36,37	10	.234	50	1000	136.8	Control Law as Designed
38,39,40	10	.26	50	1000	123.1	Off-Design Zero Operation
41,42	10	.22	50	1000	145.5	Off-Design Zero Operation
43,44	3	.234	50	1000	41.0	Off-Design Pole Operation
45,46	10	.234	50	1000	15.0	Reduced Gain Operation
47,48,49	10	.234	125	625	54.7	Operation at Low P_{t_1}

From the first run, a plot of the measured mass flow rate vs. time (Fig. 35) shows the performance of the control system with no control dynamics, just a simple unity control law feedback arrangement. This clearly demonstrates that some control law dynamics will be required to improve the system response. This is as expected from the analysis carried out in the chapter on Dynamic Modelling. Since the mass flow meter is giving a delayed response, by the time the error signal goes to zero, the mass flow rate has already gone too high. This causes the excessive overshoot and the long decay time.

The following series of plots (Figures 36 & 37) demonstrate the system operation with the control law as designed in Chapter 4. In Fig. 36, the measured mass flow rate is plotted as a function of time for the case when the controller has been implemented as designed from the theoretical considerations. The results of the nonlinear simulation which are shown on the same plot suggest that the system model is capable of predicting the true system response quite well. The plot of the control voltage at the input to the valve actuator (Fig. 37) shows that the mass flow rate had been set within about five to seven seconds which is almost twenty

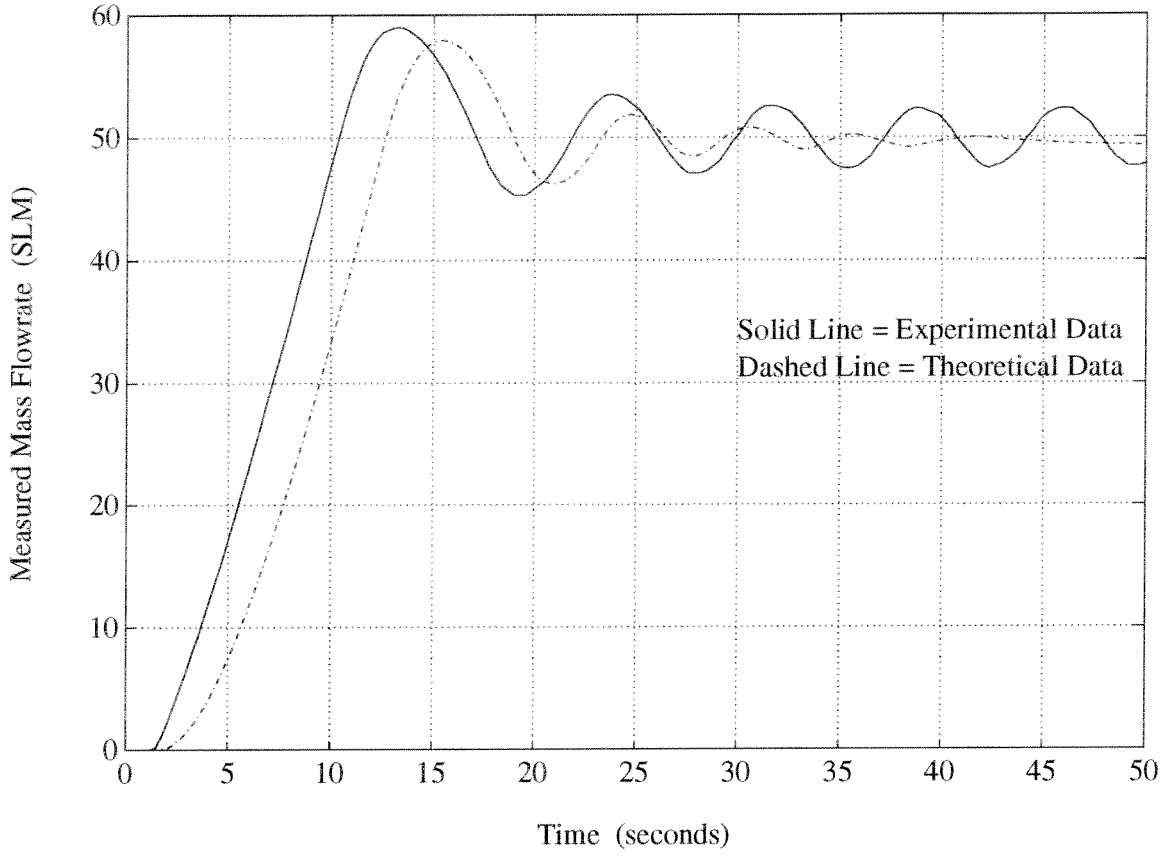

Figure 35. Experimental Results of the Mass Flow Rate Controller Operating With Unity Control Law

seconds faster than the flow meter could respond. The noise in the fluctuations in the control law output occurred because the control law gain setting had to be so high in order to ensure a steady state error of less than 0.5%. The required control gain is inversely proportional to the command flow rate so that for lower set-points, the fluctuations become greater. Of course, there comes a point when the fluctuations become so large that setting lower mass flow rates becomes impractical. For this reason, the mass flow rate controller should always be run at the highest possible flow rates in order to achieve the greatest accuracy. This should pose no problems for the Ram Accelerator facility since higher flow rates are more desirable from an operations standpoint, but for other applications, a control actuator with two different speeds of operation might solve the accuracy problem at the lower flow rate settings. Later are some results for cases when the

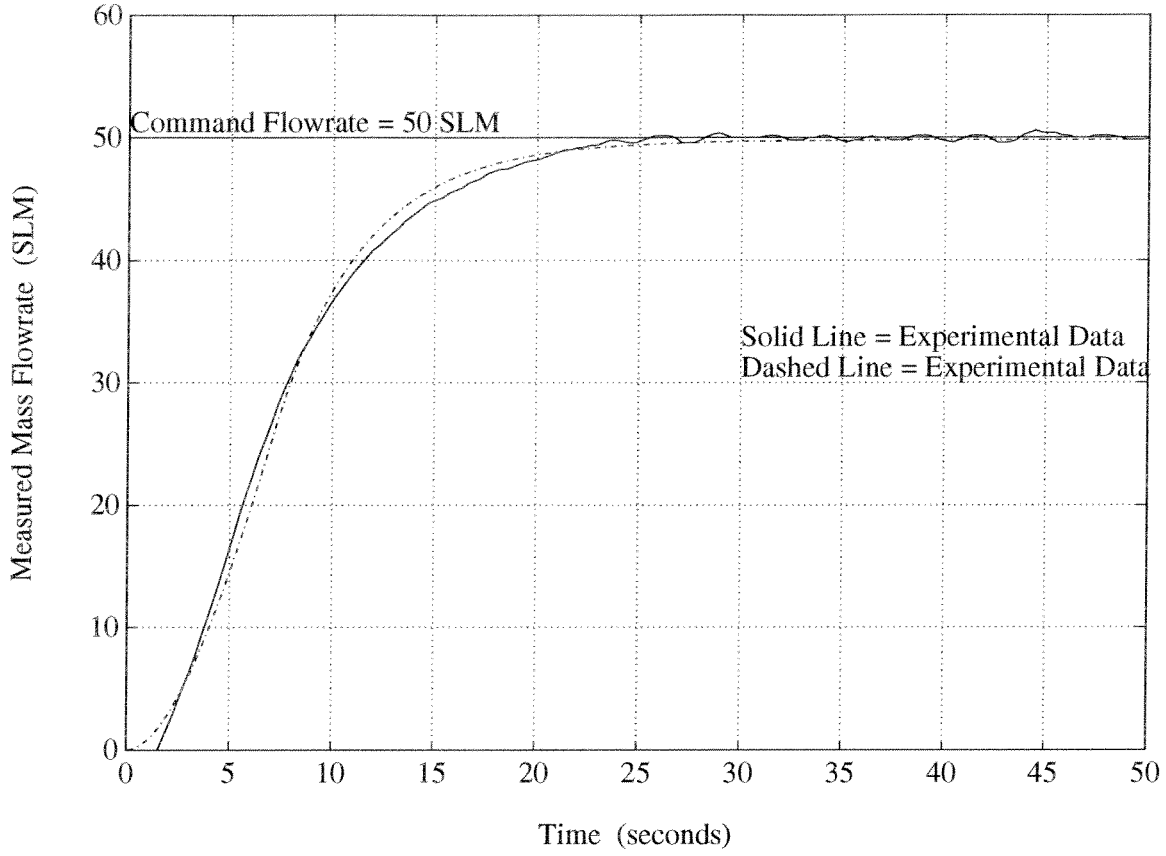

Figure 36. Experimental Results of the Mass Flow Rate Controller Operating On-Design (Zero @ 0.2339, Pole @ 10) -- Measured Mass Flow Rate

commanded mass flow rate was 100 or 150 SLM and the control voltage does, indeed, become less noisy. Notice in these plots that the theoretical prediction of the control law voltage appears somewhat delayed with respect to the experimental results. This is believed to be due to the initial unseating process within the micrometering valve. For approximately one second after the control system is turned on from rest, the valve stem is turning, but the needle remains seated inside the orifice in the valve so that flow does not begin immediately. This can also be seen in Fig. 36 where the measured mass flow rate does not begin to increase until a few seconds have passed. This slight anomaly appears in the remainder of the plots in this section as well.

The next cases that have been run show the operation of the system at off-design pole and zero locations. This demonstrates whether or not modifications to

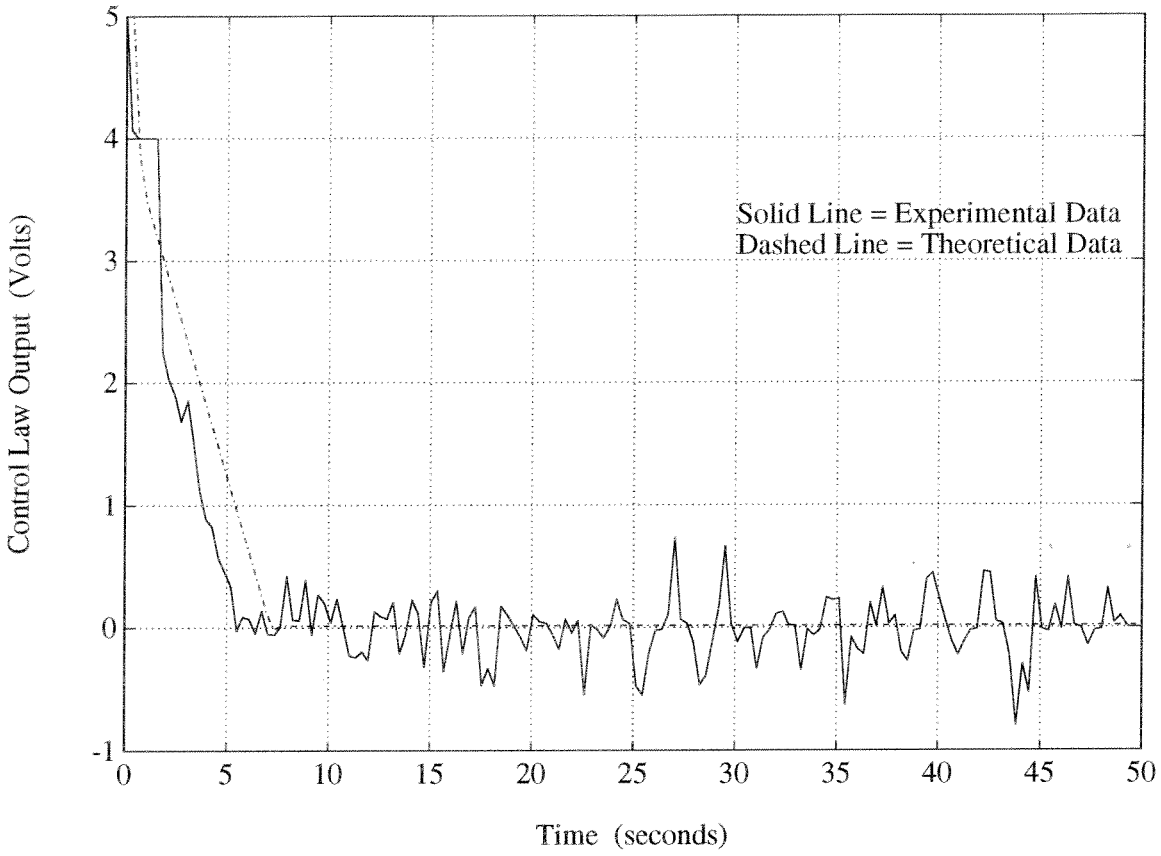

Figure 37. Experimental Results of the Mass Flow Rate Controller Operating On-Design (Zero @ 0.2339, Pole @ 10) -- Control Voltage

the control system are necessary. The plot of measured mass flow rate vs. time (Fig. 38) for a zero location 10% greater than the design value is very similar to the on-design case (Fig. 36), but the plots of control voltage vs. time (Figures 39 & 40) suggest that some small overshoot has occurred. This may only be due to the random noise fluctuations in the system, but the overshoot is notably not present in the on-design case. The close-up plot of the control voltage vs. time shows that some immediate overshoot has occurred in the experimental system which is also shown in the theoretical data, but on a smaller scale, and shifted by a few seconds along the time axis for the reasons mentioned earlier.

When the zero is placed about 10% lower than the design value, theory predicts some slight overshoot and slowing of the response. This is difficult to discern from the recorded data due to the noise in the system, but the fact that the plots of

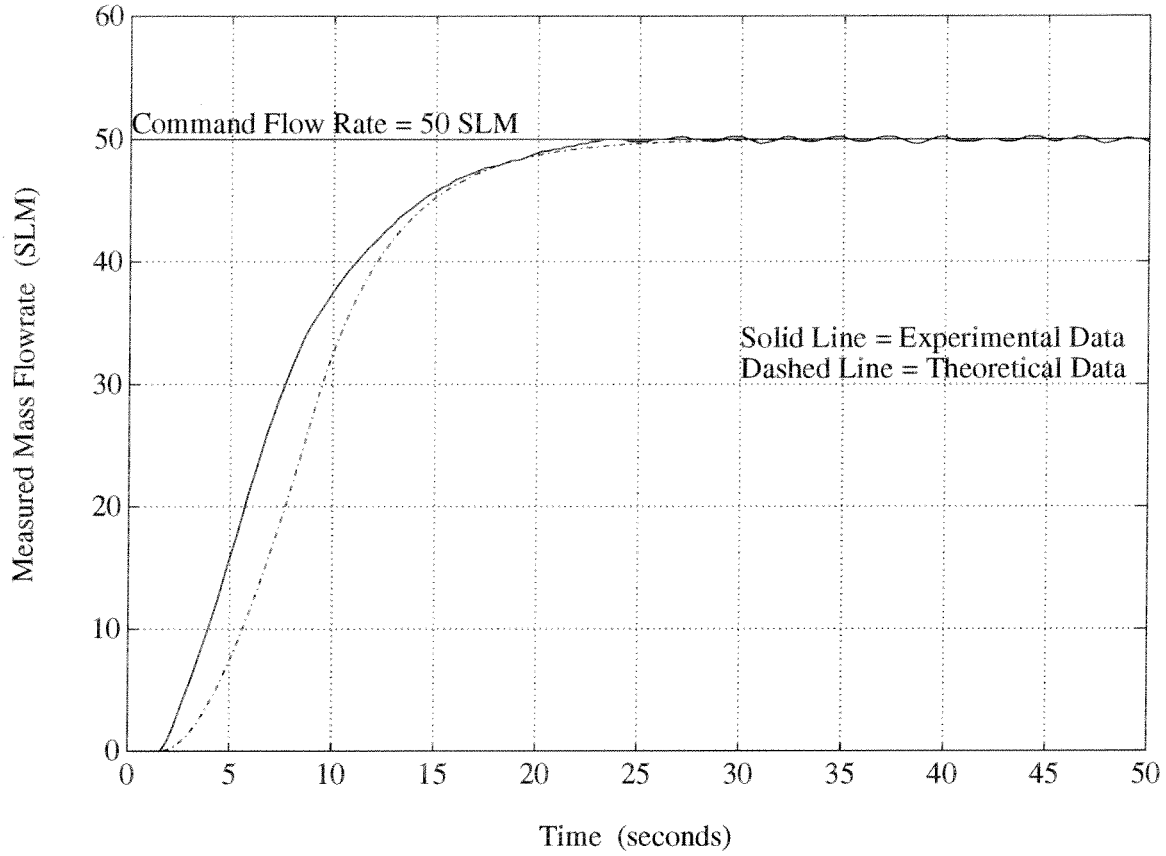

Figure 38. Experimental Results of the Mass Flow Rate Controller Operating Off-Design (Zero @ 0.26, Pole @ 10) --Measured Mass Flow Rate

measured mass flow rate and of control voltage vs. time are very similar to those for on-design conditions (Figures 36 & 37) and to theory supports the claim that the zero location should remain at the design location of 0.2339.

Now that the zero value has been fixed, the pole value can be adjusted to see if noise propagation can be reduced without sacrificing too much system response speed. The attenuation of noise is improved by moving the pole closer in towards the origin. This effectively lowers the amplification of higher frequency noise. During the design phase, however, moving the pole too close to the other system dynamics lowered the quality of the control system response so that a limit exists to the amount of noise attenuation that can be present.

A pole placement of about 2.9 has been shown theoretically to be the minimum value before system oscillations might become a problem. Experimentally, the plot

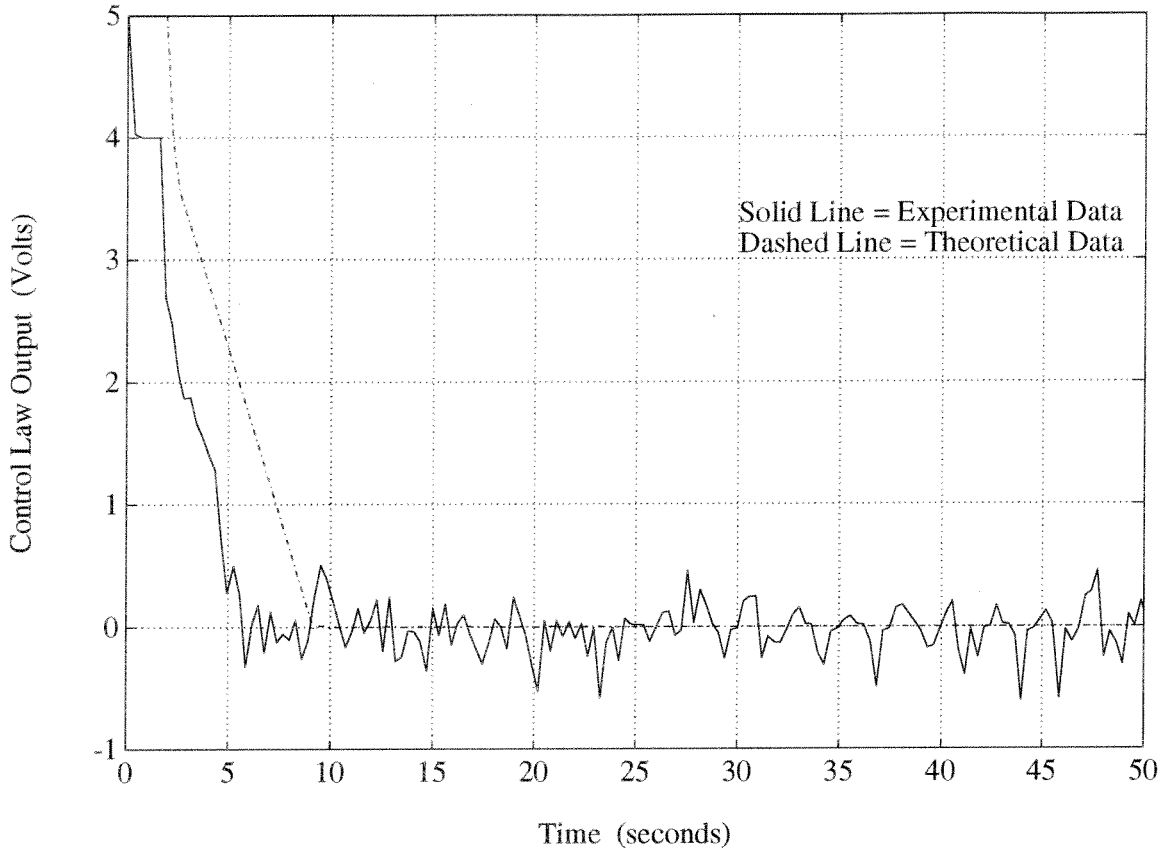

Figure 39. Experimental Results of the Mass Flow Rate Controller Operating Off-Design (Zero @ 0.26, Pole @ 10) -- Control Voltage

of control law voltage vs. time for this case (Fig. 43) does show a noticeable reduction in noise amplification. Some slight overshoot may have occurred initially, but is very minor, and the oscillations of the control law voltage appear to have become centered about zero almost immediately. An oscillation with a frequency of about 0.2 sec^{-1} is quite prominent in this case, however, which is where the system poles are supposed to be located. This means that the high gain required at this relatively low mass flow rate in order to try and keep the steady state mass flow rate within 0.5% is keeping the control system from reaching a steady state. In this way, the purpose of setting the gain has been defeated since the oscillations cause the mass flow rate to fluctuate beyond the range of ±0.5%. If these oscillations are unacceptable, the accuracy requirement may be relaxed slightly to try and remove the oscillations. This is a problem inherent in the system

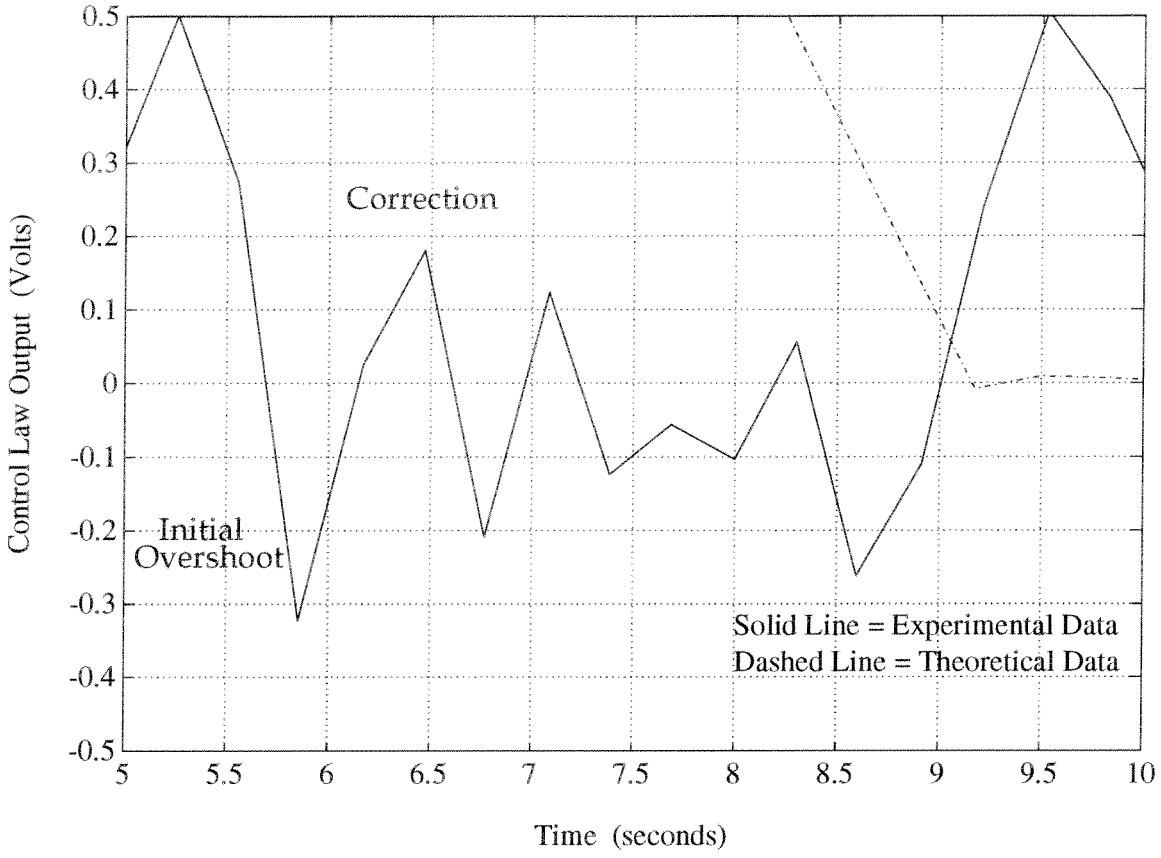

Figure 40. Experimental Results of the Mass Flow Rate Controller Operating Off-Design (Zero @0.26, Pole @ 10) -- Close-up of Fig. 39

hardware and may be solved in future systems by adding another speed of operation to the valve actuator. In this way, once the control system has brought the mass flow rate to within a specified range, the speed of the actuator can be reduced so that steady state may be more easily maintained. The plot of measured mass flow rate vs. time (Fig. 44) follows the theoretical results so that the true mass flow rate has likely been set to the proper value, but the oscillations are evident here as well. By relaxing the accuracy requirement to 1% from 0.5%, the oscillations have been reduced measurably as shown in Figures 45 & 46. In these figures, the recorded accuracy of the measurements is better than expected and suggests that the reduction in gain may increase the accuracy of the system when some noise is present. Later are some experimental results for the setting of higher mass flow rates in which the theoretical accuracy has been maintained at 0.5% and

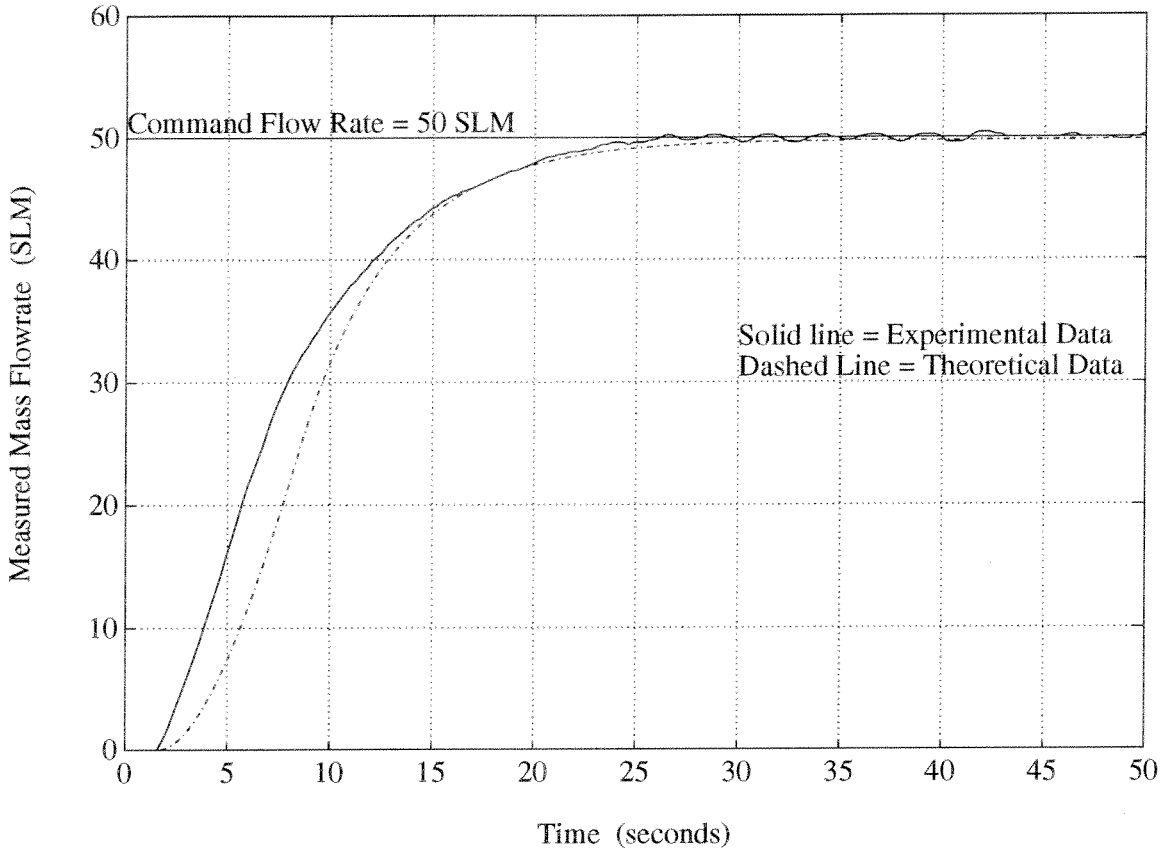

Figure 41. Experimental Results of the Mass Flow Rate Controller Operating Off-Design (Zero @ 0.22, Pole @ 10) -- Measured Mass Flow Rate

the oscillations have been virtually removed since the required gain at the higher flow rates is less.

All of the preceding results have been for the same system conditions of 1000 psig upstream pressure, choked flow through the valve orifice, and a command flow rate of 50 SLM. The following two plots (Figures 47 & 48) demonstrate the operation of the system for an upstream pressure of about 625 psia and a higher command flow rate of 125 SLM. The flow has been maintained until the pressure in the fill tank nearly equalizes with the upstream pressure to show the operation of the controller for the lower pressure setting and to show what happens as the flow unchokes.

Since the commanded flow rate is higher, the required controller gain for maintaining 0.5% accuracy is lower, and the oscillations in the flow rate have

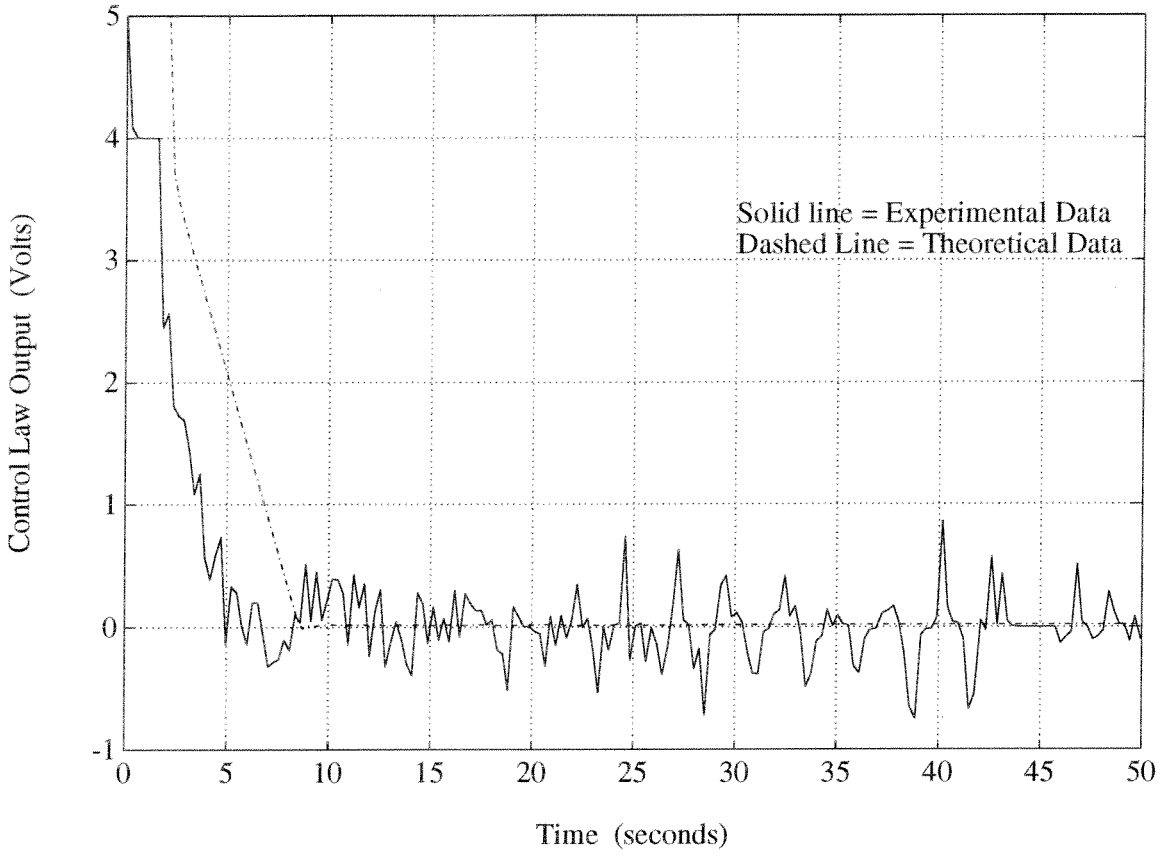

Figure 42. Experimental Results of the Mass Flow Rate Controller Operating Off-Design (Zero @ 0.22, Pole @ 10) -- Control Voltage

nearly disappeared as expected. This confirms the idea that the oscillation problem at the lower flow rates is hardware related. The first noticeable decrease in the mass flow rate occurs at about 75 seconds which, from the plot of pressure vs. time (Fig. 49), corresponds to a fill tank pressure of about 325 psia. Using the *maxvalve.m* program (Appendix A.4), a plot of orifice Mach number vs. upstream pressure for the case where the fill tank pressure is 325 psia (Fig. 50) shows that the theoretical unchoking point for these conditions is, indeed, at about 625 psia. On the plot of measured mass flow rate vs. time (Fig. 47), a line has been drawn corresponding to 99% of the commanded mass flow rate (125 SLM). The controller is able to keep the mass flow rate to within 1% of the setpoint value for about 45 seconds beyond the unchoking of the orifice after which time the pressure in the fill tank becomes too nearly equal to the upstream pressure for the flow rate to be

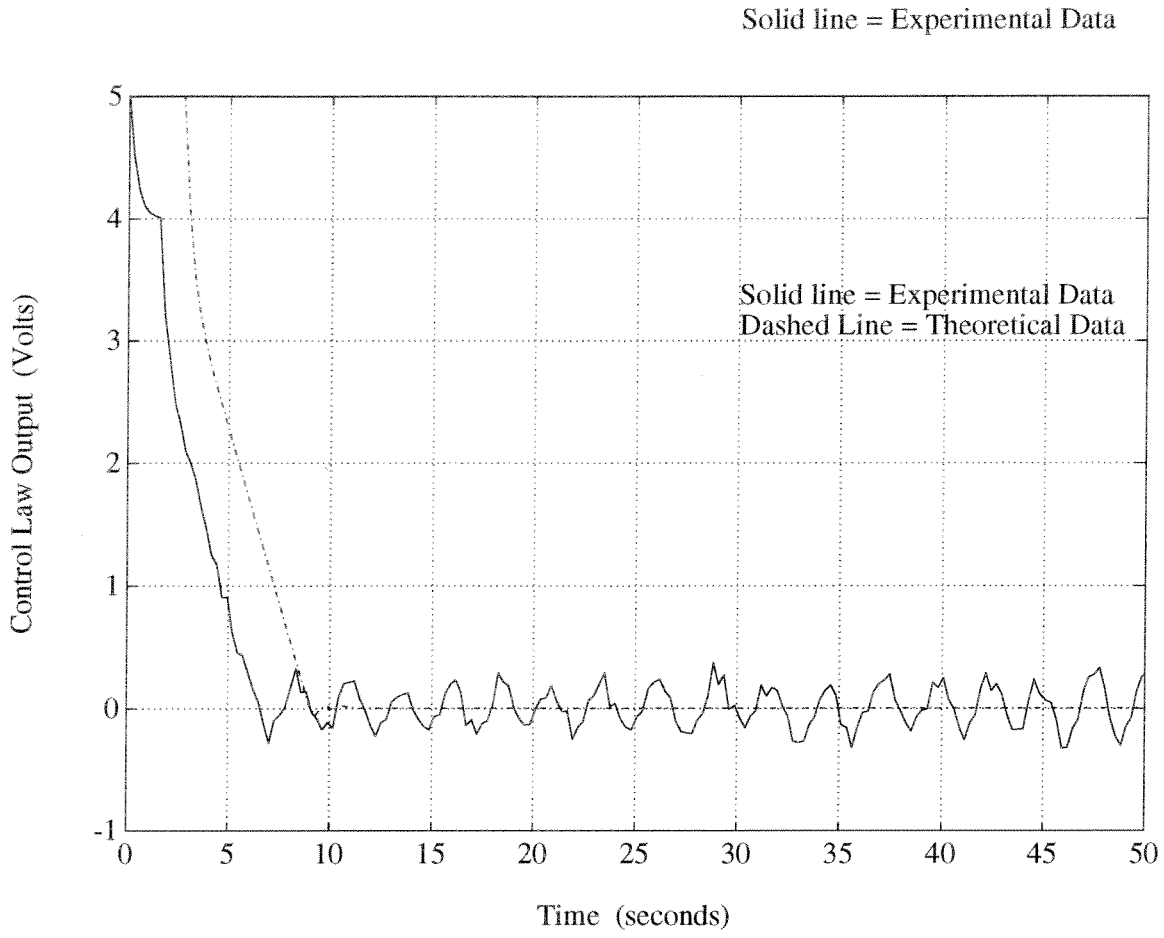

Figure 43. Experimental Results of the Mass Flow Rate Controller With Noise Attenuation (Zero @ 0.2339, Pole @ 3) -- Control Voltage

held constant. The plot of pressure vs. time shows that the flow rate is held to within 1% up to a fill tank pressure of 520 psig which is about 87% of the upstream gas pressure. In the current sonic orifice method for setting mass flow rates, however, the highest possible fill tank pressure before unchoking occurs in this case is 350 psig. The mass flow rate controller therefore offers a significant improvement in the amount of the source gas that can be utilized.

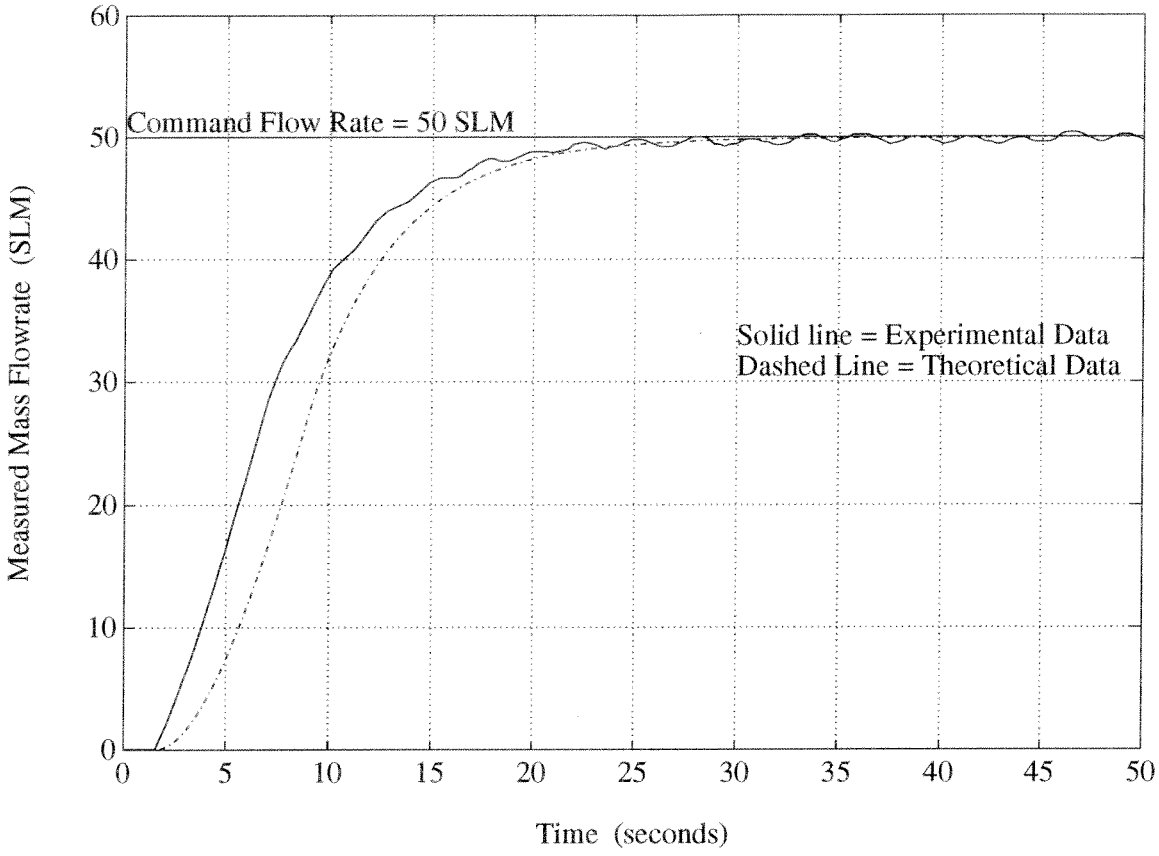

Figure 44. Experimental Results of the Mass Flow Rate Controller With Noise Attenuation (Zero @ 0.2339, Pole @ 3) -- Measured Mass Flow Rate

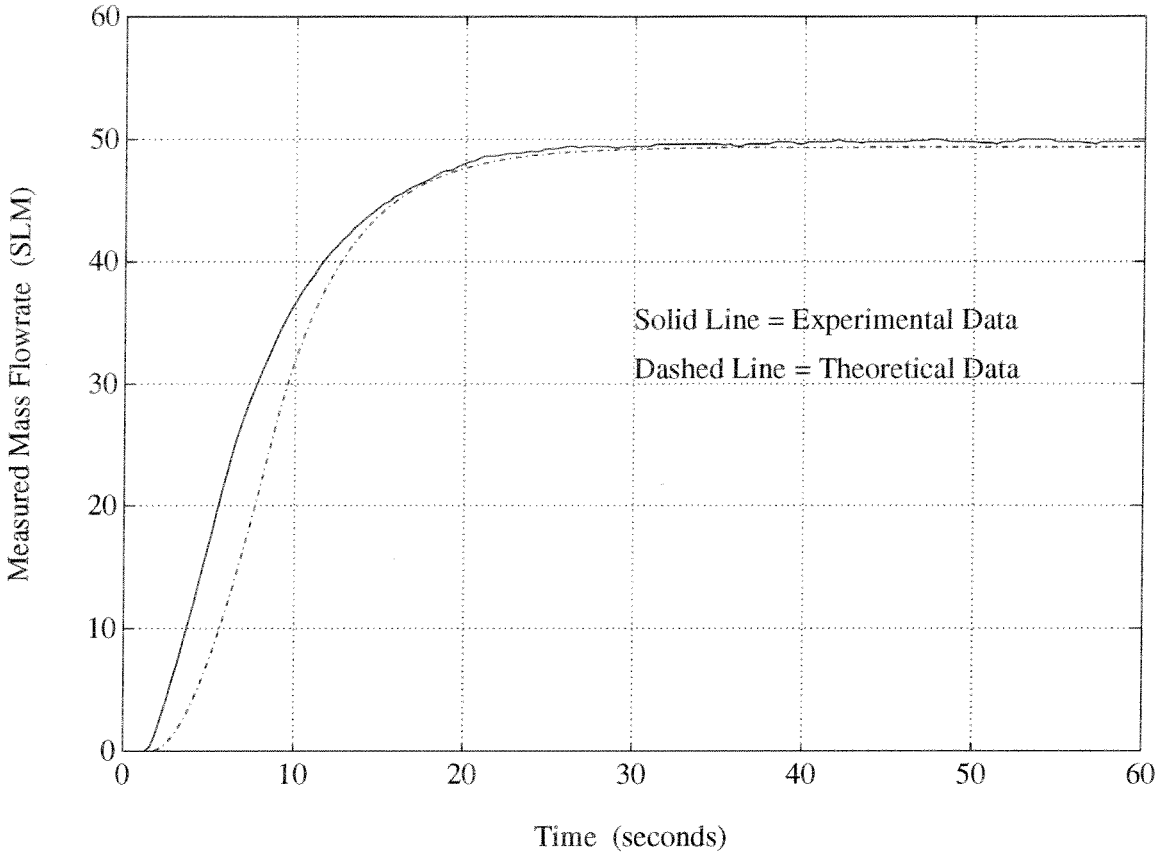

Figure 45. Experimental Results of the Mass Flow Rate Controller Operating With Reduced Controller Gain -- Measured Mass Flow Rate

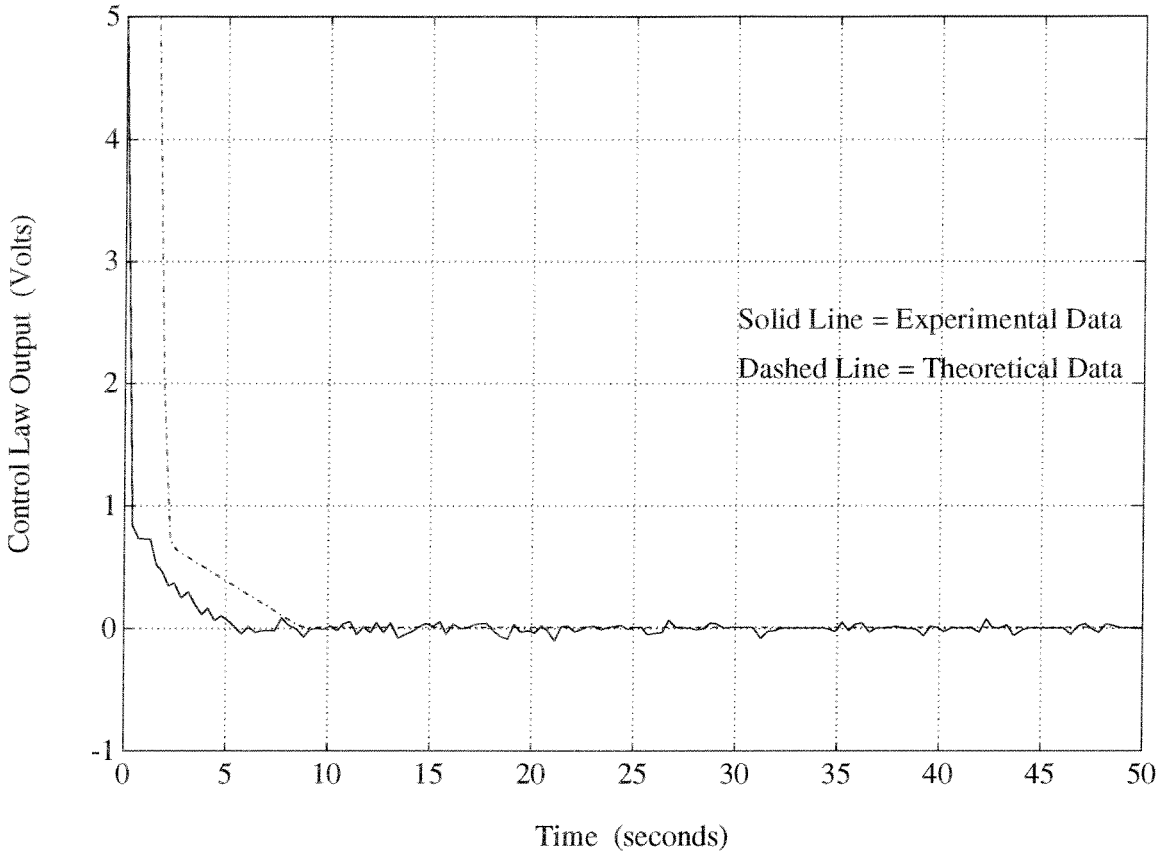

Figure 46. Experimental Results of the Mass Flow Rate Controller Operating With Reduced Control Law Gain -- Control Law Output

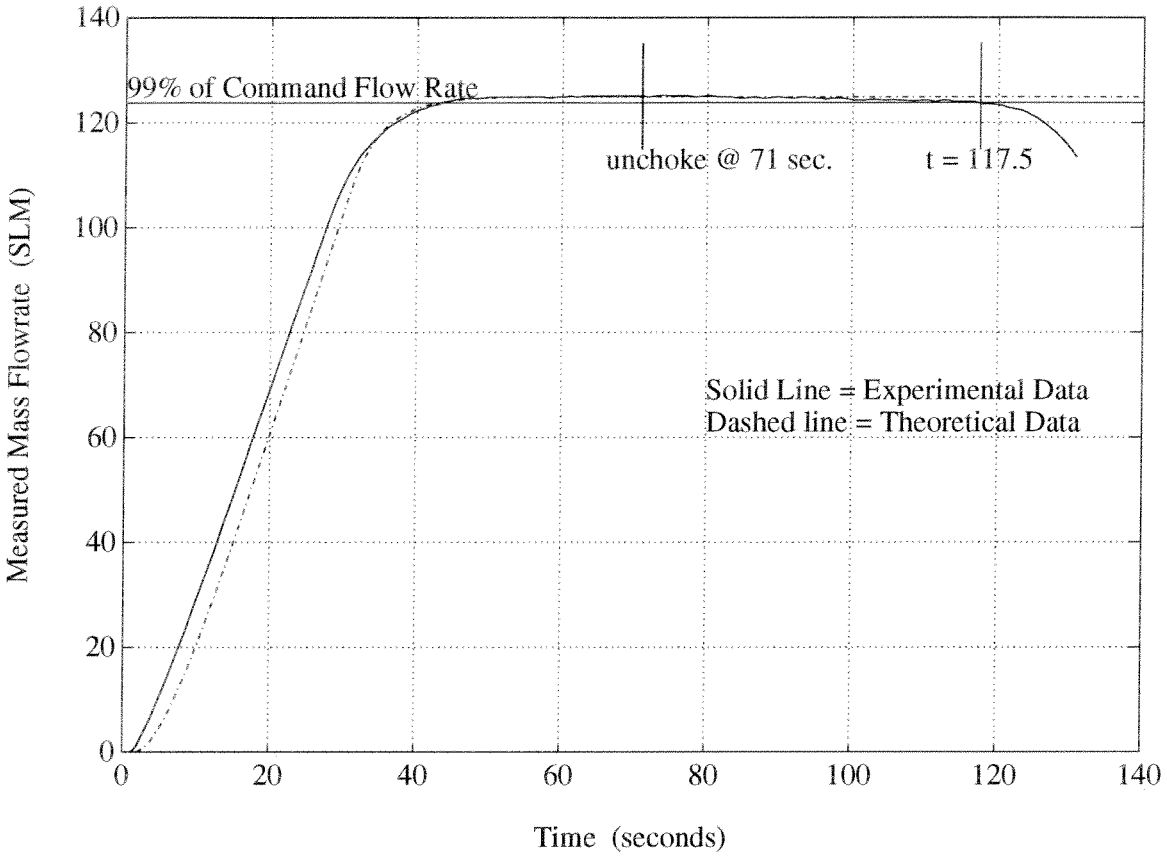

Figure 47. Experimental Results of the Mass Flow Rate Controller Operating Under Low Gain Conditions (Upstream Orifice Pressure = 625 psia)

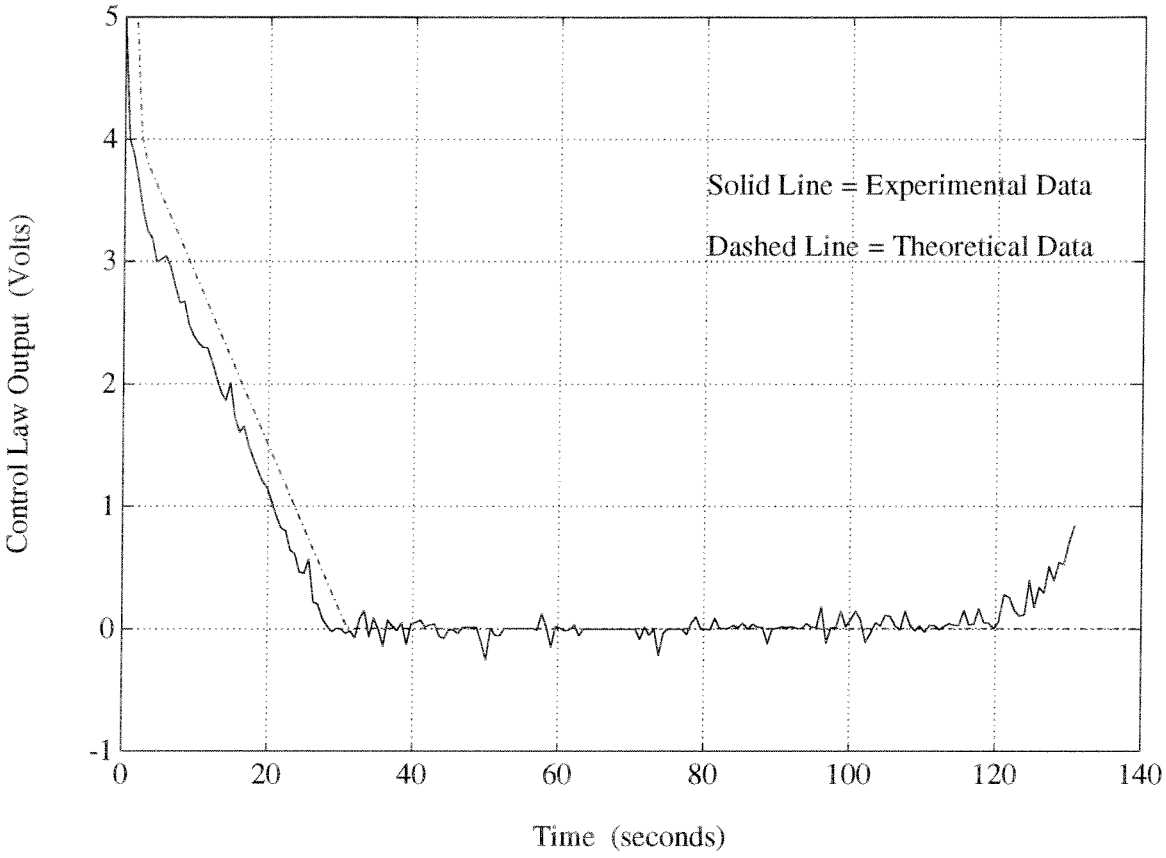

Figure 48. Experimental Results of the Mass Flow Rate Controller Operating Under Low Gain Condtions (Upstream Orifice Pressure = 625 psia)

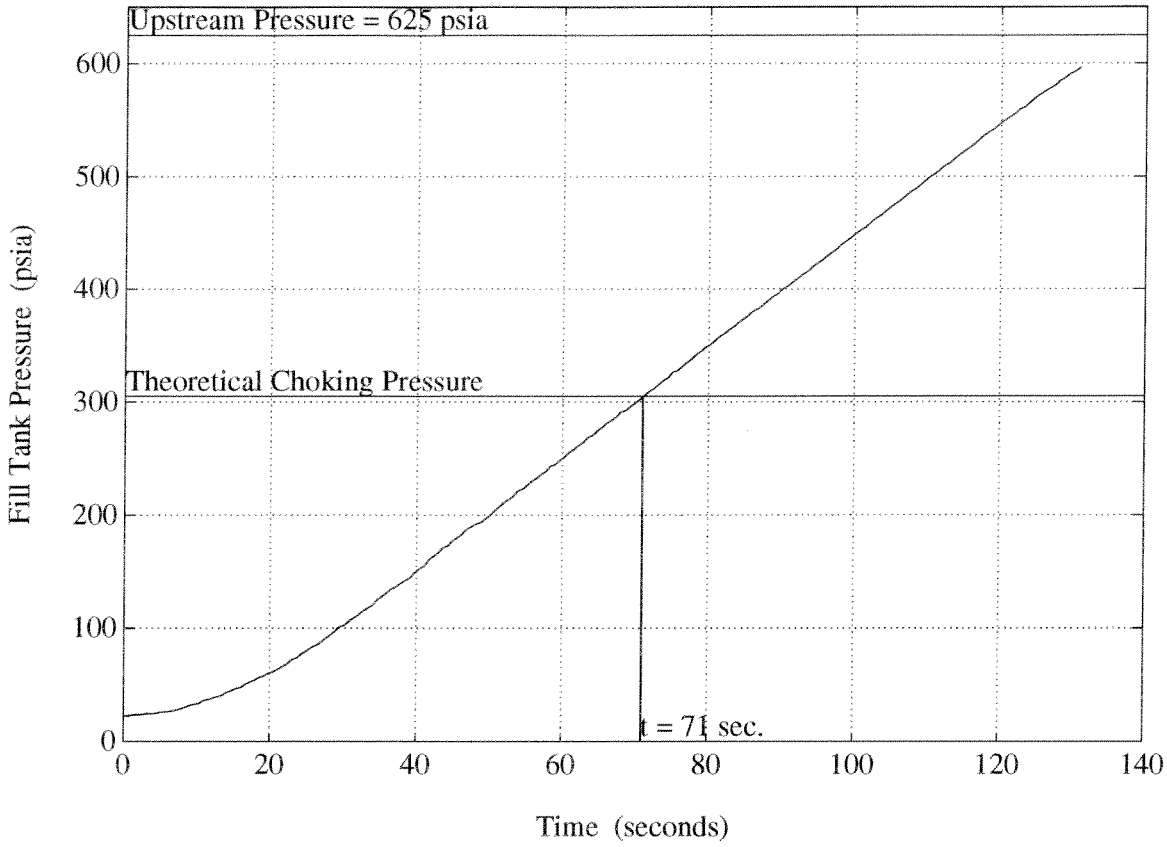

Figure 49. Experimental Results of the Mass Flow Rate Controller Operating Under Low System Gain Conditions (Upstream Pressure = 625 psia)

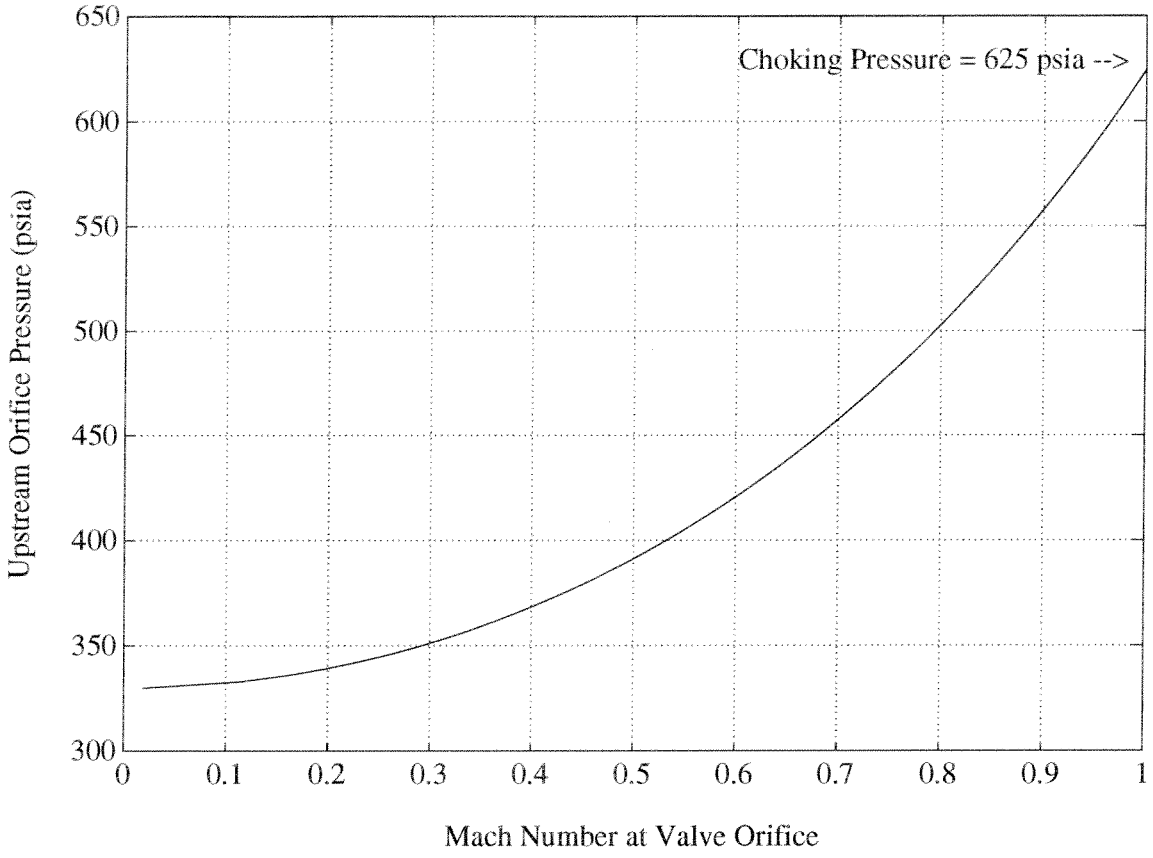

Figure 50. Theoretical Determination of Upstream Pressure for Choking Valve Orifice When P_f = 325 psia Corresponding to Figures 47-49

7.2 Mass Flow Meter Calibration Demonstration

A full calibration of the mass flow meter has not been performed here, but the mass flow meter readings at three different flow ranges have been correlated with the readings of pressure and temperature (and therefore mass since the volume and gas constant are known) from the fill tank in order to demonstrate the general calibration process. In Table 19 appear some data regarding accuracy of the

Table 19: Calibration Instrumentation

Measurement	Instrument Type	Accuracy	Value or Range
Pressure	Thin-Film Steady State Pressure Transducer	±0.4% F.S.	0-1000 psig
Temperature	J-Type Thermocouple Probe	±0.5°C	250-350°C
Volume	Displacement Measurements	±0.5%	7.00 Liters

measurements of pressure, temperature, and volume. Since the mass flow rates will be determined by taking the difference of the computed mass at two different time increments, some cancellation of error is likely to occur if the distribution of error is not entirely random in the measurement probes and if the range of measurements is not too large. When computing the measurement accuracy, however, the worst case will be assumed where the initial pressure and temperature measurements are at the lower end of their accuracy limits, and the final pressure and temperature measurements are at the higher end of their accuracy limits before the numbers are used to compute the mass differential. The equation used to compute the mass flow rate in SLM from the pressure and temperature data is given by:

$$\dot{M}_{exp} = \frac{\Delta M}{\Delta t} = \frac{V \cdot T_S}{P_S \cdot \Delta t}\left[\left(\frac{P_F}{T_F} - \frac{P_I}{T_I}\right)\right] \text{(SLM)} \qquad \text{(Eq. 71)}$$

where the volume, V, is in Liters, the standard temperature and pressure, T_s

and P_s, are 273.15 K and 1.01×10^5 Pa respectively, the pressure and temperature values are in Pascals and degrees Kelvin, and the time difference, Δt, is measured in minutes.

The demonstration will be given for three different flow rate settings: 50, 100 and 150 SLM. The plot of measured mass flow rate vs. time for the 50 SLM case has already appeared as Fig. 45 in the previous section and the plots for the other two cases as well as the pressure vs. time histories are given here (Figures 51-55).

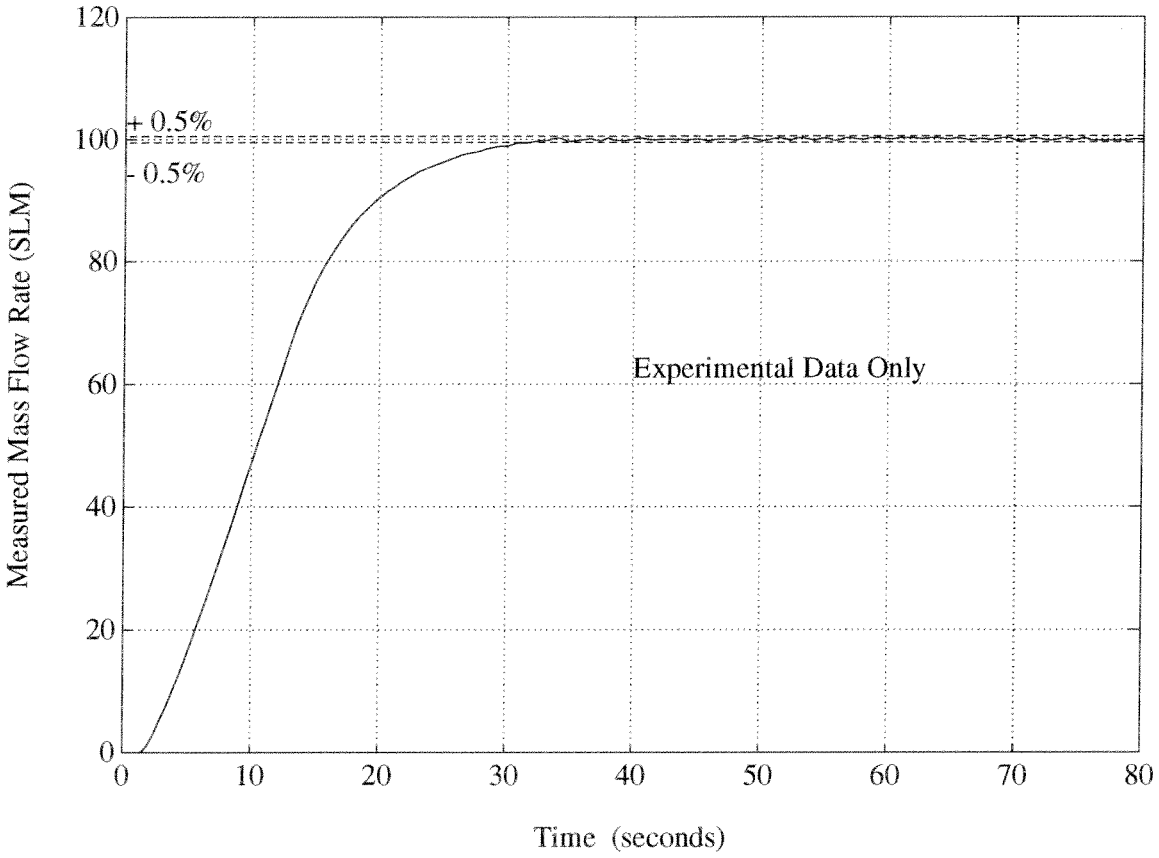

Figure 51. Calibration Run Using the Mass Flow Rate Controller to Maintain 100 SLM (Upstream Pressure = 1000 psig)

For the plots of measured mass flow rate, the voltage values have been multiplied be a factor of 40 which is the conversion factor from Volts to SLM supplied by the manufacturer. The temperature histories are not shown here in graphical form, but the data is recorded along with the pressure and flow meter measurements in Table in which the mass flow rates computed from these data have been presented.

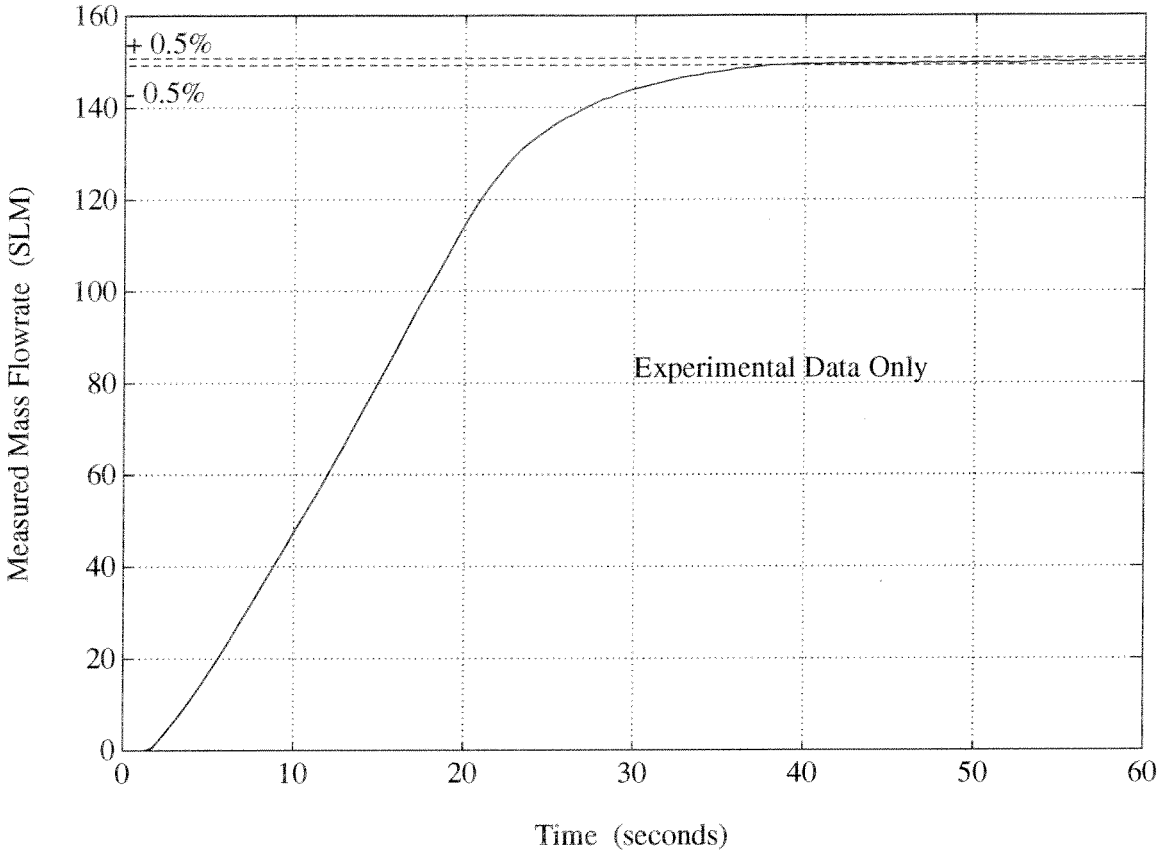

Figure 52. Calibration Run Using the Mass Flow Rate Controller to Maintain 150 SLM (Upstream Pressure = 1000 psig)

Table 20: Experimental Mass Flow Meter Calibration Results

Figs.	P_F(MPa)	T_F(K)	P_I(MPa)	T_I(K)	Δt(sec)	$\dot{M}_{exp}$(SLM)	$\dot{M}_m$(SLM)
45, 53	15.27	298.4	10.91	297.5	20	56 ±10	50
51, 54	34.19	304.5	17.52	301.5	40	104.7 ±4.6	100
52, 55	33.16	307.2	20.78	303.8	20	152.8 ±10	150

The times used to determine where to obtain the initial mass readings have been chosen near to where the mass flow rate has become within ±0.5% of the set-point value. In the interest of conserving source gas, the flows have been carried

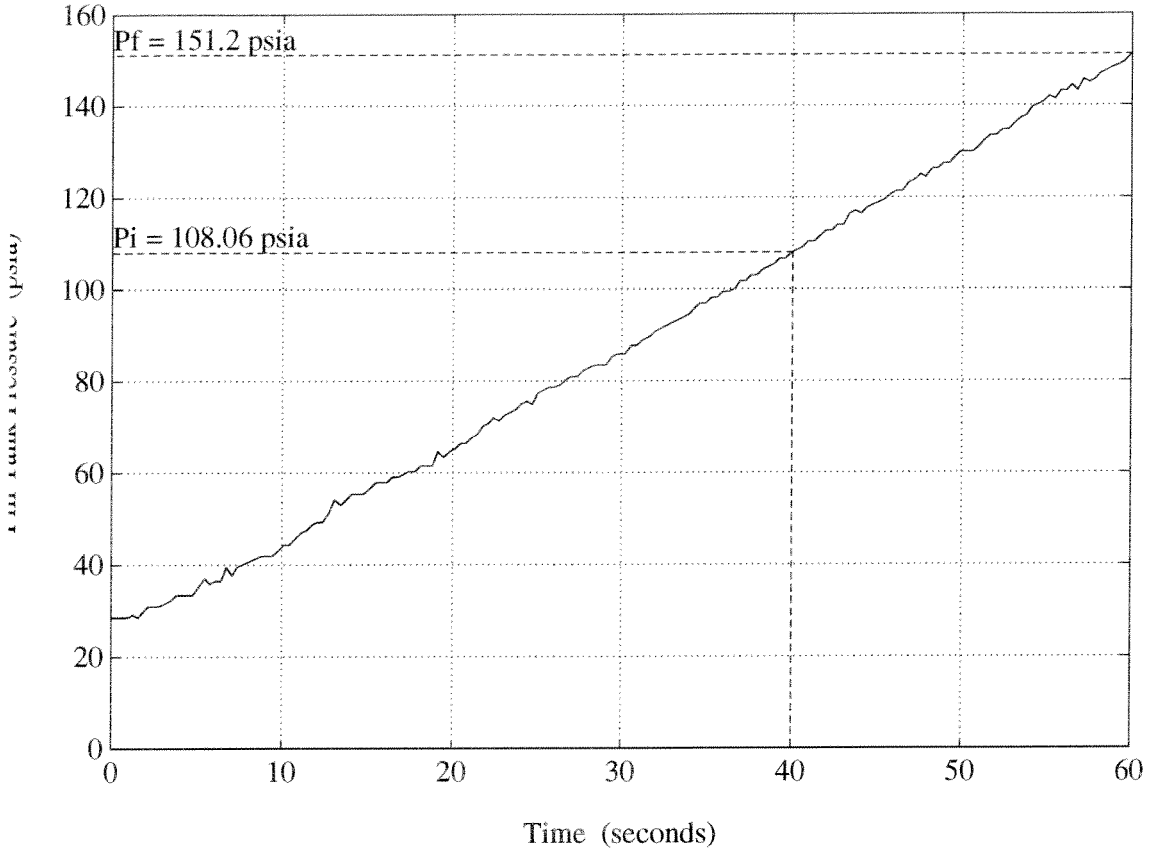

Figure 53. Pressure vs. Time History Corresponding to Fig. 45 (50 SLM)

out for 60 seconds in the 50 and 150 SLM cases, and for 80 seconds in the 100 SLM case. This resulted in time differentials of 20 seconds and 40 seconds respectively for use in computing the mass flow rates from the experimental data. The results of this analysis (Table 20) show that the mass flow rates computed from the pressure and temperature data agree with the mass flow meter measurements within the maximum error limits of the measurements. Unfortunately, for these short time differentials used to compute the mass flow rates, the error limits are higher than desirable. As the time difference between the measurements increases, the error limits decrease since the errors in each measurement will become less significant when the mass difference is greater. While these results are not entirely conclusive, the methods used may be applied to mass flow meters in the future before the mass ratio control system is put into operation. This provides a

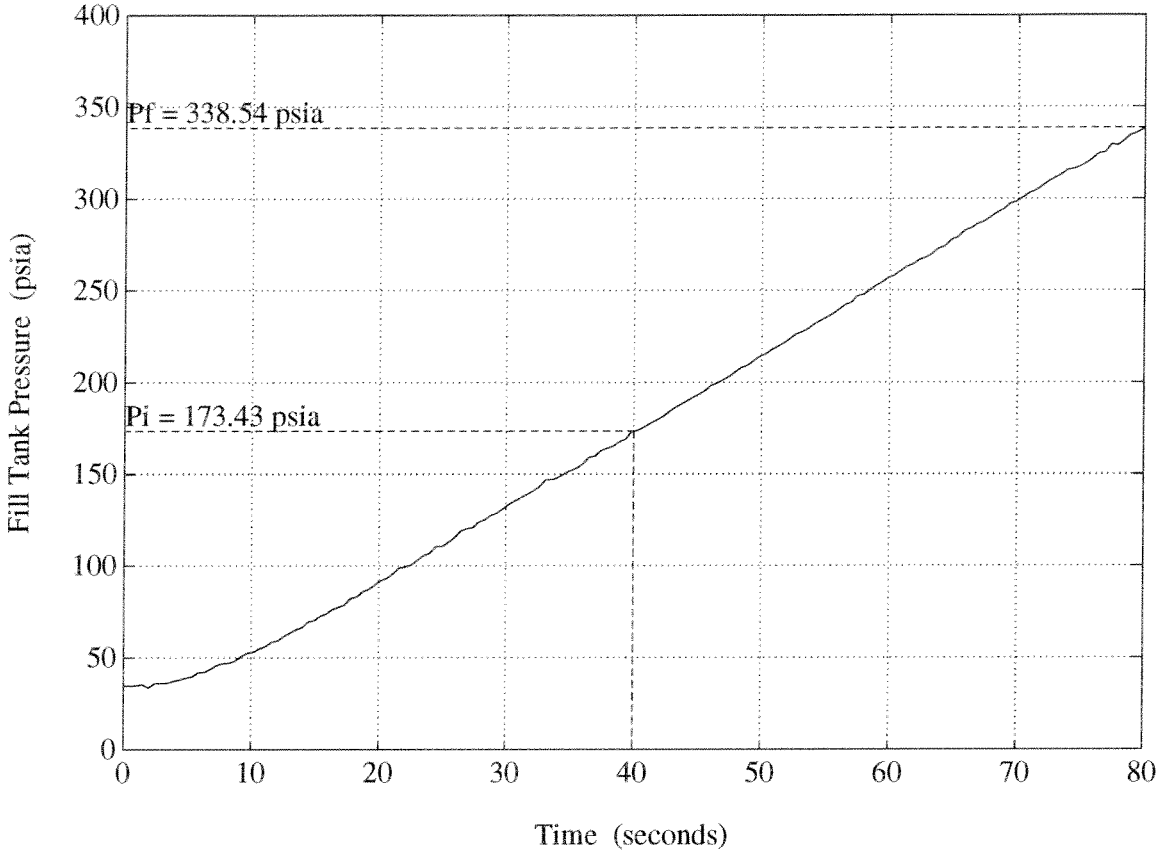

Figure 54. Pressure vs. Time History Corresponding to Fig. 51 (100 SLM)

relatively simple and inexpensive method for calibrating mass flow meters.

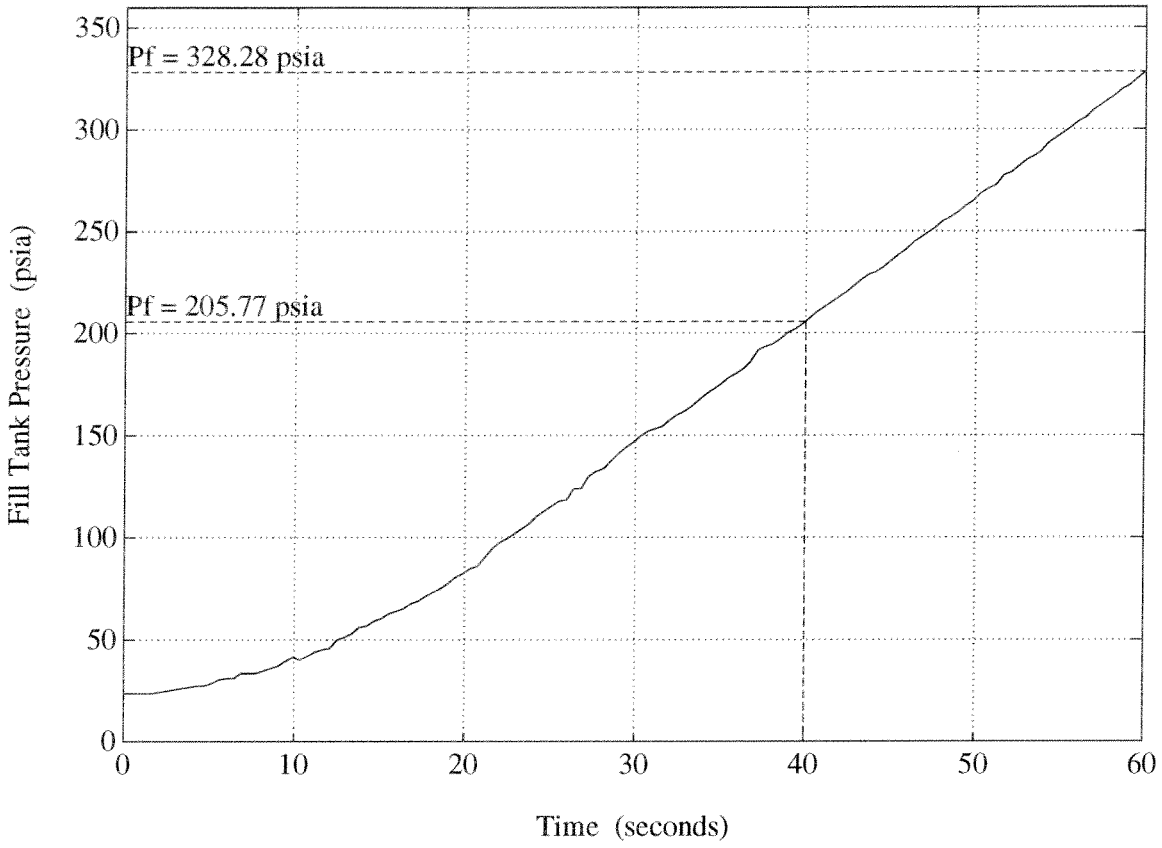

Figure 55. Pressure vs. Time History Corresponding to Fig. 52 (150 SLM)

7.3 Mass Ratio Controller

From the theoretical design considerations, the operation of the mass ratio controller without control dynamics is expected to be unstable. Rather than cause potential problems with the control system components by trying to show this instability, the analysis here begins with the operation of the controller using the control laws developed in Chapter 5.

Unfortunately, since only one set of control components is available for the prototype unit, the testing of the mass ratio controller can only be performed by simulating the output of a primary gas flow for use as a command input to the mass ratio controller. Temperature and Pressure data has been taken during these experimental runs, however, so that an independent means exists for verifying that the correct amount of mass has accumulated in the fill tank. The simulated mass flow rate of the primary gas is merely a constant for most of the experimental runs so that the results may be more easily applied to the nonlinear simulations performed in Chapter 5. One run has been performed with a fluctuation in the command mass flow rate which simulates the plugging and unplugging of the valve orifice on the primary gas line. This demonstrates the ability of the mass ratio control system to maintain constant mass ratios in the event of the disruption of the primary gas flow.

The first series of plots (Figs. 56-57) demonstrates the on-design response of the mass ratio controller. The input to the system is a constant 50 SLM which simulates a case where the primary gas is flowing at a constant mass flow rate, and then the mass ratio controller is turned on for the secondary gas. The mass ratio vs. time data (Fig. 56) shows that the mass ratio formed with the filtered mass flow rate data steadily approaches the set-point value of unity without overshoot, and comes to within 0.5% of the set-point after about 40 seconds. Verification that steady state has been achieved is obtained from Fig. 57 which shows that the control voltage has fallen permanently within the actuator dead-zone range of ± 0.02 Volts after about 12.5 seconds. To determine whether or not the mass ratio has been accurately set by use of the feedback filter reading of the mass flow rate, the pressure and temperature data can be used much as in the calibration section, only here we are concerned with the total mass which has accumulated in the fill tank. As read from Table 21, the total accumulated mass as computed by the pressure and temperature data is within the accuracy of the measurement instruments of

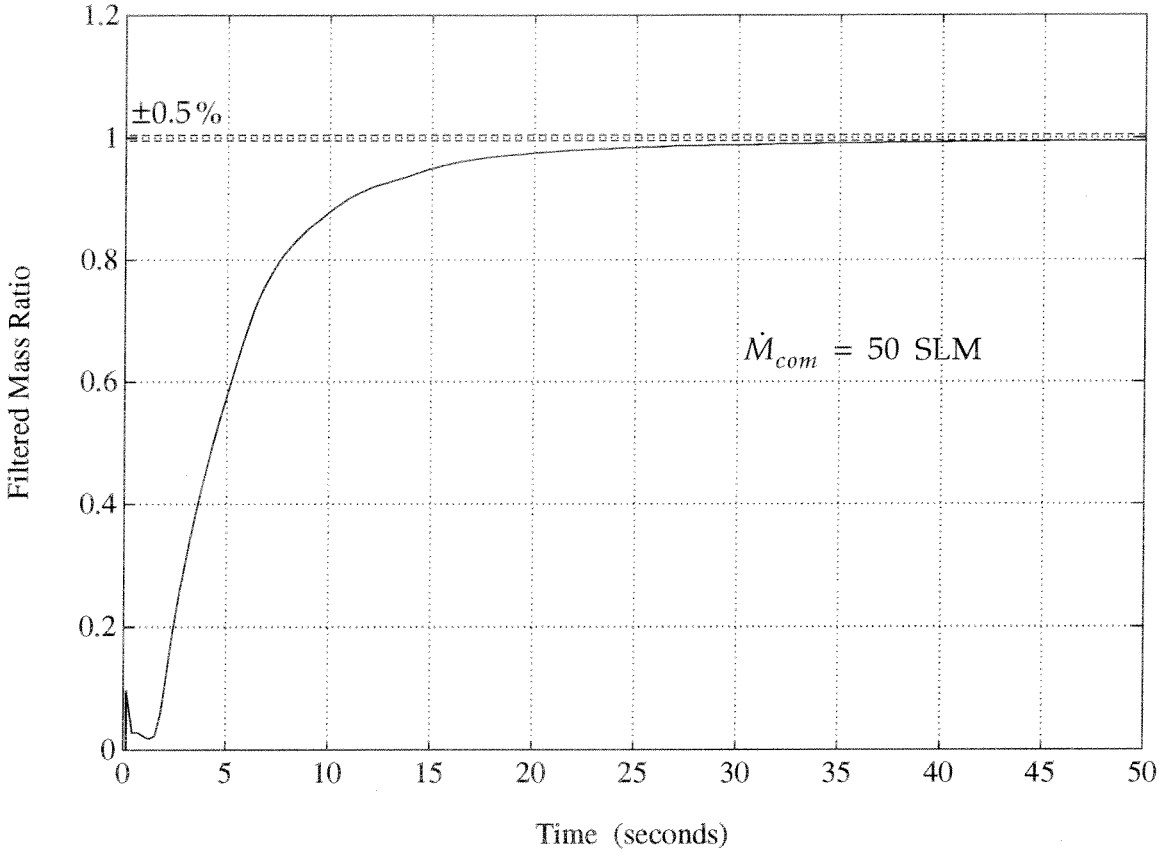

Figure 56. Experimental Results of the Mass Ratio Controller Operating at Design Conditions -- Filtered Mass Ratio Measurement

Table 21: Experimental Results for the Mass Ratio Controller

Figs.	P_F(MPa)	T_F(K)	P_I(MPa)	T_I(K)	Δt(sec)	M_{exp}(SL)	M_{com}(SL)	% E
56,57	0.8839	297.8	0.2046	295.2	50.00	43.06 ±3.4	41.67	3.2
58,59	1.073	298.7	0.2633	295.5	58.30	51.11 ±3.4	48.45	5.5
60	0.8713	297.5	0.1920	295.1	51.96	43.12 ±3.4	43.3	0.4

being equal to the command value.

The next data run has been performed to simulate the case of a non-constant flow rate of the primary gas. During the run as the measured mass ratio

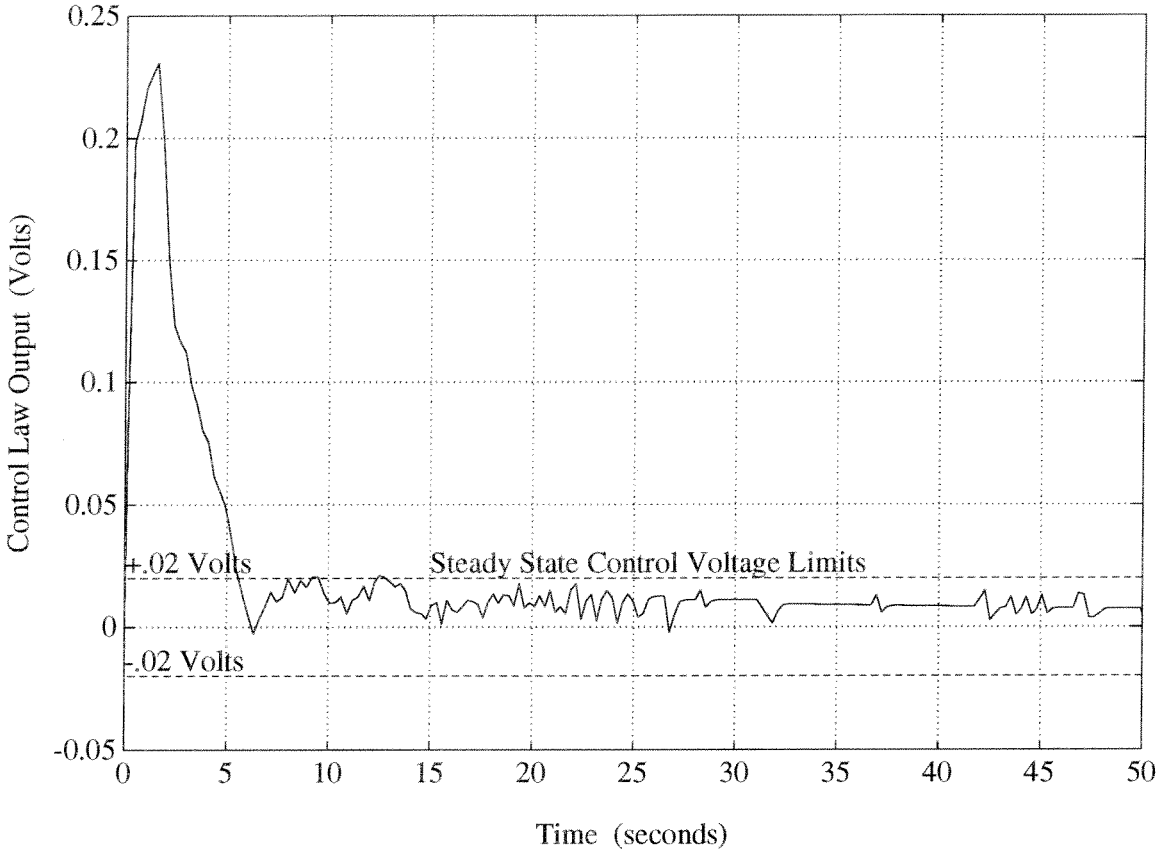

Figure 57. Experimental Results of the Mass Ratio Controller Operating at Design Conditions -- Control Voltage

approaches zero, the command flow rate has been varied from the setpoint and the response of the ratio controller measured. The plot of commanded mass flow rate vs. time (Fig. 58) shows the variations which have been made, and the corresponding plot of mass ratio vs. time (Fig. 59) suggests that the controller is still able to maintain a constant overall mass ratio. The quantitative results of this run appear back in Table 21 and further suggest that the mass ratio controller has been able to maintain a nearly constant mass ratio in the case of a low frequency unsteady input.

The final experiment has been performed to demonstrate the operation of the controller when the gas pressure upstream of the valve is dropped to 600 psig from 1000 psig. The shape of the mass ratio vs. time curve has been skewed slightly in the early time history, but the control system is able to bring the mass ratio up to

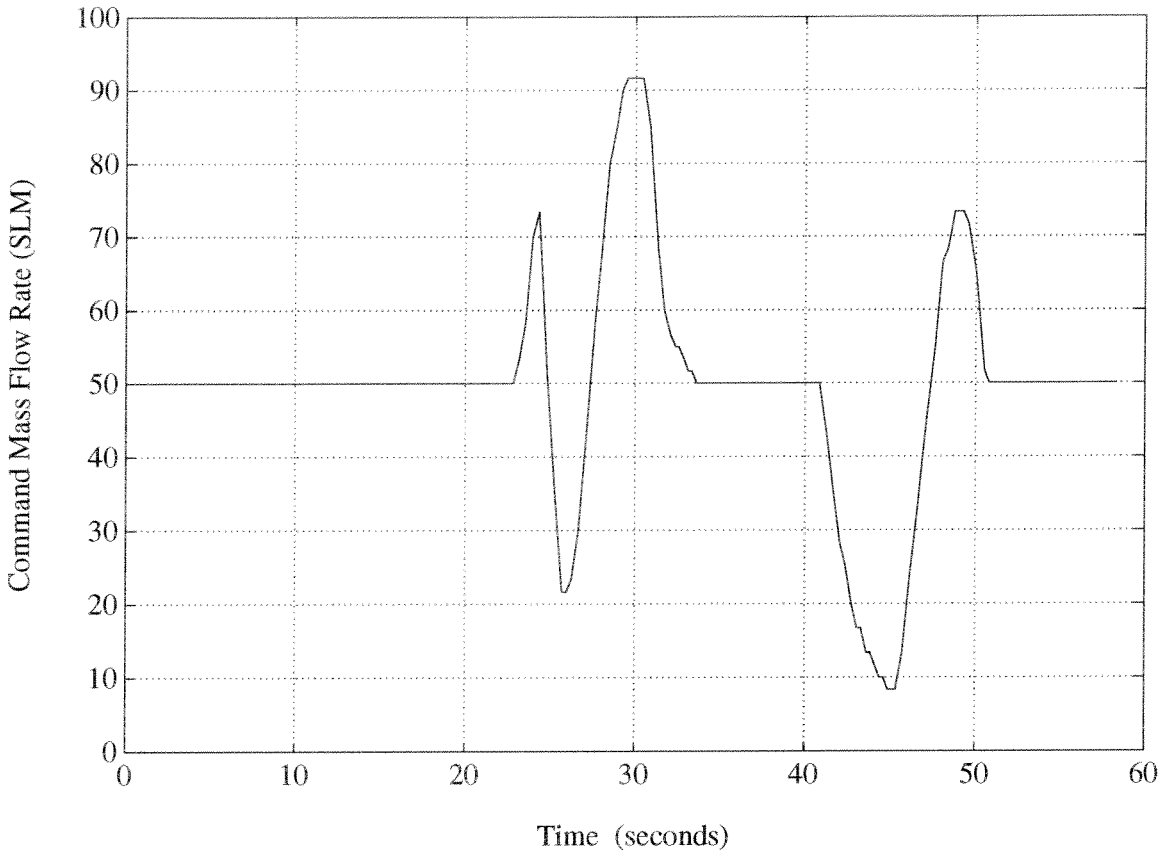

Figure 58. Variable Command Mass Flow Rate Input to the Mass Ratio Controller (see Fig. 59)

within the desired ±0.5% accuracy range after about 28 seconds. The quantitative calculations of accumulated mass also appear in Table 21 for this case, and these results also support the fact that the controller developed here is able to maintain reasonably accurate settings of mass flow ratios.

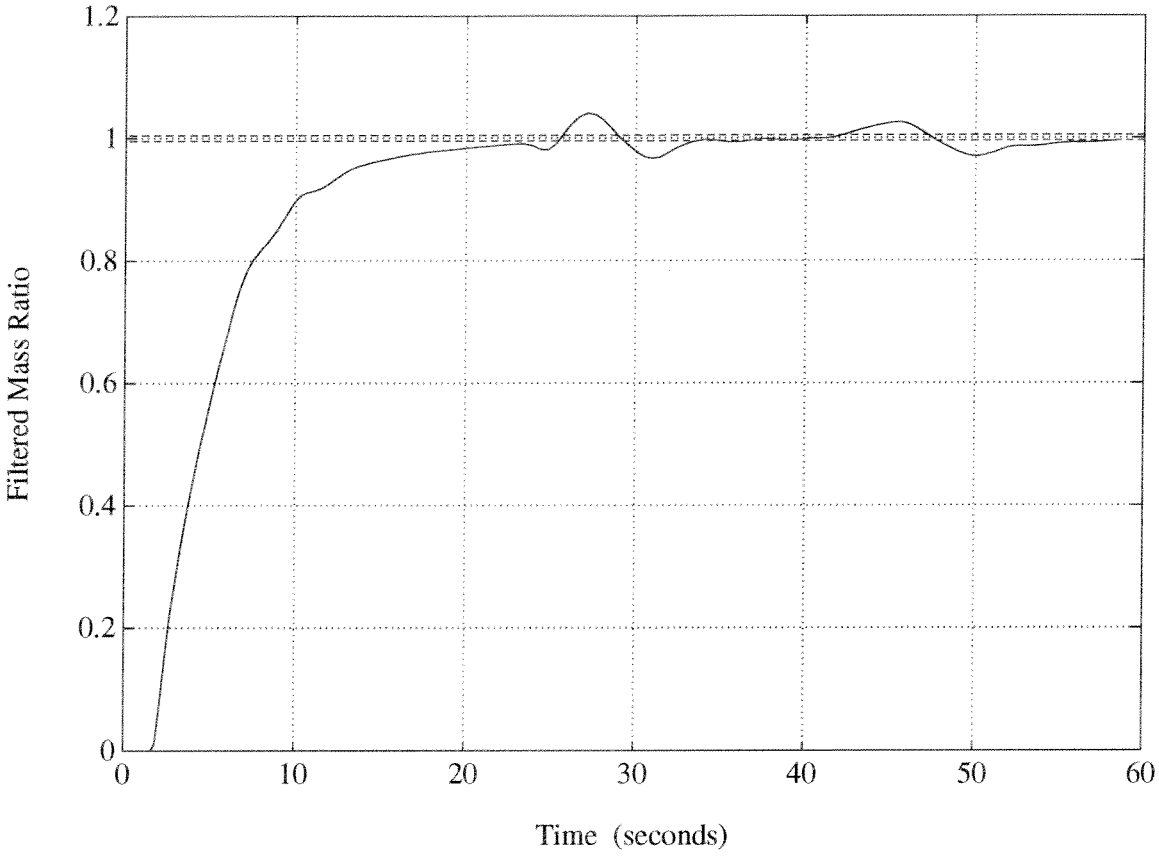

Figure 59. Measured Mass Ratio For the Case of Varying Mass Flow Rate Input to the Mass Ratio Controller

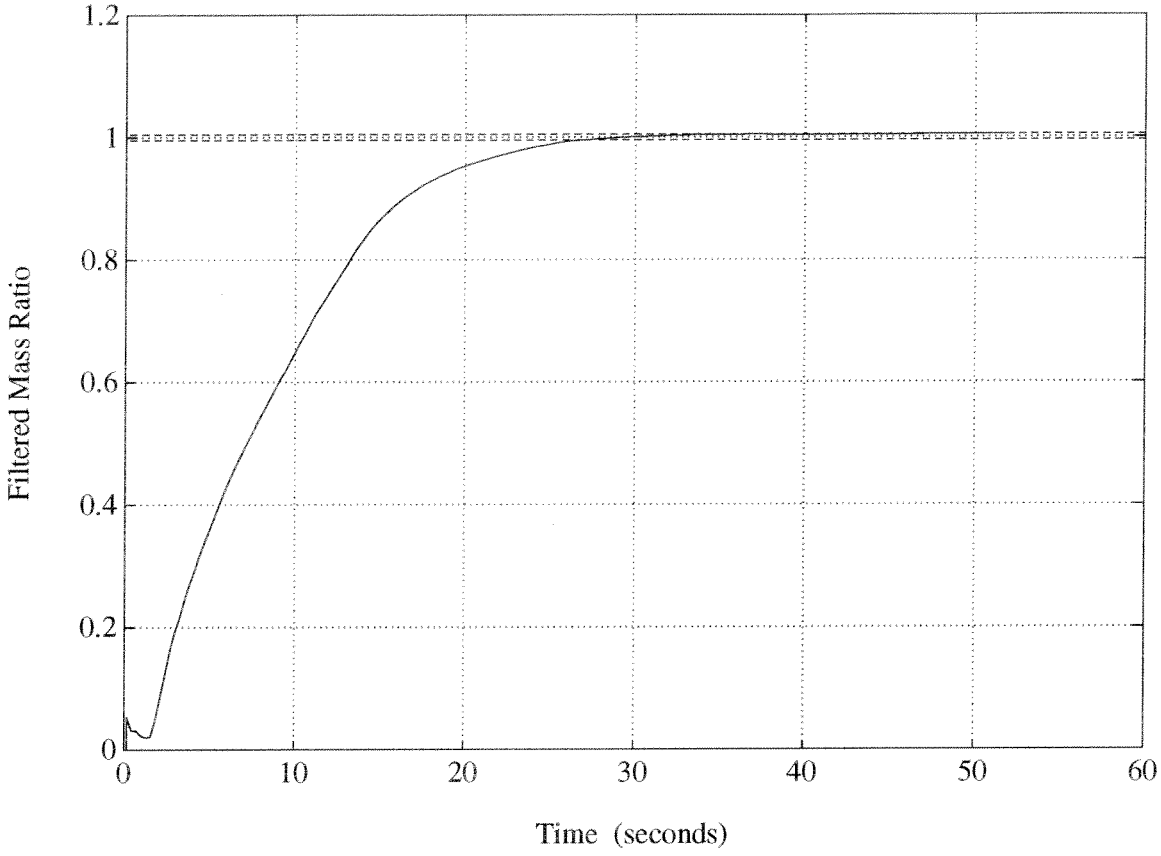

Figure 60. Experimental Results of the Mass Ratio Controller Operating at Reduced Gas Pressure Conditions (600 psig)

CHAPTER 8 CONCLUSIONS

The research and experimental work presented here has demonstrated that a feedback controlled gas mixing system may be used to accurately set the molar ratios of a multiple number of gases flowing at high pressure into a fill tank. A mass flow rate controller has been developed and shown to be capable of setting the mass flow rate of a primary gas to a constant level within a specified accuracy. A mass ratio control law has been designed which uses the mass flow rate measurements of the primary gas as an input and integrates the error signal between this flow rate and the flow rate of a secondary gas in order to set the mass ratio of the two gases to a specified value.

8.1 Comments and Reccomendations for Additional Work

A few more experiments are necessary to completely prove the control concepts by extending the analysis to other gases besides Nitrogen which exhibit non-ideal behavior such as methane and carbon dioxide. Since the prototype consists only of one flow system, the flowing of several gases simultaneously will still be necessary to discover what problems, if any, will be encountered when multiple gases are flowed together.

The overall accuracy of this system is dependent upon the calibration of the mass flow meters and upon the accuracy with which the transfer functions of the mass flow meters are known. Quantifying the performance of this control system needs to be performed more rigorously so that a certain level of accuracy can be guaranteed. The calibrations of the mass flow meters typically need to be performed only to account for slight deviations from linearity in the voltage output of the meters over a range of mass flow rates. The type of mass flow meters used (RTD) operate based upon heat transfer properties and ideally measure true mass flow rates independently of gas pressure and temperature. Some secondary effects may be encountered due to large changes in the gas pressure and temperature, but for the flow conditions experienced in the ram accelerator fill system, and in most other applications, the range of fluctuations in the gas properties will be small enough to be neglected. Even with large variations, however, the accuracy of the mass flow meter is only affected by one or two percent. If significant pressure and temperature variations are expected, and if the guaranteed accuracy needs to be

extraordinarily high, the flow meter calibrations may be broadened to account for these effects.

Even if the transfer function of the mass flow meter is not well known, the mass ratio of two gases may still be set. Given the delay in the meter readings, however, a long lag time is experienced which requires that a gas fill take a longer amout of time before the mass ratio can be set to a desired level. When the transfer function of the flow meter is known, a filter may be employed in the feedback path of the control system in order to speed the setting of the mass ratio. This has been thoroughly demonstrated in this thesis.

The method of calibration presented here has shown very promising results for being an inexpensive and simple means of calibrating the mass flow meters on-site. The pressure and temperature measurements have been made with relatively innacurate equipment, however, so that in the future, more accurate equipment should be used to perform the calibrations if higher accuracy is desired. Even with the innacurate pressure and temperature transducers, fairly high accuracy may be obtained which may be adequate for most applications.

8.2 Mass Flow Rate Controller

As this has been a first order design, many small changes can be recommended for future control systems. The most useful change would be to incorporate a control valve with the ability to reduce the actuator motor speed when lower flow rates are commanded. A fully linear actuator is not what is meant by this. Instead, the fast actuator operation is desirable when operating under the higher system gain and higher command flow rate settings, but when the controller is to be used for setting lower flow rates, the high speed operation of the control valve decreases the attainable accuracy.

The design methods for obtaining the mass flow rate control laws are simple single input single output linear control techniques. With the design of the prototype system, as long as significant changes are not made in any of the hardware components, a control law may be easily obtained for any similar control system. Fast time responses with almost no overshoot have been demonstrated so that a flow rate controller using RTD flow meters and servo actuated valves provides an accurate and easy means of controlling mass flow rates for a variety of

gas flow conditions.

8.3 Mass Ratio Controller

The most important design consideration in the case of the mass ratio controller is to know the transfer function of the flow meter as well as possible. In this way, even though the response of RTD flow meter is slow, accurate measurements of the true accumulated mass can be made by integrating the filtered output of the flow meter in a much shorter time than without a filter in the feedback path.

The experiments given here have only proven the ratio controller under a few conditions. More experiments will need to be performed in order to better define the operating envelope of the control system. The results of the analysis in this thesis do strongly suggest that the mass controller is capable of accurately setting the mass ratio of two gases for the conditions commonly experienced in the ram accelerator fill system. Defining the accuracy limits of the mass ratios obtained through the uce of the ratio controller is all that is really necessary before the control system becomes operational.

8.4 Control Implementation

A computer has been used to demonstrate the digital implementation of the ratio control system. This allows the possibility of using the computer to handle many routine tasks in perfoming gas mixing operations. For example, in the case of the ram accelerator, the computer may be easily programmed to ask for a desired set of molar gas ratios and the desired ram tube fill pressure and then perform the filling operation fully automatically.

If these extra capabilities are not necessary, the control laws are simple enough to be easily implemented through an analog control circuit. This would reduce the cost of installing a gas mixing system, but at the expense of flexibility and automation.

REFERENCES

1. Olin et al., United States Patent Number 4,487,062., Dec. 11, 1984.

2. Shames, Irving H., *Mechanics of Fluids*, 2nd ed., McGraw Hill, Chapter 11, 1982.

3. Chemical Rubber Company, *CRC Standard Mathematical Tables 28th ed.*, CRC Press.

4. The Mathworks Inc., Matlab version 3.5f, South Natick MA, June 9, 1992.

5. Lyons, Jerry L., *Lyons Valve Designers Handbook*, Van Nostrand Reinhold Co., 1982.

Appendix A. COMPUTER PROGRAMS

A.1 mdot.m

```
%       12/4/91
%
%       This program will experimentally estimate the values of
%       the roughness coefficient and final pipe diameter for the current
%       Ram accelerator fill system.  This will be done by varying values of
%       E, and dp until the theoretical points coincide with the
%       experimental ones.

clear
clg
hold off

global M2 g f L dp Af A1


po=1.01e5;                          % initial in-tube pressure

N2                                  % enters gas data
R=8314.4/MW;
T=295;
vt=.01824;                          % Ram tube volume

stop=0;
while stop==0,
 point=input('Data point 1 or 2: ');
 if point==1,                       % one point of experimental data
  L=18;
  p1=1.01e5/14.7*(14.7+1000);
  pf=1.01e5/14.7*(14.7+460);
  t=41.77;
 end
 if point==2,                       % the other point
  L=10;
  p1=1.01e5/14.7*(14.7+900);
  pf=1.01e5/14.7*(14.7+410);
```

```
  t=34.77;
 end
 E=input('E= ');                    % This section allows user iteration
 df=input('df= ');
 Af=pi*(df/2)^2;
 mdexp=(pf-po)*vt/R/T/t
 dp=.152*.0254;
 A1=pi*(dp/2)^2;
 Gexp=mdexp/A1;

 M2=fzero('mach2',.9);
 Re=Gexp*dp/mu;
 f=.25/(log(E/3.7/dp)+(5.74/Re^.9))^2;
 M1=fzero('mach1',.1);
 mdcomp=A1*p1*M1*(g*(1+(g-1)/2*M1^2)/R/T)^.5

 stop=input('anything but zero to end: ')
end
```

A.2 mach1.m

```
%       12/2/91
%
%       This function is used to iteratively solve for the Mach Number
%       at an upstream location in a tube with friction (adiabatic) given
%       the downstream Mach Number.

function m1zero=mach1(M)

T1=M^(-2)-M2^(-2);

m1zero=T1+(g+1)/2*log(M^2*(2+(g-1)*M2^2)/(M2^2*(2+(g-1)*M^2)))-f*g*L/dp;
```

A.3 mach2.m

```
%       12/2/91
%
%       This function is used by the Fzero routine called in the mdot.m
%       program in order to compute the Mach # at the end of the fill tube
%       just prior to the final constricting orifice.

function m2zero=mach2(M)

m2zero=(Af/A1)*(2/(g+1)*(1+(g-1)/2*M^2))^((g+1)/2/(g-1))-M;
```

A.4 maxvalve.m

```
%       maxvalve.m
%       11/22/92
%
%       This program will allow the user to input several parameters
%       for the Ram Accelerator (or any similar system) and then calculate
%       the approximate Cv factor required in order to maintain the desired
%       input mass flow rate.
%       The calculations are performed for a range of upstream pressures
%       between the downstream pressure value and the maximum pressure
%       before choking occurs.

clear
clg
hold off
%%%%%%%%%%%%%%%%%%%%%%%%
%       User Inputs %
%%%%%%%%%%%%%%%%%%%%%%%%

choice=input('1=CH4, 2=CO2, 3=H2, 4=He, 5=O2, 6=N2: ');
gas(choice)
Pf=input('Fill Tank Pressure (psig), Pf: ');
Pf=(14.7+Pf)*1.01e5/14.7;

%%%%%%%%%%%%%%%%%%%%%%%%
%       Fixed Inputs%
%%%%%%%%%%%%%%%%%%%%%%%%

flag=0;
E=.00125;%              Pipe roughness coefficient  inches
dmin=.00143;%           minimum line diameter, meters
Amin=atan(1)*dmin^2;
dp=.152*.0254;%         Fill Pipe Diameter, meters
Ap=atan(1)*dp^2;%       Fill Pipe Area, square meters
Tf=295;%                Temperature in Fill Tank, Kelvin
Ru=8314.4;%             SI Units
Kcv=7.1475e-5;%input('Kcv= ');
L=18;%                  Fill Line length in meters.
```

```
%%%%%%%%%%%%%%%%%%%%%%
%       Calculations%
%%%%%%%%%%%%%%%%%%%%%%

Kcf=1315.74*sqrt(g/(MW*(g-1)));
pterm=sqrt((2/(g+1))^(2/(g-1))-(2/(g+1))^((g+1)/(g-1)));
Mdmax=input('Molar Flow Rate= ')
Mfsq=(Mdmax*1.01e5*sqrt(MW)/Pf/Ap/60000/sqrt(g*Tf*Ru))^2;
Mf=sqrt(Mfsq)
Re=MW*(5.706e-3)/Ru*Mdmax*dp/Ap/mu;
f=.25/(log(E/3.7/dp)+(5.74/Re^.9))^2;
M2=fzero('mach1mv',Mf*.9)


A2s=Ap*M2*((2/(g+1))*(1+(g-1)/2*M2^2))^(-(g+1)/2/(g-1));%critical area

P2=MW*(5.706e-3)/Ru*Mdmax/M2/Ap*(Ru*Tf/g/MW/(1+((g-1)/
2)*M2^2))^.5;
P2o=P2*(1+(g-1)/2*M2^2)^(1/(g-1));
P2o*14.7/1.01e5

PRcrit=(2/(g+1))^(g/(g-1));
P1o=P2o:(P2/PRcrit-P2o)/100:P2/PRcrit;
for i=1:length(P1o)
 PR(i)=P2/P1o(i);
 Cv(i)=(Mdmax*(Kcf*Kcv*P1o(i)*((PR(i))^(2/g)-(PR(i))^((g+1)/g))^.5)^(-1));
 P1opsi(i)=P1o(i)*14.7/1.01e5;
 Mvplot(i)=(((PR(i))^((1-g)/g)-1)*2/(g-1))^.5;
end

%%%%%%%%%%%%%%%%%%%%%%
%       Output
%%%%%%%%%%%%%%%%%%%%%%

axis([0, 1000, 0, .05])
plot(P1opsi,Cv)
hold
plot([Pf*14.7/1.01e5 Pf*14.7/1.01e5],[0 .05])
grid
```

```
xlabel('Upstream Stagnation Pressure  psia')
ylabel('Cv Factor')
text(.5,.8,'Kcv=','sc')
text(.5,.75,'Pf=','sc')
text(.5,.7,'gamma=','sc')
text(.5,.65,'MW=','sc')
text(.56,.8,num2str(Kcv),'sc')
text(.56,.75,num2str(Pf*14.7/1.01e5),'sc')
text(.58,.7,num2str(g),'sc')
text(.56,.65,num2str(MW),'sc')
text(.62,.75,'psia','sc')

end
```

A.5 mach1mv.m

```
%       12/2/91
%
%       This function is used to iteratively solve for the Mach Number
%       at an upstream location in a tube with friction (adiabatic) given
%       the downstream Mach Number.

function m1zero=mach1(M)

T1=M^(-2)-Mf^(-2);

m1zero=T1+(g+1)/2*log(M^2*(2+(g-1)*Mf^2)/(Mf^2*(2+(g-1)*M^2)))-f*g*L/dp;
```

A.6 gas.m

```
%       gas.m
%       11/22/92
%
%       This program is simple.  It is a function which returns the Molecular
%       Weight, gamma, and the viscosity of the chosen gas.

function gas(choice)
 if choice==1, CH4
 elseif choice==2, CO2
 elseif choice==3, H2
 elseif choice==4, He
 elseif choice==5, O2
 elseif choice==6, N2
 else N2
  input('Nitrogen will be used. <RETURN> to continue.');
 end
```

A.7 N2.m

```
%       N2, Nitrogen
%       SI Units


MW=28;
g=1.4;
mu=178.2e-7;
```

A.8 metertf.m

```
%       metertf.m
%       6/1/92
%
%       This program uses the data in the mtfdata#.m files to compute the
%       empirical eigenvalue for the flow meter with a least squares
%       algorithm.  The meter response is modelled as: y=1-e^(-lam*t).
%       Rewriting with the exponential term on one side, and 1-y on the
%       other, taking the logarithm gives the following linear equation:
%               (1-y)=z=lam*t
%       After the least squares fit is done for this equation using the
%       foexpfit.m function file, the values obtained for lam for six
%       different runs are averaged to give the final value to be used
%       as the model for the flow meter transfer function.

clear
clg
hold off
lambdasq=0;
offsetsq=0;

mtfdata1
t1=t;
y1=y;
[la,of]=foexpfit(t,y);
lambdasq=lambdasq+la^2;
offsetsq=offsetsq+of^2;
tc=t(1):(10+t(length(t))-t(1))/50:t(length(t))+10;
for i=1:length(tc)
 yc(i)=1-exp(-(la*tc(i)+of));
end

plot(tc,yc,t,y,'x'),grid
pause

mtfdata2
t2=t;
y2=y;
[la,of]=foexpfit(t,y);
```

```
lambdasq=lambdasq+la^2;
offsetsq=offsetsq+of^2;
tc=t(1):(10+t(length(t))-t(1))/50:t(length(t))+10;
for i=1:length(tc)
  yc(i)=1-exp(-(la*tc(i)+of));
end

plot(tc,yc,t,y,'x'),grid
pause

mtfdata3
t3=t;
y3=y;
[la,of]=foexpfit(t,y);
lambdasq=lambdasq+la^2;
offsetsq=offsetsq+of^2;
tc=t(1):(10+t(length(t))-t(1))/50:t(length(t))+10;
for i=1:length(tc)
  yc(i)=1-exp(-(la*tc(i)+of));
end

plot(tc,yc,t,y,'x'),grid
pause

mtfdata4
t4=t;
y4=y;
[la,of]=foexpfit(t,y);
lambdasq=lambdasq+la^2;
offsetsq=offsetsq+of^2;
tc=t(1):(10+t(length(t))-t(1))/50:t(length(t))+10;
for i=1:length(tc)
  yc(i)=1-exp(-(la*tc(i)+of));
end

plot(tc,yc,t,y,'x'),grid
pause

mtfdata5
```

```
t5=t;
y5=y;
[la,of]=foexpfit(t,y);
lambdasq=lambdasq+la^2;
offsetsq=offsetsq+of^2;
tc=t(1):(10+t(length(t))-t(1))/50:t(length(t))+10;
for i=1:length(tc)
  yc(i)=1-exp(-(la*tc(i)+of));
end

plot(tc,yc,t,y,'x'),grid
pause

mtfdata6
t6=t;
y6=y;
[la,of]=foexpfit(t,y);
lambdasq=lambdasq+la^2;
offsetsq=offsetsq+of^2;
tc=t(1):(10+t(length(t))-t(1))/50:t(length(t))+10;
for i=1:length(tc)
  yc(i)=1-exp(-(la*tc(i)+of));
end

plot(tc,yc,t,y,'x'),grid
pause

lambda=sqrt(lambdasq/6);
offset=sqrt(offsetsq/6);

time=0:40/100:40;
for i=1:length(time)
  y(i)=1-exp(-lambda*time(i));
end

plot(time,y),hold,grid
plot(t1,y1,'o')
plot(t2,y2,'o')
plot(t3,y3,'o')
```

```
plot(t4,y4,'x')
plot(t5,y5,'x')
plot(t6,y6,'x')
xlabel('Time   seconds')
ylabel('Normalized Flow Meter Response')
text(.5,.7,'y(t)=1-exp(-t/T)','sc')
text(.5,.65,'T=','sc')
text(.6,.65,num2str(lambda),'sc')
```

A.9 foexpfit.m

```
%       foexpfit.m
%       6/1/92
%
%       This function returns the time constant for a first order
%       approximation to the flow meter response.  As inputs, it requires
%       two vectors:  the time vector, and the normalized voltage response
%       vector.

function [lambda,offset]=foexpfit(t,y)

for i=1:length(y)
  ya(i)=-log(1-y(i));
end

p=polyfit(t,ya,1)
lambda=p(1)
offset=p(2)
```

A.10 mtfdata1.m

```
%       Data for the flow meter.  See foexpfit.m and metertf.m for details.
y=[0 .4688 .5575 .6634 .7306 .7834 .825 .8567];
t=[0 2.988 3.77 5.02 5.996 7.012 7.988 9.004];
```

A.11 mtfdata2.m

```
%       Data for the flow meter.  See foexpfit.m and metertf.m for details.
y=[0 .4576 .5485 .6564 .7218 .7747 .8127 .8451];
t=[0 2.988 3.789 5.078 5.996 7.031 7.988 9.004];
```

A.12 mtfdata3.m

```
%       Data for the flow meter.  See foexpfit.m and metertf.m for details.
y=[0 .4764 .5677 .676 .7399 .7938 .8344 .8673];
t=[0 2.988 3.789 5.078 5.996 7.031 7.988 9.023];
```

A.13 mtfdata4.m

```
%       Data for the flow meter.  See foexpfit.m and metertf.m for details.
y=[0 .5514 .6349 .7441 .7969 .8446 .881 .9098];
t=[0 2.988 3.789 5.078 5.996 7.031 7.988 9.023];
```

A.14 mtfdata5.m

```
%       Data for the flow meter.  See foexpfit.m and metertf.m for details.
y=[0 .5314 .6359 .7148 .7794 .8257 .8613 .8911];
t=[0 2.988 4.004 5 6.035 7.031 7.988 9.023];
```

A.15 mtfdata6.m

```
%       Data for the flow meter.  See foexpfit.m and metertf.m for details.
y=[0 .5317 .6335 .7102 .7706 .8160 .8516 .8793];
t=[0 3.008 4.004 5 6.016 7.012 8.008 9.004];
```

A.16 Graphical Representation of Simulab Program for Nonlinear Simulation of Mass Flow Rate Controller

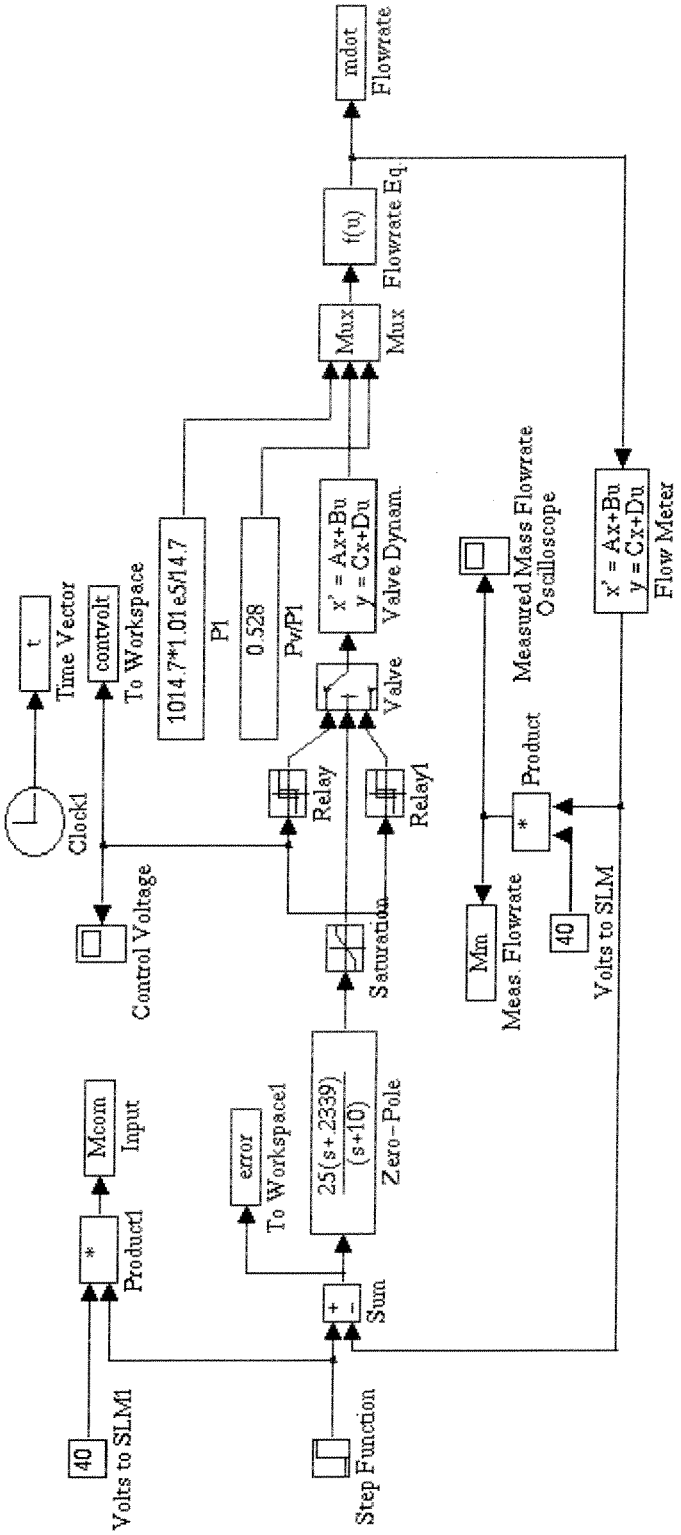

A.17 nlrateth.m (Creates Graphical and Numerical Simulation Shown in Appendix A.16)

```
function [ret,x0,str]=nlrateth(t,x,u,flag);
%NLRATETHis the M-file description of the SIMULINK system named NLRATETH.
%       The block-diagram can be displayed by typing: NLRATETH.
%
%       SYS=NLRATETH(T,X,U,FLAG) returns depending on FLAG certain
%       system values given time point, T, current state vector, X,
%       and input vector, U.
%       FLAG is used to indicate the type of output to be returned in SYS.
%
%       Setting FLAG=1 causes NLRATETH to return state derivitives, FLAG=2
%       discrete states, FLAG=3 system outputs and FLAG=4 next sample
%       time. For more information and other options see SFUNC.
%
%       Calling NLRATETH with a FLAG of zero:
%       [SIZES]=NLRATETH([],[],[],0),  returns a vector, SIZES, which
%       contains the sizes of the state vector and other parameters.
%             SIZES(1) number of states
%             SIZES(2) number of discrete states
%             SIZES(3) number of outputs
%             SIZES(4) number of inputs.
%       For the definition of other parameters in SIZES, see SFUNC.
%       See also, TRIM, LINMOD, LINSIM, EULER, RK23, RK45, ADAMS, GEAR.

% Note: This M-file is only used for saving graphical information;
%       after the model is loaded into memory an internal model
%       representation is used.

% the system will take on the name of this mfile:
sys = mfilename;
new_system(sys)
simver(1.2)
if(0 == (nargin + nargout))
   set_param(sys,'Location',[100,385,910,786])
   open_system(sys)
end;
set_param(sys,'algorithm','RK-45')
```

```
set_param(sys,'Start time','0.0')
set_param(sys,'Stop time','999999')
set_param(sys,'Min step size','0.001')
set_param(sys,'Max step size','.01')
set_param(sys,'Relative error','1e-3')
set_param(sys,'Return vars','')

add_block('built-in/Constant',[sys,'/','Zero'])
set_param([sys,'/','Zero'],...
                'Value','.26',...
                'position',[115,275,135,295])

add_block('built-in/Constant',[sys,'/','Pole'])
set_param([sys,'/','Pole'],...
                'Value','3',...
                'position',[115,240,135,260])

add_block('built-in/Sum',[sys,'/','Sum'])
set_param([sys,'/','Sum'],...
                'inputs','+-',...
                'position',[115,200,135,220])

add_block('built-in/Mux',[sys,'/','Mux1'])
set_param([sys,'/','Mux1'],...
                'inputs','4',...
                'position',[160,178,190,237])

add_block('built-in/Fcn',[sys,'/','Gain'])
set_param([sys,'/','Gain'],...
                'Expr','u(2)*.02/.005*u(3)/u(4)/u(1)',...
                'position',[200,200,240,220])

add_block('built-in/Constant',[sys,'/','Pv//P1'])
set_param([sys,'/','Pv//P1'],...
                'Value','0.528',...
                'position',[415,155,530,175])

add_block('built-in/Constant',[sys,'/','P1'])
set_param([sys,'/','P1'],...
```

```
                'Value','1014.7*1.01e5/14.7',...
                'position',[415,113,530,137])

add_block('built-in/Mux',[sys,'/','Mux'])
set_param([sys,'/','Mux'],...
                'inputs','3',...
                'position',[610,194,640,226])

add_block('built-in/Fcn',[sys,'/','Flow Rate Eq.'])
set_param([sys,'/','Flow Rate Eq.'],...
                'Expr','0.03325*u(1)*((u(3))^(1.428)-(u(3))^(1.714))^(.5)*u(2)',...
                'position',[660,196,700,224])

add_block('built-in/State-space',[sys,'/','Valve Dynam.'])
set_param([sys,'/','Valve Dynam.'],...
                'A','0',...
                'B','1',...
                'C','1',...
                'D','0',...
                'position',[470,195,550,225])

add_block('built-in/To Workspace',[sys,'/','Cv'])
set_param([sys,'/','Cv'],...
                'mat-name','valve',...
                'buffer','10000',...
                'position',[580,282,630,298])

add_block('built-in/To Workspace',[sys,'/','Input'])
set_param([sys,'/','Input'],...
                'mat-name','inp',...
                'buffer','10000',...
                'position',[80,147,130,163])

add_block('built-in/Step Fcn',[sys,'/','Step Function'])
set_param([sys,'/','Step Function'],...
                'Time','0',...
                'Before','0',...
                'After','2.5',...
                'position',[35,195,55,215])
```

```
add_block('built-in/To Workspace',[sys,'/','Meas. Flow Rate'])
set_param([sys,'/','Meas. Flow Rate'],...
                'orientation',2,...
                'mat-name','mdotm',...
                'buffer','10000',...
                'position',[305,302,355,318])

add_block('built-in/To Workspace',[sys,'/','Flow Rate'])
set_param([sys,'/','Flow Rate'],...
                'mat-name','mdot',...
                'buffer','10000',...
                'position',[745,157,795,173])

add_block('built-in/State-space',[sys,'/','Flow Meter'])
set_param([sys,'/','Flow Meter'],...
                'orientation',2,...
                'A','[0 1;0 -.2339]',...
                'B','[0;.00583]',...
                'C','[0 1]',...
                'D','0',...
                'position',[480,336,555,364])

add_block('built-in/Switch',[sys,'/','Valve'])
set_param([sys,'/','Valve'],...
                'ForeGround',0,...
                'position',[420,194,445,226])

add_block('built-in/Zero-Pole',[sys,'/','Zero-Pole'])
set_param([sys,'/','Zero-Pole'],...
                'Zeros','[-.26]',...
                'Poles','[-3]',...
                'Gain','[1]',...
                'position',[260,192,330,228])

add_block('built-in/Clock',[sys,'/','Clock1'])
set_param([sys,'/','Clock1'],...
                'position',[355,35,390,65])
```

```
add_block('built-in/To Workspace',[sys,'/','Time Vector'])
set_param([sys,'/','Time Vector'],...
                'mat-name','t',...
                'buffer','10000',...
                'position',[440,42,490,58])

add_block('built-in/Scope',[sys,'/',['Mass Flow Rate',13,'Oscilloscope']])
set_param([sys,'/',['Mass Flow Rate',13,'Oscilloscope']],...
                'Vgain','200',...
                'Hgain','10',...
                'Vmax','400',...
                'Hmax','20',...
                'Window',[0,0,280,220])
open_system([sys,'/',['Mass Flow Rate',13,'Oscilloscope']])
set_param([sys,'/',['Mass Flow Rate',13,'Oscilloscope']],...
                'position',[750,197,770,223])

add_block('built-in/Scope',[sys,'/','Valve Output '])
set_param([sys,'/','Valve Output '],...
                'orientation',2,...
                'Vgain','7e-05',...
                'Hgain','10',...
                'Vmax','0.00014',...
                'Hmax','20',...
                'Window',[0,0,280,220],...
                'position',[515,277,535,303])

add_block('built-in/Relay',[sys,'/','Relay'])
set_param([sys,'/','Relay'],...
                'On_switch_value','.02',...
                'Off_switch_value','.02',...
                'On_output_value','1.177e-4',...
                'Off_output_value','0',...
                'position',[360,170,385,190])

add_block('built-in/Relay',[sys,'/','Relay1'])
set_param([sys,'/','Relay1'],...
                'On_switch_value','-.02',...
                'Off_switch_value','.02',...
```

```
                'On_output_value',0',...
                'Off_output_value',-1.177e-4',...
                'position',[360,225,385,245])
add_line(sys,[705,210;715,210;715,350;560,350])
add_line(sys,[715,210;745,210])
add_line(sys,[715,210;715,165;740,165])
add_line(sys,[245,210;255,210])
add_line(sys,[140,285;150,285;155,230])
add_line(sys,[140,250;140,215;155,215])
add_line(sys,[140,210;140,200;155,200])
add_line(sys,[60,205;110,205])
add_line(sys,[70,205;75,155])
add_line(sys,[72,185;155,185])
add_line(sys,[195,210;195,210])
add_line(sys,[475,350;100,350;100,215;110,215])
add_line(sys,[535,125;580,125;580,200;605,200])
add_line(sys,[535,165;565,165;565,220;605,220])
add_line(sys,[555,210;605,210])
add_line(sys,[645,210;655,210])
add_line(sys,[450,210;465,210])
add_line(sys,[395,350;395,310;360,310])
add_line(sys,[395,50;435,50])
add_line(sys,[555,210;555,290;575,290])
add_line(sys,[555,290;540,290])
add_line(sys,[390,180;400,180;400,200;415,200])
add_line(sys,[390,235;400,235;400,220;415,220])
add_line(sys,[335,210;415,210])
add_line(sys,[340,210;340,180;355,180])
add_line(sys,[340,210;340,235;355,235])
% Return any arguments.
if (nargin | nargout)
        % Must use feval here to access system in memory
        if (nargin > 3)
                if (flag == 0)
                        eval(['[ret,x0,xstr]=',sys,'(t,x,u,flag);'])
                else
                        eval(['ret =', sys,'(t,x,u,flag);'])
                end
        else
```

```
            [ret,x0,str] = feval(sys);
        end
    end
```

A.18 thor.m

```
%       thor.m
%       11/2/92
%
%       This program allows the user to choose the pole values for the
%       closed loop transfer function of a 3rd order open loop system
%       and returns the poles and zeros of a 3rd order controller which
%       will achieve the desired pole locations.

clear
clg
hold off

k=input('Gain: ');
pm1=input('pm1= ');
pm2=input('pm2= ');
pm3=input('pm3= ');
pm4=input('pm4= ');
pm5=input('pm5= ');
pm6=input('pm6= ');

y=zeros(6);
a=zeros(6,6);
s=[-pm1 -pm2 -pm3 -pm4 -pm5 -pm6];
for i=1:length(s)
dg=(s(i))^2;
dh=(s(i)+.2332);
ng=k;
nh=5.83e-3;
 for j=1:3
  a(i,j)=dg*dh*(s(i))^(3-j);
  a(i,j+3)=ng*nh*(s(i))^(3-j);
 end
 y(i)=-(dg*dh+ng*nh)*(s(i))^3;
end


c=inv(a)*y;
p2=-max(s);
```

```
p3=-max(s)*.9;
tol=1;
count=0;
while tol>=1e-7,
 count=count+1;
 pold=p3;
 p1=c(1)-p3-p2;
 p2=(c(2)-p1*p3)/(p1+p3);
 p3=(c(3))/p2/p1;
 tol=abs((p3-pold)/p3);
 if count>2e4,tol=1e-7;,p3,end
end
p1
p2
p3


z2=1;
z3=1;
tol=1;
count=0;
while tol>=1e-6,
 count=count+1;
 zold=z3;
 z1=c(4)-z3-z2;
 z2=(c(5)-z1*z3)/(z1+z3);
 z3=(c(6))/z2/z1;
 tol=abs((z3-zold)/z3);
 if count>2e3,tol=1e-7;,z3,end
end
z1
z2
z3
end
```

A.19 Graphical Representation of Simulabe Program for Nonlinear Simulation of Mass Ratio Controller

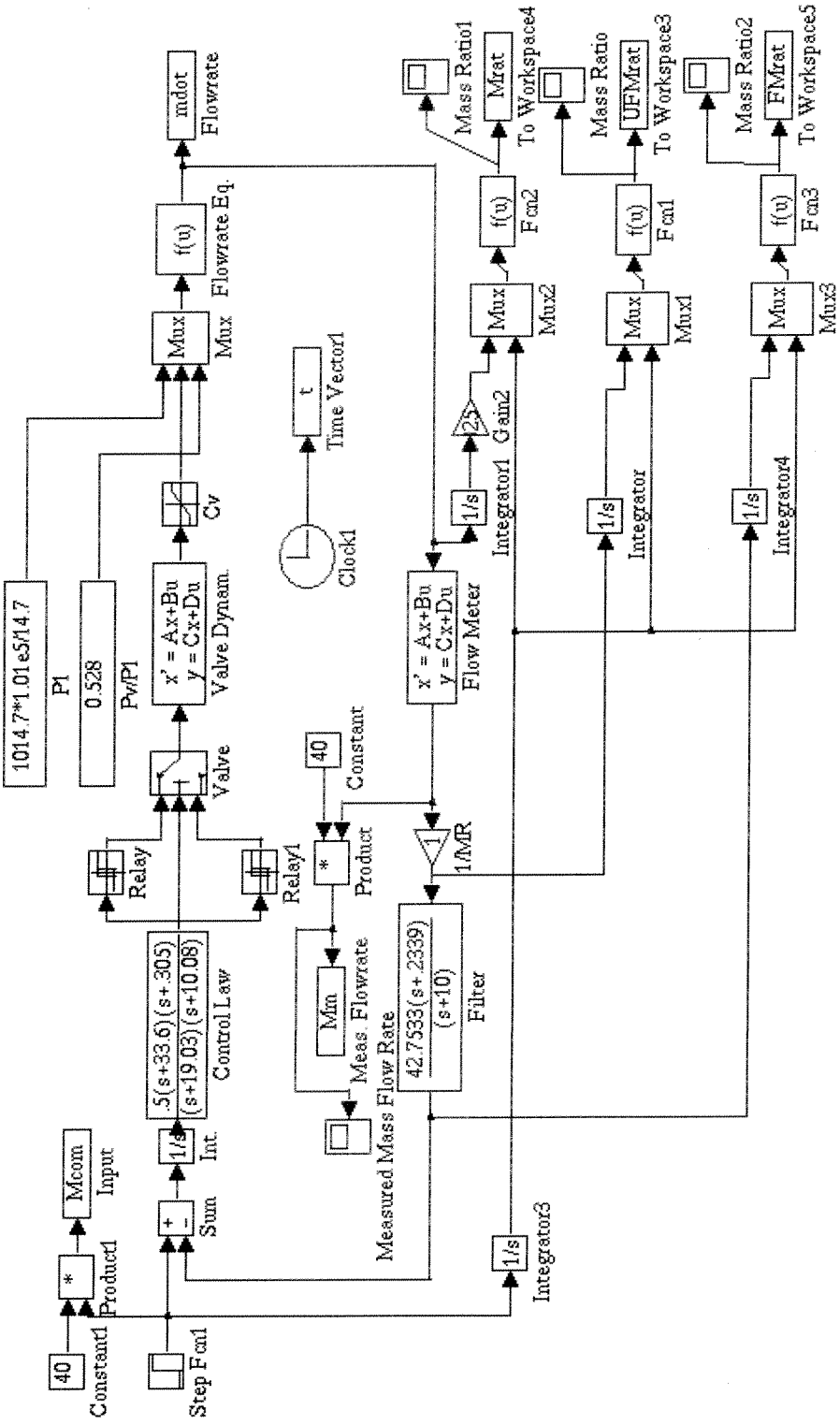

A.20 nlratioth.m (Creates graphical and numerical simulation shown in Appendix)

```
function [ret,x0,str]=nlratioth(t,x,u,flag);
%NLRATIOTHis the M-file description of the SIMULINK system named NLRA-
TIOTH.
%       The block-diagram can be displayed by typing: NLRATIOTH.
%
%       SYS=NLRATIOTH(T,X,U,FLAG) returns depending on FLAG certain
%       system values given time point, T, current state vector, X,
%       and input vector, U.
%       FLAG is used to indicate the type of output to be returned in SYS.
%
%       Setting FLAG=1 causes NLRATIOTH to return state derivitives, FLAG=2
%       discrete states, FLAG=3 system outputs and FLAG=4 next sample
%       time. For more information and other options see SFUNC.
%
%       Calling NLRATIOTH with a FLAG of zero:
%       [SIZES]=NLRATIOTH([],[],[],0),  returns a vector, SIZES, which
%       contains the sizes of the state vector and other parameters.
%             SIZES(1) number of states
%             SIZES(2) number of discrete states
%             SIZES(3) number of outputs
%             SIZES(4) number of inputs.
%       For the definition of other parameters in SIZES, see SFUNC.
%       See also, TRIM, LINMOD, LINSIM, EULER, RK23, RK45, ADAMS, GEAR.

% Note: This M-file is only used for saving graphical information;
%       after the model is loaded into memory an internal model
%       representation is used.

% the system will take on the name of this mfile:
sys = mfilename;
new_system(sys)
simver(1.2)
if(0 == (nargin + nargout))
   set_param(sys,'Location',[13,61,992,832])
   open_system(sys)
end;
set_param(sys,'algorithm','RK-45')
```

```
set_param(sys,'Start time','0.0')
set_param(sys,'Stop time','999999')
set_param(sys,'Min step size','0.1')
set_param(sys,'Max step size','.1')
set_param(sys,'Relative error','1e-3')
set_param(sys,'Return vars','')

add_block('built-in/Constant',[sys,'/','Constant'])
set_param([sys,'/','Constant'],...
                'orientation',2,...
                'Value','40',...
                'position',[390,205,410,225])

add_block('built-in/Product',[sys,'/','Product'])
set_param([sys,'/','Product'],...
                'orientation',2,...
                'inputs','2',...
                'position',[325,210,350,230])

add_block('built-in/Zero-Pole',[sys,'/','Filter'])
set_param([sys,'/','Filter'],...
                'orientation',2,...
                'Zeros','[-.2339]',...
                'Poles','[ -10]',...
                'Gain','[42.7533]',...
                'position',[210,257,315,293])

add_block('built-in/Zero-Pole',[sys,'/','Control Law'])
set_param([sys,'/','Control Law'],...
                'ForeGround',0,...
                'Zeros','[-33.6;-.305]',...
                'Poles','[-19.03;-10.08]',...
                'Gain','[.5]',...
                'position',[195,118,300,152])

add_block('built-in/Integrator',[sys,'/','Integrator'])
set_param([sys,'/','Integrator'],...
                'Initial','0',...
                'position',[520,360,540,380])
```

```
add_block('built-in/Scope',[sys,'/','Mass Ratio'])
set_param([sys,'/','Mass Ratio'],...
                'Vgain','1.2',...
                'Hgain','100',...
                'Vmax','2.4',...
                'Hmax','200',...
                'Window',[0,0,280,220],...
                'position',[760,332,780,358])

add_block('built-in/To Workspace',[sys,'/','To Workspace3'])
set_param([sys,'/','To Workspace3'],...
                'mat-name','UFMrat',...
                'buffer','10000',...
                'position',[745,377,795,393])

add_block('built-in/Fcn',[sys,'/','Fcn1'])
set_param([sys,'/','Fcn1'],...
                'Expr','u(1)/u(2)',...
                'position',[675,375,715,395])

add_block('built-in/Mux',[sys,'/','Mux1'])
set_param([sys,'/','Mux1'],...
                'inputs','2',...
                'position',[625,370,655,405])

add_block('built-in/Scope',[sys,'/','Measured Mass Flow Rate'])
set_param([sys,'/','Measured Mass Flow Rate'],...
                'orientation',2,...
                'Vgain','200',...
                'Hgain','160',...
                'Vmax','416.667',...
                'Hmax','320',...
                'Window',[0,0,231,217],...
                'position',[175,217,195,243])

add_block('built-in/To Workspace',[sys,'/','Time Vector1'])
set_param([sys,'/','Time Vector1'],...
                'mat-name','t',...
```

```
                'buffer','10000',...
                'position',[575,197,625,213])

add_block('built-in/Clock',[sys,'/','Clock1'])
set_param([sys,'/','Clock1'],...
                'position',[490,190,525,220])

add_block('built-in/Switch',[sys,'/','Valve'])
set_param([sys,'/','Valve'],...
                'ForeGround',0,...
                'position',[375,119,400,151])

add_block('built-in/State-space',[sys,'/','Flow Meter'])
set_param([sys,'/','Flow Meter'],...
                'orientation',2,...
                'A','[0 1;0 -.2339]',...
                'B','[0;.0058475]',...
                'C','[0 1]',...
                'D','0',...
                'position',[425,261,500,289])

add_block('built-in/Sum',[sys,'/','Sum'])
set_param([sys,'/','Sum'],...
                'inputs','+-',...
                'position',[130,125,150,145])

add_block('built-in/To Workspace',[sys,'/','Flow Rate'])
set_param([sys,'/','Flow Rate'],...
                'mat-name','mdot',...
                'buffer','10000',...
                'position',[740,127,790,143])

add_block('built-in/To Workspace',[sys,'/','Meas. Flow Rate'])
set_param([sys,'/','Meas. Flow Rate'],...
                'orientation',2,...
                'mat-name','Mm',...
                'buffer','10000',...
                'position',[230,212,280,228])
```

```
add_block('built-in/To Workspace',[sys,'/','Input'])
set_param([sys,'/','Input'],...
                'mat-name','Mcom',...
                'buffer','10000',...
                'position',[140,72,190,88])

add_block('built-in/State-space',[sys,'/','Valve Dynam.'])
set_param([sys,'/','Valve Dynam.'],...
                'A','0',...
                'B','1',...
                'C','1',...
                'D','0',...
                'position',[425,120,505,150])

add_block('built-in/Note',[sys,'/','Nonlinear Simulation of the Flow Rate Con-
troller'])
set_param([sys,'/','Nonlinear Simulation of the Flow Rate Controller'],...
                'position',[200,11,201,12])

add_block('built-in/Saturation',[sys,'/','Cv '])
set_param([sys,'/','Cv '],...
                'Upper Limit','.007',...
                'Lower Limit','0',...
                'position',[525,125,550,145])

add_block('built-in/Gain',[sys,'/','1//MR'])
set_param([sys,'/','1//MR'],...
                'orientation',2,...
                'Gain','1',...
                'position',[335,265,355,285])

add_block('built-in/Step Fcn',[sys,'/','Step Fcn1'])
set_param([sys,'/','Step Fcn1'],...
                'Time','0',...
                'Before','0',...
                'After','1.25',...
                'position',[45,120,65,140])

add_block('built-in/Relay',[sys,'/','Relay1'])
```

```
set_param([sys,'/','Relay1'],...
                'On_switch_value','-.02',...
                'Off_switch_value','-.02',...
                'On_output_value','0',...
                'Off_output_value','-1.177e-4',...
                'position',[320,170,345,190])

add_block('built-in/Relay',[sys,'/','Relay'])
set_param([sys,'/','Relay'],...
                'On_switch_value','.02',...
                'Off_switch_value','.02',...
                'On_output_value','1.177e-4',...
                'Off_output_value','0',...
                'position',[320,85,345,105])

add_block('built-in/Constant',[sys,'/','Pv//P1'])
set_param([sys,'/','Pv//P1'],...
                'Value','0.528',...
                'position',[380,80,495,100])

add_block('built-in/Constant',[sys,'/','P1'])
set_param([sys,'/','P1'],...
                'Value','1014.7*1.01e5/14.7',...
                'position',[380,38,495,62])

add_block('built-in/Fcn',[sys,'/','Flow Rate Eq.'])
set_param([sys,'/','Flow Rate Eq.'],...
                'Expr','0.03325*u(1)*((u(3))^(1.428)-(u(3))^(1.714))^(.5)*u(2)',...
                'position',[665,121,705,149])

add_block('built-in/Mux',[sys,'/','Mux'])
set_param([sys,'/','Mux'],...
                'inputs','3',...
                'position',[615,119,645,151])

add_block('built-in/Integrator',[sys,'/','Int.'])
set_param([sys,'/','Int.'],...
                'Initial','0',...
                'position',[170,125,190,145])
```

```
add_block('built-in/Integrator',[sys,'/','Integrator3'])
set_param([sys,'/','Integrator3'],...
                'Initial','0',...
                'position',[110,310,130,330])

add_block('built-in/Product',[sys,'/','Product1'])
set_param([sys,'/','Product1'],...
                'inputs','2',...
                'position',[95,70,120,90])

add_block('built-in/Constant',[sys,'/','Constant1'])
set_param([sys,'/','Constant1'],...
                'Value','40',...
                'position',[45,65,65,85])

add_block('built-in/Integrator',[sys,'/','Integrator1'])
set_param([sys,'/','Integrator1'],...
                'Initial','0',...
                'position',[525,285,545,305])

add_block('built-in/Scope',[sys,'/','Mass Ratio1'])
set_param([sys,'/','Mass Ratio1'],...
                'Vgain','1.2',...
                'Hgain','100',...
                'Vmax','2.4',...
                'Hmax','200',...
                'Window',[0,0,280,220],...
                'position',[765,257,785,283])

add_block('built-in/To Workspace',[sys,'/','To Workspace4'])
set_param([sys,'/','To Workspace4'],...
                'mat-name','Mrat',...
                'buffer','10000',...
                'position',[750,302,800,318])

add_block('built-in/Fcn',[sys,'/','Fcn2'])
set_param([sys,'/','Fcn2'],...
                'Expr','u(1)/u(2)',...
```

```
                'position',[680,300,720,320])

add_block('built-in/Mux',[sys,'/','Mux2'])
set_param([sys,'/','Mux2'],...
                'inputs','2',...
                'position',[630,295,660,330])

add_block('built-in/Gain',[sys,'/','Gain2'])
set_param([sys,'/','Gain2'],...
                'Gain','.025',...
                'position',[575,285,595,305])

add_block('built-in/Integrator',[sys,'/','Integrator4'])
set_param([sys,'/','Integrator4'],...
                'Initial','0',...
                'position',[525,440,545,460])

add_block('built-in/Scope',[sys,'/','Mass Ratio2'])
set_param([sys,'/','Mass Ratio2'],...
                'Vgain','1.2',...
                'Hgain','100',...
                'Vmax','2.4',...
                'Hmax','200',...
                'Window',[0,0,280,220],...
                'position',[765,412,785,438])

add_block('built-in/To Workspace',[sys,'/','To Workspace5'])
set_param([sys,'/','To Workspace5'],...
                'mat-name','FMrat',...
                'buffer','10000',...
                'position',[750,457,800,473])

add_block('built-in/Fcn',[sys,'/','Fcn3'])
set_param([sys,'/','Fcn3'],...
                'Expr','u(1)/u(2)',...
                'position',[680,455,720,475])

add_block('built-in/Mux',[sys,'/','Mux3'])
set_param([sys,'/','Mux3'],...
```

```
                'inputs','2',...
                'position',[630,450,660,485])
add_line(sys,[205,275;105,275;105,140;125,140])
add_line(sys,[195,275;195,450;520,450])
add_line(sys,[320,220;285,220])
add_line(sys,[300,220;300,200;210,200;210,230;200,230])
add_line(sys,[385,215;355,215])
add_line(sys,[330,275;320,275])
add_line(sys,[720,385;720,345;755,345])
add_line(sys,[720,385;740,385])
add_line(sys,[660,390;670,385])
add_line(sys,[530,205;570,205])
add_line(sys,[405,135;420,135])
add_line(sys,[555,135;610,135])
add_line(sys,[510,135;520,135])
add_line(sys,[305,135;305,95;315,95])
add_line(sys,[305,135;305,180;315,180])
add_line(sys,[305,135;370,135])
add_line(sys,[350,95;350,125;370,125])
add_line(sys,[350,180;350,145;370,145])
add_line(sys,[500,50;585,50;585,125;610,125])
add_line(sys,[500,90;565,90;565,145;610,145])
add_line(sys,[650,135;660,135])
add_line(sys,[155,135;165,135])
add_line(sys,[195,135;190,135])
add_line(sys,[70,130;125,130])
add_line(sys,[85,130;90,85])
add_line(sys,[85,130;85,320;105,320])
add_line(sys,[125,80;135,80])
add_line(sys,[70,75;90,75])
add_line(sys,[710,135;725,135;725,275;505,275])
add_line(sys,[725,135;735,135])
add_line(sys,[545,370;600,370;600,380;620,380])
add_line(sys,[550,295;570,295])
add_line(sys,[600,295;610,295;610,305;625,305])
add_line(sys,[515,275;520,295])
add_line(sys,[665,315;675,310])
add_line(sys,[725,310;745,310])
add_line(sys,[725,310;745,270;760,270])
```

```
add_line(sys,[725,465;726,425;760,425])
add_line(sys,[725,465;745,465])
add_line(sys,[665,470;675,465])
add_line(sys,[550,450;606,450;606,460;625,460])
add_line(sys,[420,275;360,275])
add_line(sys,[370,275;370,225;355,225])
add_line(sys,[330,275;330,370;515,370])
add_line(sys,[135,320;625,320])
add_line(sys,[465,320;465,395;620,395])
add_line(sys,[465,395;465,475;625,475])
% Return any arguments.
if (nargin | nargout)
        % Must use feval here to access system in memory
        if (nargin > 3)
                if (flag == 0)
                        eval(['[ret,x0,xstr]=',sys,'(t,x,u,flag);'])
                else
                        eval(['ret =', sys,'(t,x,u,flag);'])
                end
        else
                [ret,x0,str] = feval(sys);
        end
end
```